PB95-231452

Publication No. FHWA-RD-94-151
June 1995

Finite Element Model of a Small Automobile Impacting a Rigid Pole

U.S. Department of Transportation
Federal Highway Administration

Research and Development
Turner-Fairbank Highway Research Center
6300 Georgetown Pike
McLean, Virginia 22101-2296

FOREWORD

This report describes the development of a finite element model of a small passenger car similar to the 820C test vehicle recommended in NCHRP Report 350. The finite element model was developed to provide a tool for performing finite element analyses of impacts with roadside safety hardware. This model was designed such that it can be easily integrated into finite element analyses of a variety of frontal narrow-object impact problems such as the design of luminaire and small sign supports. The report describes the development of the model and then compares the results with full-scale crash tests.

This report will be of interest to developers of roadside safety hardware since it describes a powerful analysis tool that can be integrated into the safety appurtenance development process. Researchers and policy makers will also be interested in the use of this type of finite element model for exploring policy options.

Lyle Saxton
Director, Office of Safety and Traffic
Operations Research and Development

NOTICE

Technical Report Documentation Page

1. Report No.	2.	3. Recipient's Catalog No.
FHWA-RD-94-151	PB95-231452	

4. Title and Subtitle	5. Report Date
FINITE ELEMENT MODEL OF A SMALL AUTOMOBILE IMPACTING A RIGID POLE	June 1995
	6. Performing Organization Code
7. Author(s) Emmanual Cofie	8. Performing Organization Report No.
9. Performing Organization Name and Address Turner-Fairbank Highway Research Center 6300 Georgetown Pike McLean, Virginia 22101-2296	10. Work Unit No. (TRAIS) 3A5I
	11. Contract or Grant No. NHI GRF Project #93-31
12. Sponsoring Agency Name and Address Office of Safety and Traffic Operations R&D Federal Highway Administration 6300 Georgetown Pike McLean, Virginia 22101-2296	13. Type of Report and Period Covered Final Report June 1993 - July 1994
	14. Sponsoring Agency Code

15. Supplementary Notes

16. Abstract

A finite element simulation of a small automobile impacting a rigid instrumented pole using the nonlinear finite element code DYNA3D is presented in this report. The vehicle model was based on a 1989 Ford Festiva, a member of the 820C class of vehicles defined in NCHRP Report 350. The Ford Festiva is a good representative of the 820C class based on FOIL tests of three different 820C vehicles. The model consists of beam, shell, and solid elements. The objective of this report was to develop a computationally efficient finite-element model using as few elements as possible, that can be analyzed "overnight", without unduly sacrificing the accuracy of the results. Nodes were merged at junctions where parts met. Contact surfaces were defined between parts of the model where contacts was anticipated during the impact. The rigid pole was modeled as a hollow semicircle of solid elements with a very large mass. Three impact scenarios were anlyzed for this study: (1) centerline impact, (2) left-of-centerline impact (strongest spot), and (3) right-of-centerline impact (weakest spot). Accelerations, velocities, and displacements at the center of gravity of the vehicle and reaction forces on the rigid pole of the finite element model are plotted. Results of the centerline impact are compared with full-scale test results. These finite element analysis results indicate that computationally accurate results can be obtained with a relatively simple vehicle model for the test conditions under consideration.

17. Key Words	18. Distribution Statement
820C, simulation, finite element model, accelerations, velocities, displacements, rigid pole force, centerline, left-of-centerline, right-of-centerline, INGRID, TRUEGRID, TAURUS, DYNA3D.	No restrictions. This document is available to the public through the National Technical Information Service, 5385 Port Royal Road, Springfield, Virginia 22161.

19. Security Classif. (of this report)	20. Security Classif. (of this page)	21. No. of Pages	22. Price
Unclassified	Unclassified	91	

Form DOT F 1700.7 (8-72)
(PF V2.1, 12/13/93)

SI* (MODERN METRIC) CONVERSION FACTORS

APPROXIMATE CONVERSIONS TO SI UNITS

Symbol	When You Know	Multiply By	To Find	Symbol
		LENGTH		
in	inches	25.4	millimeters	mm
ft	feet	0.305	meters	m
yd	yards	0.914	meters	m
mi	miles	1.61	kilometers	km
		AREA		
in^2	square inches	645.2	square millimeters	mm^2
ft^2	square feet	0.093	square meters	m^2
yd^2	square yards	0.836	square meters	m^2
ac	acres	0.405	hectares	ha
mi^2	square miles	2.59	square kilometers	km^2
		VOLUME		
fl oz	fluid ounces	29.57	milliliters	mL
gal	gallons	3.785	liters	L
ft^3	cubic feet	0.028	cubic meters	m^3
yd^3	cubic yards	0.765	cubic meters	m^3

NOTE: Volumes greater than 1000 l shall be shown in m^3.

Symbol	When You Know	Multiply By	To Find	Symbol
		MASS		
oz	ounces	28.35	grams	g
lb	pounds	0.454	kilograms	kg
T	short tons (2000 lb)	0.907	megagrams (or "metric ton")	Mg (or "t")
		TEMPERATURE (exact)		
°F	Fahrenheit temperature	5(F-32)/9 or (F-32)/1.8	Celcius temperature	°C
		ILLUMINATION		
fc	foot-candles	10.76	lux	lx
fl	foot-Lamberts	3.426	candela/m^2	cd/m^2
		FORCE and PRESSURE or STRESS		
lbf	poundforce	4.45	newtons	N
lbf/in^2	poundforce per square inch	6.89	kilopascals	kPa

APPROXIMATE CONVERSIONS FROM SI UNITS

Symbol	When You Know	Multiply By	To Find	Symbol
		LENGTH		
mm	millimeters	0.039	inches	in
m	meters	3.28	feet	ft
m	meters	1.09	yards	yd
km	kilometers	0.621	miles	mi
		AREA		
mm^2	square millimeters	0.0016	square inches	in^2
m^2	square meters	10.764	square feet	ft^2
m^2	square meters	1.195	square yards	yd^2
ha	hectares	2.47	acres	ac
km^2	square kilometers	0.386	square miles	mi^2
		VOLUME		
mL	milliliters	0.034	fluid ounces	fl oz
L	liters	0.264	gallons	gal
m^3	cubic meters	35.71	cubic feet	ft^3
m^3	cubic meters	1.307	cubic yards	yd^3
		MASS		
g	grams	0.035	ounces	oz
kg	kilograms	2.202	pounds	lb
Mg (or "t")	megagrams (or "metric ton")	1.103	short tons (2000 lb)	T
		TEMPERATURE (exact)		
°C	Celcius temperature	1.8C + 32	Fahrenheit temperature	°F
		ILLUMINATION		
lx	lux	0.0929	foot-candles	fc
cd/m^2	candela/m^2	0.2919	foot-Lamberts	fl
		FORCE and PRESSURE or STRESS		
N	newtons	0.225	poundforce	lbf
kPa	kilopascals	0.145	poundforce per square inch	lbf/in^2

* SI is the symbol for the International System of Units. Appropriate rounding should be made to comply with Section 4 of ASTM E380.

(Revised September 1993)

TABLE OF CONTENTS

LIST OF FIGURES

LIST OF TABLES

CHAPTER 1. INTRODUCTION

The past few decades have seen a major effort on the part of the Federal Highway Administration (FHWA), highway designers, and researchers to improve the crash performance of highway safety hardware. The design of roadside safety hardware has been based largely on empirical data, a limited number of full-scale crash tests, and, in some cases, analysis results based on crash simulation computer codes developed for a specific impact scenario. Full-scale crash tests provide only limited information on the specific test conducted, and can be very expensive, very elaborate, and time consuming, making it less attractive for parametric studies. Various special-purpose computer codes for analyzing the dynamics of a vehicle during impact have been developed in the past. BARRIER VII, developed for FHWA to evaluate automobile barrier systems, uses a two-dimensional mathematical model to simulate the behavior of an automobile striking a deformable barrier.(1) The vehicle was represented as a planar body surrounded by inelastic springs and the barrier was idealized as a collection of beams, cables, posts, springs, and dampers. GUARD, another program developed for FHWA for guardrail impact simulations, relied on a three-dimensional force-displacement mathematical representation of the barrier and vehicle.(2) Motions at node points were divided into two categories: primary nodal motions, which were independent, and secondary nodal motions, which were dependent on the motion at the primary nodes. This approach allowed for proper modeling of connection details. Because of the lack of large storage and high computing speed, most of these earlier computer codes relied on simplifying assumptions such as lumped mass parameters and the use of beams instead of plates in the code development. These simplifications tended to limit these programs to relatively simple cases. The availability of high-speed large-storage computers, coupled with the development of nonlinear dynamic three-dimensional finite element codes such as DYNA3D, have made it possible to capture these detailed nonlinear deformation modes and have resulted in an increased use of finite element models to analyze the behavior of vehicles during collisions into roadside structures.(3,4)

FHWA is funding research studies into the use of general-purpose finite element codes in predicting the behavior of vehicles during impacts with roadside safety hardware.(5) It is within this framework and those of other ongoing crash studies that this investigation was conducted. The primary focus of this research was to investigate the feasibility and reliability of using simplified finite element models that can be analyzed "overnight" on a workstation to study the behavior of vehicles during impacts into roadside structures. One indirect benefit of this study was that it helped in exploring the full capabilities and potential benefits of using the DYNA3D nonlinear finite element code.

A 1989 Ford Festiva was used as the basis for this finite element model; partly because it is representative of the 820C class of vehicles specified in NCHRP Report 350 and partly because full-scale test data on centerline impacts were available for three similar Ford Festivas for comparison and validation studies.(6) The development of the finite element model, the element and material types, the contact surface definitions, and the modeling strategies and techniques used are all described. Results from the nonlinear finite element analysis program DYNA3D are presented for three different rigid pole impact cases: (1) a centerline impact, (2) a left-of-centerline impact, and (3) a right-of-centerline impact. Comparisons between the finite element results and those from full-scale tests for the centerline impact are presented and discussed.[7] This model was tested for only frontal impacts.

CHAPTER 2. FINITE ELEMENT MODEL

GEOMETRIC MODEL

Since an accurate representation of the finite element model of the vehicle is a crucial part of a roadside safety hardware finite element analysis, careful considerations were given to the following three factors:

1. Structural and functional members - Parts that were considered critical to structure were represented in greater detail in the model. This consisted of mainly structural (load-bearing) components in the front of the car. Non-structural members (non-load-bearing) were excluded from the model or included in a coarse form to keep the model as simple as possible.

2. Contact surfaces - The sequence of events that takes place during an impact, coupled with the complex geometry and nonlinear deformation and material behavior, make it important to identify and define all surfaces that will come in contact during the impact event. The proper identification of contacting surfaces is based on intuition, on viewing films of full-scale tests, and on observing the performance of the simulations.

3. Kinematic constraints - Specified kinematic constraints, such as part connections and boundary constraints, matched the kind of kinematic constraint that existed in the actual structure. All nodes had six degrees of freedom.

The model was developed using the INGRID preprocessor to the DYNA3D analysis program, but was later converted to the TRUEGRID preprocessor, an updated commercial version of INGRID.[8,9] The coordinate system used for this model is the right-handed system. The vehicle model consists of 28 parts, 4295 nodes, 60 beams, 2898 shell elements, and 633 solid elements. The following assumptions were made in the development of this model:

- Only structural components of the vehicle considered to be part of the load path in a frontal collision were modeled.

- Dimensions and shapes used in this model were based on physical measurements taken on a 1989 Ford Festiva used at the Federal Outdoor Impact Laboratory (FOIL).

- The mass of the various parts of the model was distributed in a manner as to ensure that the center of mass of the model approximately agreed with the actual 1992 Ford Festiva measured at the FOIL. No effort was made to match the mass moments of inertia.

- Parts were generally joined by merging adjacent nodes. Tied contact surface definitions were used to merge parts with incompatible meshes.

- The suspension system was modeled using beams elements.
- Shell element aspect ratios were generally kept below four.

MODEL DESCRIPTION

The model (1989 Ford Festiva) was 3510 mm long, 1420 mm high, and 1500 mm wide. The major components of the finite element model together with the element and material types used to model them are shown in table 1.

The bumper and lower core supports were both constructed with shell elements and shaped into a box section. The bumper consisted of a front, back, top, and bottom plate, each with a thickness of 1.54 mm. The top of the bumper was located 520 mm above the ground. The lower core support also consisted of a front, back, top, and bottom plate, also with a thickness of 1.54 mm. The bottom of the lower core support was located 241 mm above the ground. The bumper and lower core support were supported by a left and right frame horn. The frame horns, also box-shaped sections, were constructed from shell elements and were merged to the bumper and lower core support at its front end. All parts, except for the lower core support, are shown in figure 1. The back of the frame horns were merged to the firewall. The left and right fenders were modeled with shell elements, each consisting of an inner and outer fender wall. The inner fender walls were attached to the outer walls of the frame horns with a tied-node contact surface as shown in figure 2.

The radiator was mounted on the lower core support. It was modeled using solid elements. The evaporator core, also modeled with solid elements, was merged to the back of the radiator. Figure 3 shows the radiator supported on the lower core support.

The engine block was modeled using solid elements. It consisted of two parts – the transmission and the engine. The total mass of the engine block was 170 kg. The engine block was supported by front, back, and right side engine mounts. The engine mounts were modeled with shell elements and merged to the engine. The other ends of the front and back engine mounts were supported on the engine cradle and the right side mount was attached to the frame horn. The engine cradle was modeled as shell elements and merged at the front to the lower core support and at the back to the firewall. Figure 4 shows the engine block with the engine mounts and the engine cradle.

The wheel system, comprising the tires and rims, were modeled as solid elements and merged to the front and back axles that were modeled as beam elements. The front wheels were connected to the engine block with tied rod beams. The wheels were attached to the main body using front and back shock absorbers modeled as beam elements. The lower crossbar was modeled as beam elements and located behind the lower core support. Figure 5 shows a view of the lower crossbar, the engine block, the front wheels, the axle, and the tied rods to the engine block. The front shock absorbers are not shown.

The hood and the main body were modeled with shell elements as shown in figure 6. The hood was merged to the main body at only three nodes – two back nodes and a front node that represented the latch. Figure 7 is a view of the underside of the model showing the engine cradle and its attachment point to the lower core support and firewall, the tires, the rims, and the floor pan.

Table 1. Major components of finite element model.

Components	Element type	Material type
Bumper	Shell	Elastic-plastic
Lower core support	Shell	Elastic-plastic
Frame horns	Shell	Elastic-plastic
Fenders	Shell	Elastic-plastic
Radiator and evaporator core	Solid	Elastic-plastic
Engine block	Solid	Elastic
Engine mounts	Shell	Elastic-plastic
Engine cradle	Shell	Elastic-plastic
Firewall	Shell	Elastic-plastic
Tires and rims	Solid	Elastic
Main body	Shell	Elastic
Windscreen/windows	Shell	Elastic
Hood and front strip	Shell	Elastic-plastic
Front and back axles	Beam	Elastic-plastic
Lower crossbar	Beam	Elastic-plastic
Shock absorbers	Beam	Elastic
Floor pan brackets	Beam	Elastic

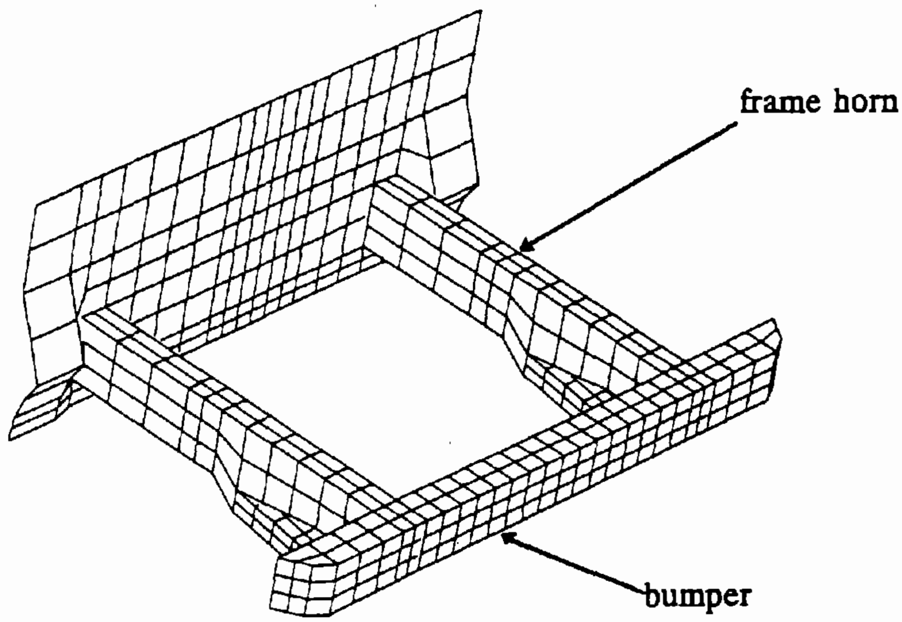

Figure 1. Bumper, lower core support, and frame horn.

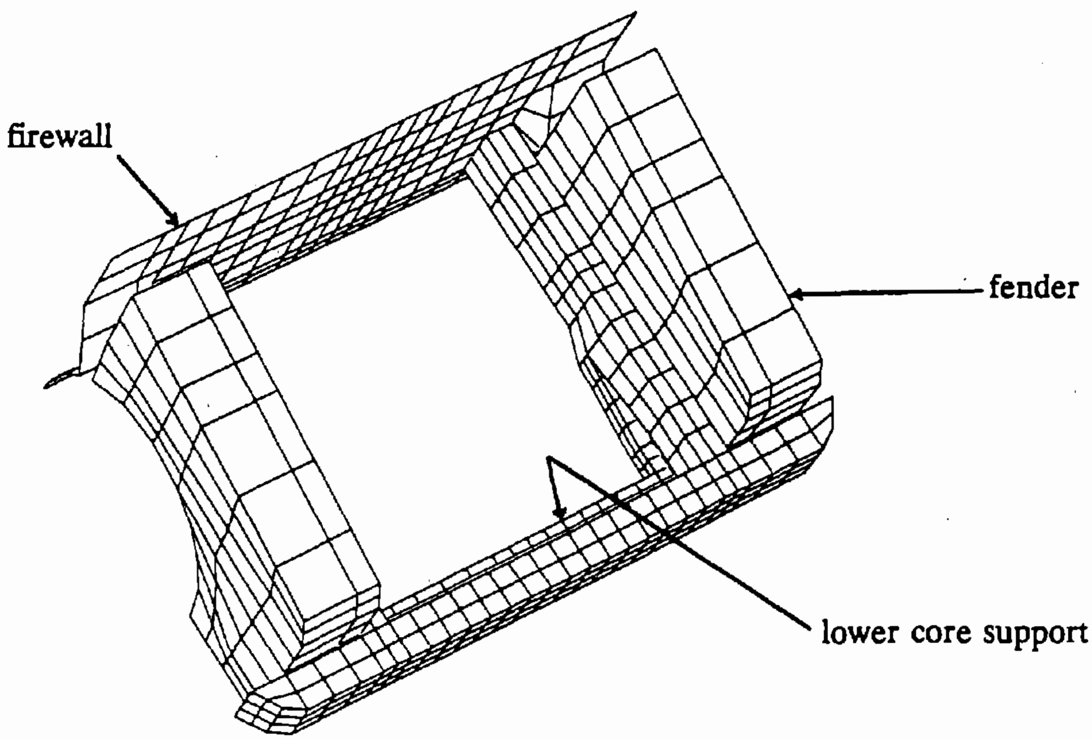

Figure 2. Fender, frame horn, and firewall.

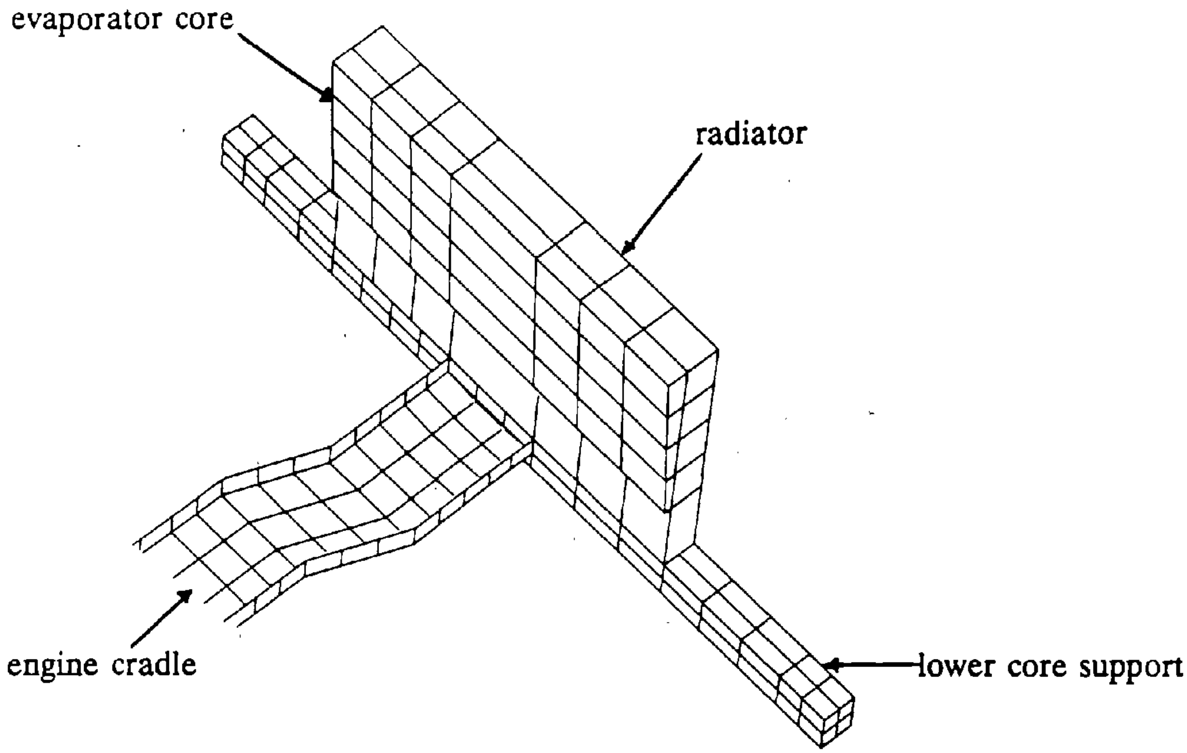

Figure 3. Radiator and evaporator core.

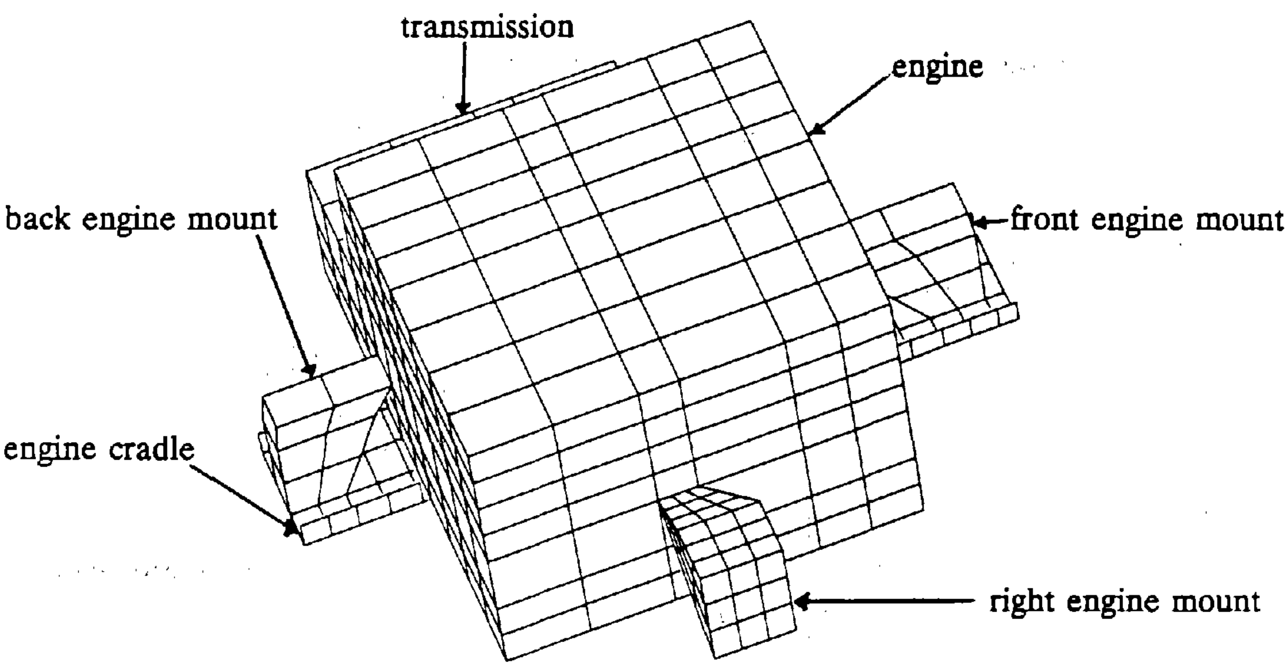

Figure 4. Engine block with engine mounts.

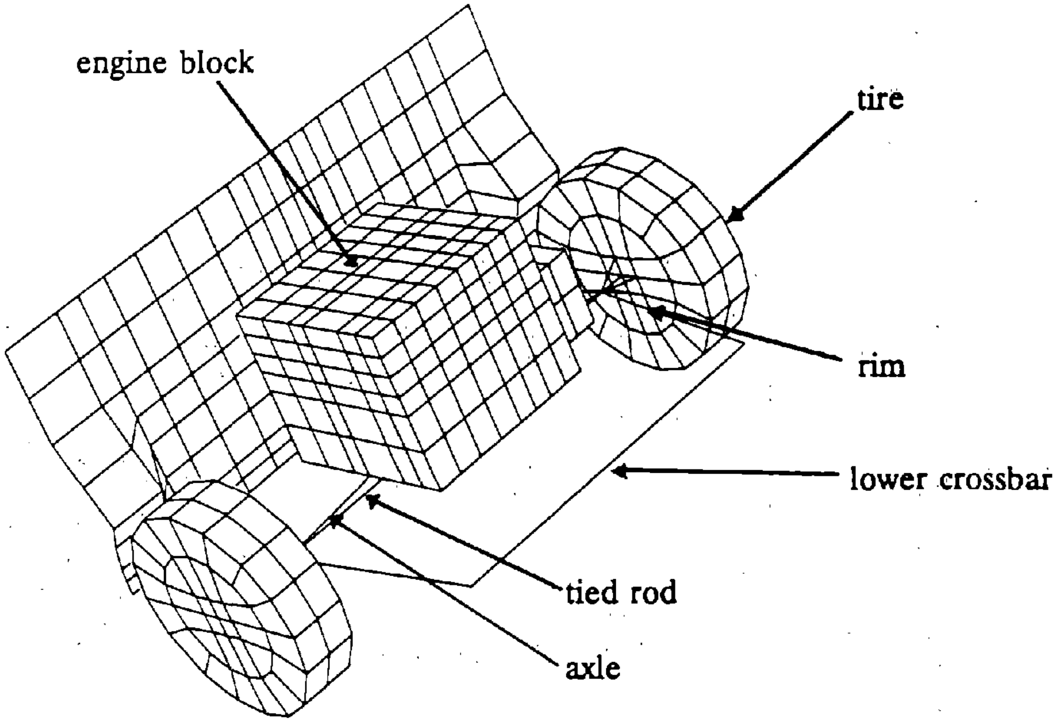

Figure 5. Wheels, lower crossbar, and axle attachment.

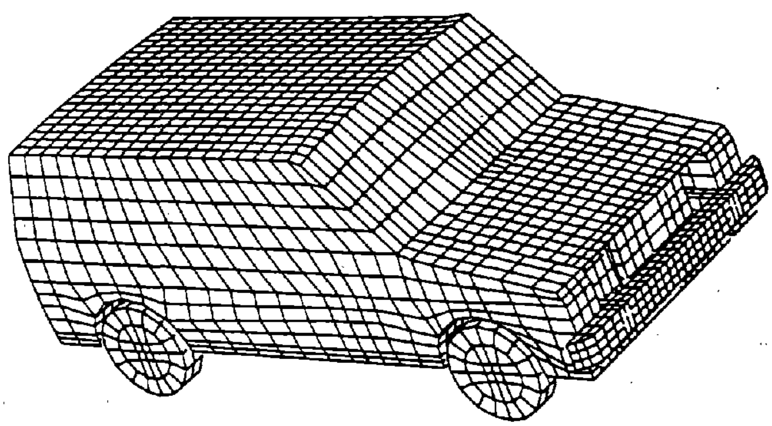

Figure 6. Full view of vehicle.

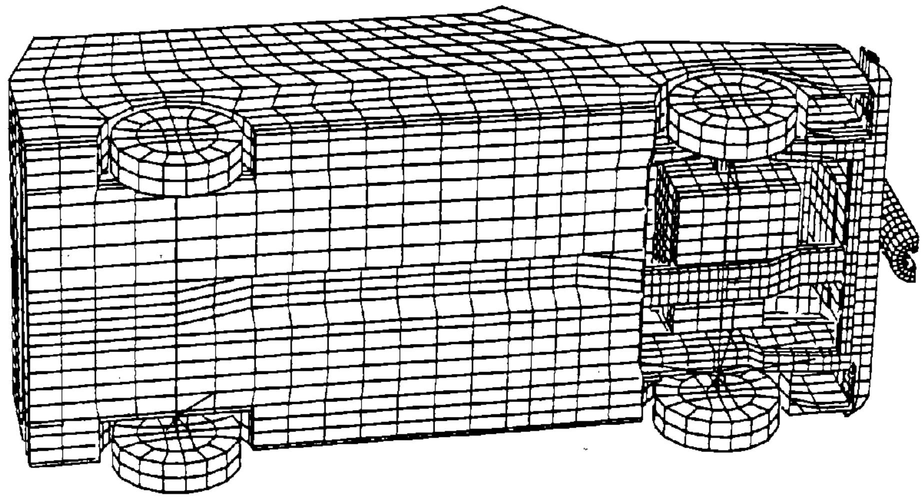

Figure 7. View from below the vehicle.

Table 2. Summary of geometric properties for 1989 Ford Festiva.

Property	Measurement			
	Model	91F049	92F032	92F033
Total mass (kg)	820	817	817	817
Mass of engine block (kg)	170			
Dimensions (mm)				
Wheelbase	2300	2300	2261	2261
Track width	1350	1350		
Overall length	3510	3510		
Overall width	1500	1500		
Height of bumper above ground	381	381		
Center of mass (mm)				
Aft of front axle (x-direction)	850	831	831	856
Above ground (z-direction)	560	577	564	533

The center of gravity of the vehicle model was located in space inside the occupant compartment and did not coincide with any physical part of the model. To gather acceleration, velocity, and displacement data from the location on the finite element model corresponding to the full-scale test, a solid box representing the accelerometer mounting bracket was rigidly merged to the floor near the center of gravity.

To allow for easy modification and changes to the finite element model, most of the dimensions and properties were defined in terms of parameters. The TRUEGRID input data for the finite element model is included in appendix A. All thicknesses of the sheet metals were based on actual measurements taken on the Ford Festiva. A summary of mass and geometric properties of the vehicle is shown in table 2.

MATERIAL PROPERTIES DESCRIPTION

All materials in front of the firewall, except the engine block, tires rims, and shock absorbers, were defined as elastic-plastic material (material type 3) to allow for inelastic deformation.[3] Yield stresses and mechanical properties were obtained from published data. All parts behind the firewall, including the tires, axles, rims, and shock absorbers, were modeled as linear elastic materials (type 1) since no inelastic deformations were expected.

The engine block had the mechanical properties of steel, the tires had the mechanical properties of rubber, and the radiator had the mechanical properties of aluminum. All shell elements, with the exception of the windshield and windows, had the mechanical properties of sheet steel. The thickness of most of the sheet metal body parts was 1.54 mm. The windows and windshield had the mechanical properties of glass. All beams used had the mechanical properties of steel.[10] Table 3 shows the material type and the materials used for the various parts of the model. Since the major load-bearing and energy-dissipating components were made of steel, only the mechanical properties of the sheet steel, as published in the American Iron and Steel Institute (AISI) Automobile Steel Design Manual and used in the finite element model, are shown in table 4.[11]

Table 3. Part name and material description.

Part Name	Material	Material type
Bumper, frame horn, cradle, fender, hood, lower core support, engine mount	Sheet metal (steel)	
Radiator	Aluminum	3
Lower crossbar	Steel rod	
Firewall, back body	Sheet metal (steel)	
Windscreen & windows	Glass	1
Tires	Rubber	
Rims, axles, shock absorbers, engine block	Steel	

Table 4. Mechanical properties of steel.

Modulus of elasticity	= 200 GPa	Poisson's ratio	= 0.30
Tangent modulus	= 200 MPa	Density	= 7.9 $kN \cdot s/m^4$
Yield stress	= 207 MPa	Hardening type	kinematic

CONTACT SURFACE DEFINITIONS

Contacting surfaces were identified by defining sets of nodes on one or more master and slave surfaces.[8,9] The position of nodes on the slave surface are checked against the positions of the nodes on the master surface at each time step during the analysis. A total of 26 different contact surfaces consisting of slideline type 3 (sliding-with-void), slideline type 4 (self-contacting), and slideline type 6 (tied-nodes) were used. The bumper contact with the rigid pole is an example of a sliding-with-voids (type 3) contact. Self-contacting surfaces were used when the surfaces on the same part were expected to collapse upon themselves due to local buckling or folding deformations. Crushing the bumper so the inside of the front flange touches the inside of the back flange is an example of this type of contact. Tied-node contact surfaces were particularly useful in tying together surfaces with incompatible meshes that would be difficult to join by merging nodes. The frame horn and the inner fender were examples of parts joined using a tied-node contact surface. To keep computational time for the contact surface algorithm at a minimum, only nodes on the surface of parts expected to make contact were placed on the contact surface. For example, only the middle half of the front surface of the bumper was placed on the contact surface with the rigid pole for a centerline impact. The tires were placed on a horizontal contact surface with friction to provide frictional effects with the ground. Table 5 is a summary of the contact surface definitions used in the model.

MODELING TECHNIQUES AND GUIDELINES

Due to the complex geometric shape of the vehicle, the fact that many parts were eliminated, coupled with the fact that DYNA3D does not generate any detailed error messages, the following special techniques and strategies were used to locate and distribute part masses, merge parts, and check the soundness of the model:

- Engine Compartment: The proper location of parts, particularly those in the engine compartment, influences the overall impact response of the model during a frontal impact. The engine block accounts for about one-fifth of the total mass of the vehicle and thus one-fifth of the initial kinetic energy of the vehicle. The engine, therefore, has to be accurately placed and correctly supported to produce the correct force-time or force-displacement response. Ford Festivas have three engine mounts that are made of thin-walled metal brackets attached to the engine. Because of the complexity and importance of the engine mounts, a number of modeling approaches have been tried.

Table 5. Contact surface definitions

Contact surface	Type	Slave	Master
1	3	bumper, fender, engine cradle, lower core support	rigid pole
2	3	radiator, fender	bumper
3	3	engine, front engine mount	radiator, evaporator core
4	3	engine, back engine mount	firewall
5	3	radiator, engine	hood
6, 8	3	left frame horn, left fender	engine, radiator
7, 9	3	right frame horn, right fender	engine, radiator
10	3	engine	engine cradle
11	4	bumper	
12	4	lower core support	
13	4	left frame horn	
14	4	right frame horn	
15	6	left frame horn	left fender
16	6	right frame horn	right fender
17	6	accelerometer box	floor
18	3	left frame horn	front left tire
19	3	right frame horn	front right tire
20	4	hood	
21	3	tires	ground
22	4	engine cradle	
23	3	left fender	front tire
24	3	right fender	front tire
25	4	left fender	
26	4	right fender	
27	4	front engine mount	
28	4	back engine mount	

Beams, truss, and shell elements were all considered during the preliminary stages. Each of these had its own unique difficulties. Beams tended to introduce high local stresses at the point where the mounts were attached to the engine cradle. Beams were generally difficult to define on contact surfaces, so modeling the interactions between the cradle, the engine block, the inner fender, and the three mounts was difficult. Beams tended to make the response too stiff, resulting in too little deformation. Truss elements, in addition to allowing large rotational motion of the engine block, also imposed high localized stresses at the point where they were attached to the cradle and the fender. Shell elements were found to be most reliable and were used in the final model. Contact surfaces were easily defined using shell elements. Although shell elements of steel produced acceptable response results, the proper modeling of the engine mounts is an area that deserves additional efforts in the future.

- Vehicle Mass: The proper mass distribution of the model (or location of the overall center of gravity) was obtained using two approaches: (1) the true total mass was assigned using the "tmm" command or (2) the density that resulted in the correct mass was assigned to a particular material. To account for the rear and front seats (not modeled), the mass of the floor was increased by increasing its thickness. It must, however, be pointed out that when assigning part masses, one must keep in mind that the overall center of gravity of the model must reasonably match that of the actual vehicle being modeled. No effort was made in matching the mass moments of inertia of the model to that of the actual vehicle.

- Merging of Parts: An appropriate tolerance must be defined to ensure the correct merging of parts. Nodes that were within this tolerance were combined as one node. Adjacent parts thus share nodes ensuring the continuity of the connection between the parts. Each group of parts was carefully examined to ensure that the correct nodes merged. A tolerance of 2 mm was used throughout the model.

CHAPTER 3. FINITE ELEMENT ANALYSIS

SIMULATION

The finite element model of the 820C vehicle was designed to simulate an impact into a 218-mm-diameter rigid pole at a zero-degree impact angle, and a 8940-mm/s (32-km/h) impact velocity. Three rigid pole impact scenarios were simulated: a centerline impact, a 254-mm offset to the right of the centerline (weak spot) impact, and a 457-mm offset to the left of the centerline (strong spot) impact. The finite element analysis results were compared with full-scale test results for the centerline impact only. The finite element analysis results for the two off-center impacts were not compared with test data since no test data were available at the time of the test report.

The total impact simulation time for all three test was 120 ms. This allowed the vehicle to strike the pole, reach its maximum deformation, rebound from the pole, and then lose contact. Plot states were collected at 2-ms intervals and the time history data were collected at 0.5-ms intervals.

RIGID POLE FORCES

The rigid pole was modeled as a hollow semicircle of solid elements. Because reaction forces cannot be directly calculated during the DYNA3D analysis, two indirect approaches were used to obtain reaction forces on the rigid pole.

In the first approach, the pole is given a relatively large mass compared to that of the vehicle and is restrained from displacement in all but the longitudinal direction (of impact). If the relative displacement of the pole in the direction of motion is very small compared to the total deformation of the vehicle (i.e., below 1 mm), the pole may still be considered "rigid" (i.e., not deforming). In this case, the acceleration of the pole multiplied by the mass of the pole can be assumed to be approximately equal to the impact force acting on the rigid pole. Thus, the force acting on the pole, F_x , shown in figure 8, can be found directly from Newton's second law:

$$F_x = ma_x \tag{1}$$

where m is the total mass of the pole and a_x is the acceleration of the pole in the longitudinal direction.

The second approach relies on the interface force features of DYNA3D. Interface forces can be written to a file during an analysis and then examined with the TAURUS post-processor.[12] From equilibrium considerations, the sum of interface forces on the vertical face of the pole equals the reaction force on the pole. Clearly, the sum of the interface forces should equal the pole impact force calculated in the earlier approach.

Preceding Page Blank

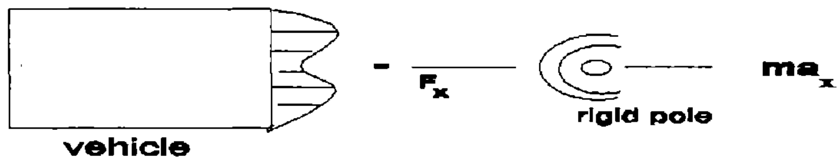

Figure 8. Free-body diagram of forces on rigid pole.

CENTERLINE IMPACT

Figures 9 through 11 show plots of the deformed shape at various times during the event. In order to get a good view of the engine compartment, the hood was removed from the plots although the hood is present in the simulations. Figure 9 is a top view of the deformed shape of the vehicle between 0.0 and 120.0 ms. At 1.0 ms into the impact, the vehicle bumper first makes contact with the rigid pole. At this point, the only part of the vehicle resisting the impact is the bumper. At about 20.0 ms into the impact, the rigid pole first makes contact with the lower core support and the bumper contacts the radiator. At 40.0 ms, the engine cradle starts to buckle and the back face of the evaporator core makes contact with the front face of the engine block, crushing the front engine mount between the radiator face and the engine block. The acceleration continues to increase until 70.0 ms, when the back engine mount yields and the engine block makes contact with the firewall. During this time, the evaporator core, radiator, bumper, lower core support, and pole are all in contact with the engine block and all components in the engine compartment, including the firewall, are involved in the impact. Kinetic energy of impact has been transferred to plastic strain energy and subsequently into heat energy through the buckling and local deformation of the engine cradle, engine mounts, frame horns, bumper, radiator, and fenders. At 90.0 ms, most of the kinetic energy in the system has been expended and the vehicle begins to rebound from the rigid pole due to residual elastic strain energy "stored" in the deformed parts. Figure 10 is a view from below the vehicle, showing the deformed states of the engine cradle during the impact. The cradle first makes contact with the bottom of the engine block, then later buckles, causing the front engine mount to deform downward, resulting in pitching of the vehicle. Figure 11 is a deformation plot from a side view of the vehicle with the hood included between 0.0 ms and 120.0 ms.

The centerline impact simulation results were compared with actual full-scale crash-test results. Crash-test accelerations were collected, and velocities and displacements were calculated at the center of gravity (CG) of the vehicle. During the test, impact forces were also collected at the rigid pole. Since the CG may not necessarily coincide with a specific node, the average results of several nodes on a box around the vicinity of the CG of the model were gathered for time-history plots of the simulated vehicle. The test data used for the comparisons were obtained from tests performed at the FOIL between 1992 and 1993.

Figure 12 is the plot of the acceleration in g's (gravity) versus time for full-scale crash tests 91F049, 92F032, 92F033, and the simulation. All three tests were performed with identical vehicles and impact conditions.[6] The simulation results generally corresponded reasonably well with the three tests. The initial stages of the impact were very noisy as evidenced by the fluctuations in the accelerations in the three tests. Figure 13 is a plot of the average accelerations from the three tests and the CG acceleration from the simulation. The peak acceleration from the simulation (35 g's) was within 5 percent of the average peak acceleration reported in the three tests. Averaging the three test accelerations dampens the noise in the earlier part of the event and removes the variability between tests. The shape of the simulation curve agrees reasonably well with that of the average acceleration. The first peak on figure 13, at 20.0 ms, corresponds to the time when the bumper, radiator, and lower core support first compress together in contact with the rigid pole (see figure 10 for the deformed shape). At this point during the impact, very little deformation takes place in the engine compartment. The second peak occurs at around 40.0 ms into the event, when the evaporator core first makes contact with the engine block. The next peak, at about 70.0 ms, corresponds to the time when contact is first made between the engine and the firewall, as shown in figure 9. At this time, the vehicle starts to reverse direction and begins to move away from the pole.

The whole impact can be divided into three stages. The first stage was from the beginning of the impact to the time when the bumper contacted the radiator and lower core support. This part was referred to as the "external impact stage" because very little deformation took place in the engine compartment. The component most deformed in the impact at this point (the bumper) was external to the vehicle. The second stage was referred to as the "internal impact stage" because most of the components involved in the impact at this point were internal to the vehicle (located in the engine compartment) as shown in figure 9. The third and final stage, termed the "rebound stage," described the event from the end of the internal stage, when the vehicle began to recoil to the time when the vehicle came to a rest.

Figure 14 is a plot of the displacement versus time for both the simulation and the three test cases. The displacement curves of the test and simulation agree very well until the rebound occurs. The maximum displacement of the event is within 8 percent of those recorded in the test. From the displacement plot, one observes that the displacement curve is linear during the initial stages of impact. Figure 15 is the combined plot of the average test and simulated acceleration and displacement at the CG of the vehicle versus time. The maximum displacement occurs at approximately the same time as the peak acceleration was reached. The vehicle begins to recoil around the time it reaches its peak acceleration as is evident in figure 15.

Figure 16 is a plot of the velocity versus time for the three tests cases and the finite element simulation. Again, there is reasonable agreement between the simulation and test results. The variations in the curves toward the end of the event may be due to a number of possible factors, e.g., in the actual test, the weight of the vehicle and the attendant friction between the tires and the ground provides resistance to the motion of the vehicle during the rebound. Whereas for the simulation, gravity is not applied, which results in no resisting force on the finite element model during its rebounding phase. During the initial stages of the impact, the variation between the curves (test data versus simulation) are again noticeable. The reason for this variation is not well understood and needs further investigation.

Figure 17 is a plot of the resultant force on the rigid pole versus time for the simulation and tests. The area under the curve is the total impulse of the event. The test results are from load cell readings. The force on the rigid pole for the simulation was obtained by multiplying the acceleration of the rigid pole by the mass of the pole. The maximum simulated pole force is about 220 kN, which is about 15 percent higher than that obtained from the test. The reason for this variation has been fully explained earlier.

The first sharp peak force in figure 17 (at approximately 20 ms) is coincident with initial contact with the edge of the hood. This impact causes an increase in the forces applied to the pole, but stabilizes within a short time. The second sharp peak (at approximately 40 ms) is coincident with the impact with the front face of the engine. From the plot, one observes that the pole force builds up very quickly, remains at or near the peak over a period of time, then decreases, first rapidly and then gradually, towards the end of the event.

Figure 18 shows the plot of the rigid pole force against the velocity. The pole force reaches a maximum when approximately 33 percent of the initial energy in the vehicle has been expended (velocity decreases to 7.5 m/s) and maintains a constant force until 66 percent of the energy of the vehicle is dissipated (velocity decreases to 4.8 m/s). This constant force may be attributed mainly to the resistance provided by the engine mounts and the engine cradle and the deformation of the fenders and frame horns. Figure 19 is a plot of the rigid pole force versus displacements. The area under this curve represents the total work done in the longitudinal direction.

Figure 20 shows the plot of the total energy, the kinetic energy, and the work done on the vehicle due to the impact in the longitudinal direction. There is reasonable agreement between the test results and the simulated results until the end of the impact event, i.e., when rebound of the vehicle initiates at approximately 70 ms. The simulated vehicle does not rebound as much as the actual test vehicles. Also, during the initial stages of the impact, until approximately 15 ms, the simulated results deviated markedly from the test results. During this period of the impact, the kinetic energy actually "goes" positive, indicating a velocity increase in the simulated vehicle.

The deviation at the end of the event may be due to the reasons explained earlier, e.g., the strain hardening modulus of the simulated materials (after yield) may be less than the modulus of the materials in the actual vehicles. The cause for this deviation will be investigated. The increase in kinetic energy of the simulated vehicle during the initial stages of the event may be due to the initial pitching motion of the vehicle. The vertical location of the accelerometers in the test vehicles is not accurately known and, thus, the vertical location in the simulated vehicle is the best approximation possible. It is reasonable to suspect that the accelerometer location in the simulated vehicle may have been slightly higher than the actual test vehicle. Also, because the simulated curve "goes" positive, the location chosen may have been above the center of gravity of the simulated vehicle. If all of this is true, the longitudinal component of the rotary (pitch) acceleration artificially increased and distorted the longitudinal acceleration of the simulated vehicle versus the test vehicles.

One interesting observation from this curve is that the maximum longitudinal work done on both the test and simulated vehicles is approximately 96 percent of the initial kinetic energy at impact. This tends to indicate that little yawing took place in the vehicle and that the overall simulation and test results are reasonable.

The longitudinal changes in velocities, kinetic energy, impulse transferred, and the longitudinal work done on the vehicle at rebound and at the end of impact is shown in table 6. These changes agreed well up until the rebound (70 ms). The changes in velocities, kinetic energy, impulse transferred, and work done was lower for the finite element simulation than for the tests. This may be due to some of the reasons stated earlier.

t = 0 ms

t = 20 ms

t = 40 ms

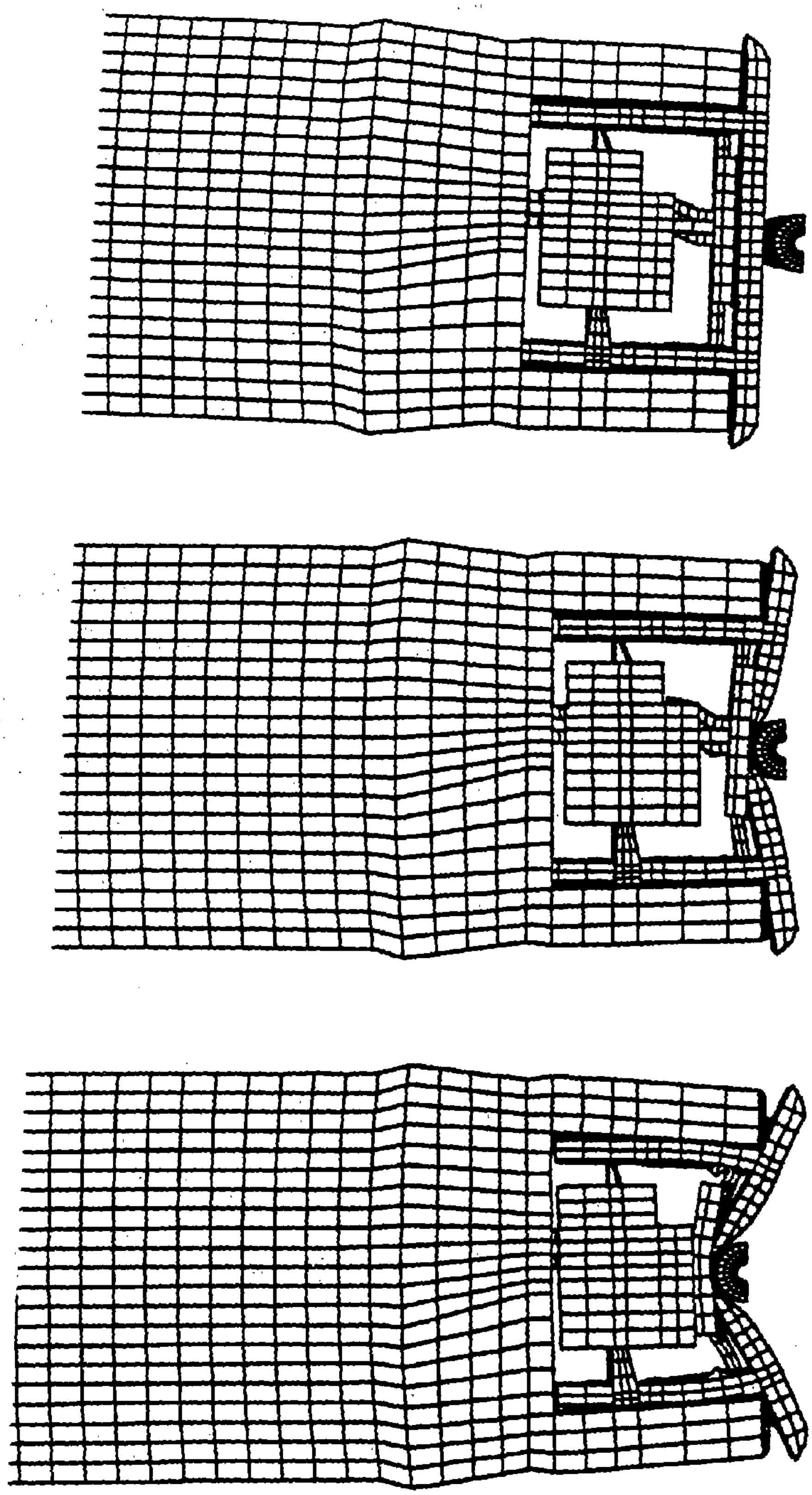

Figure 9. Top view of engine compartment for centerline impact: 0 to 120 ms.

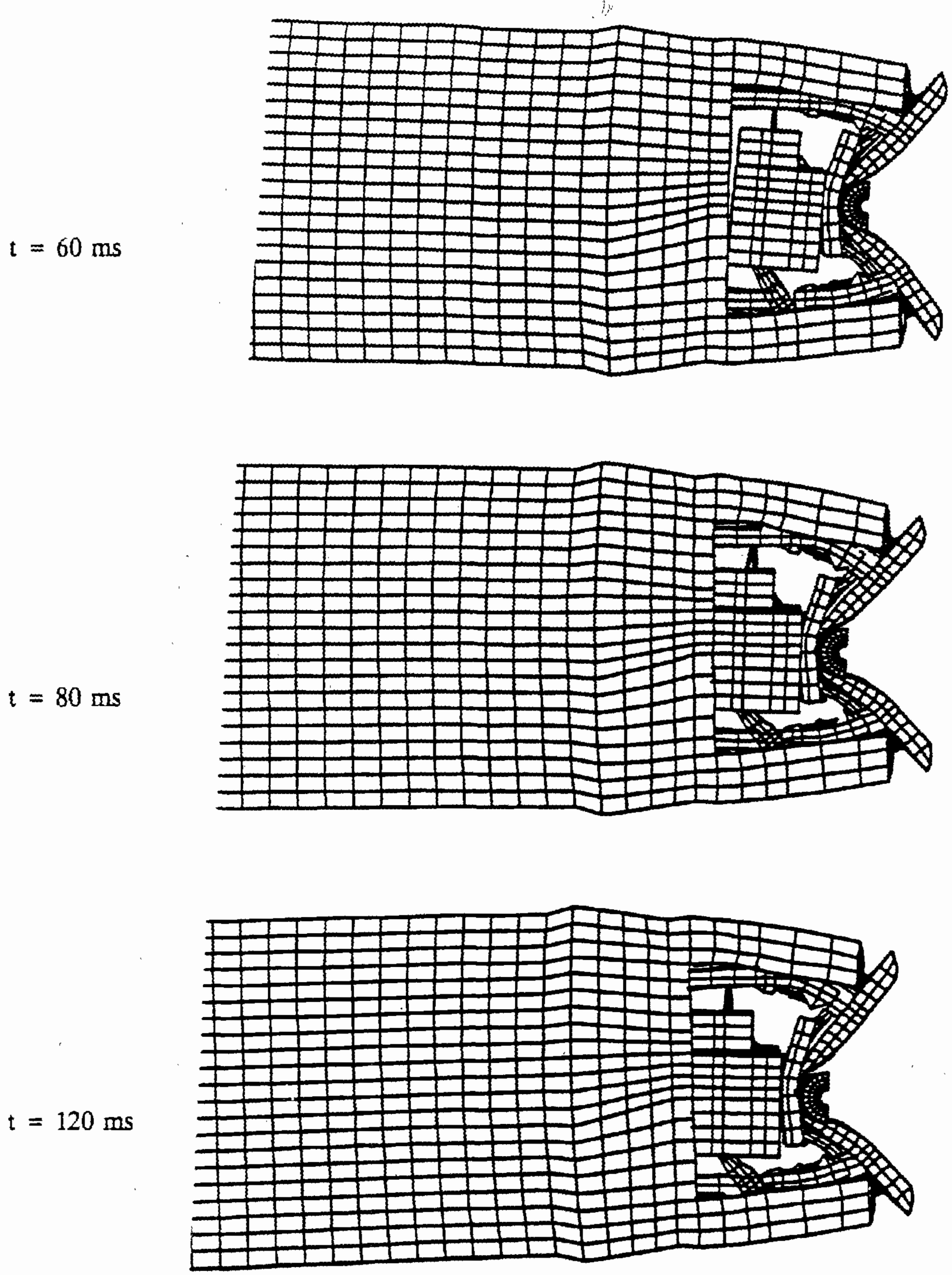

Figure 9. Top view of engine compartment for centerline impact:
0 to 120 ms (continued).

t = 0 ms

t = 20 ms

t = 40 ms

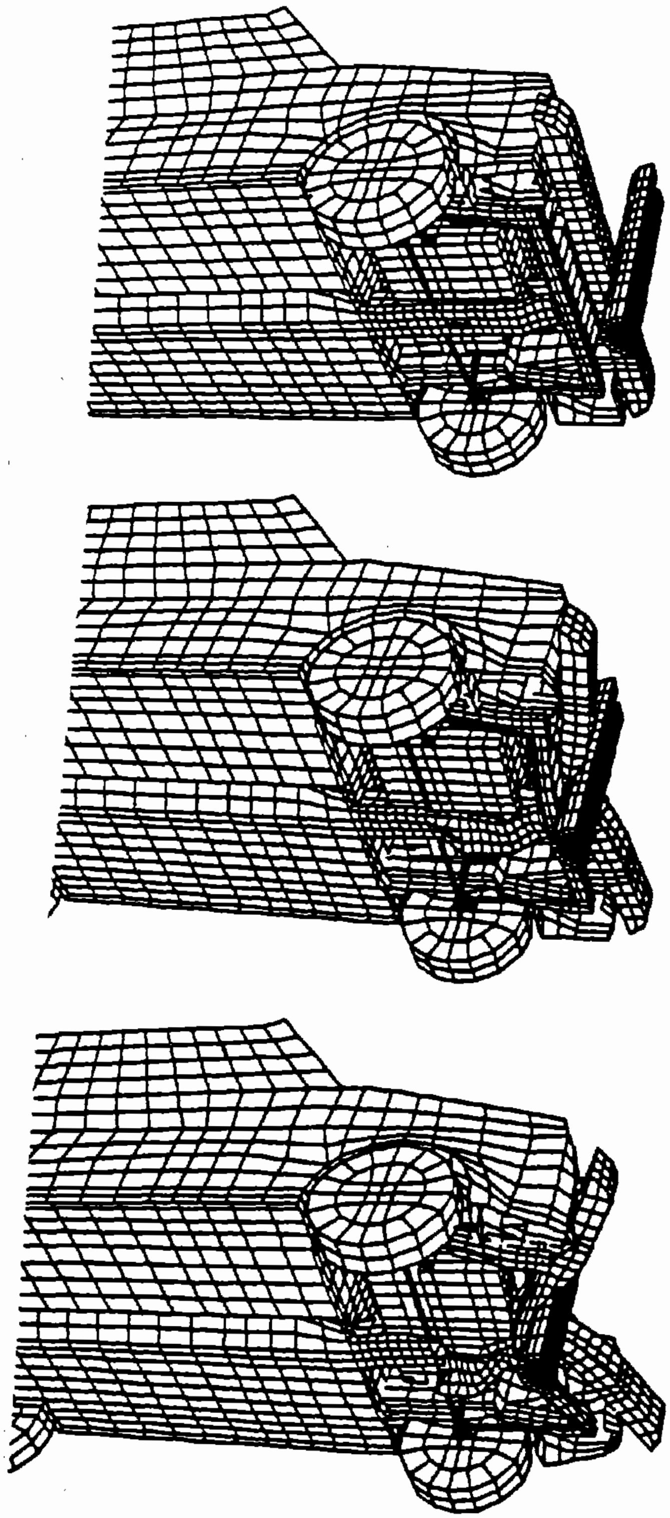

Figure 10. View from below engine compartment for centerline impact: 0 to 120 ms.

t = 60 ms

t = 80 ms

t = 120 ms

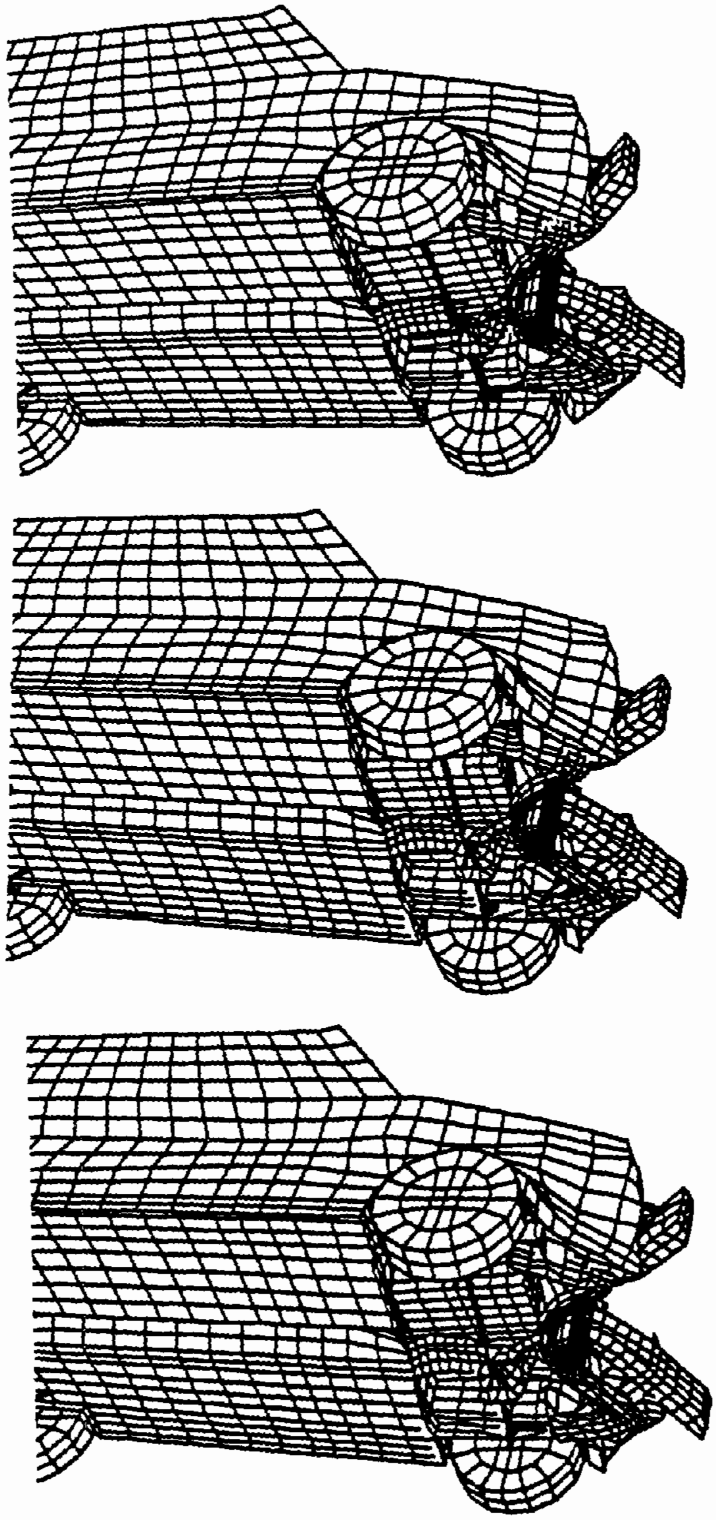

Figure 10. View from below engine compartment for centerline impact: 0 to 120 ms (continued).

t = 0 ms

t = 20 ms

t = 40 ms

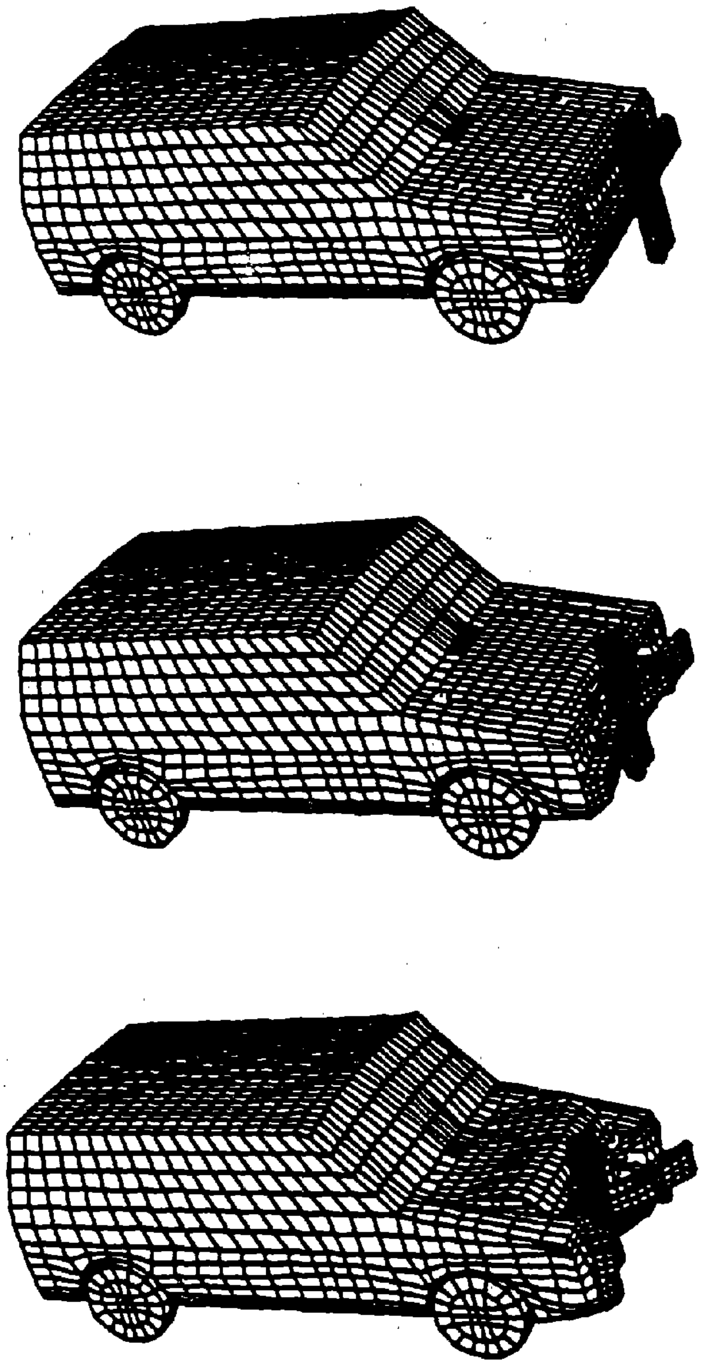

Figure 11. Side view of vehicle for centerline impact: 0 to 120 ms.

t = 60 ms

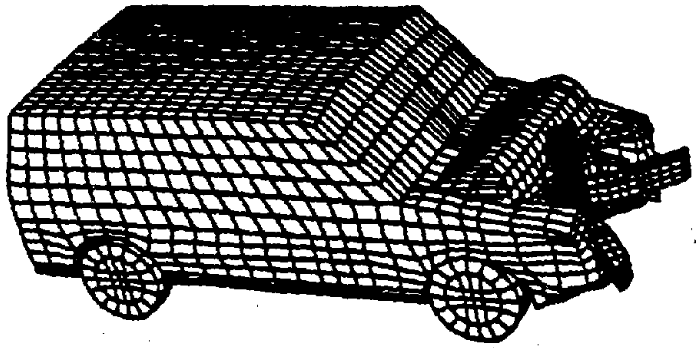

t = 80 ms

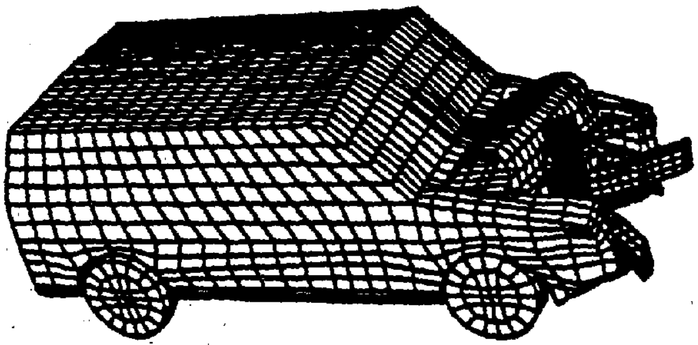

t = 120 ms

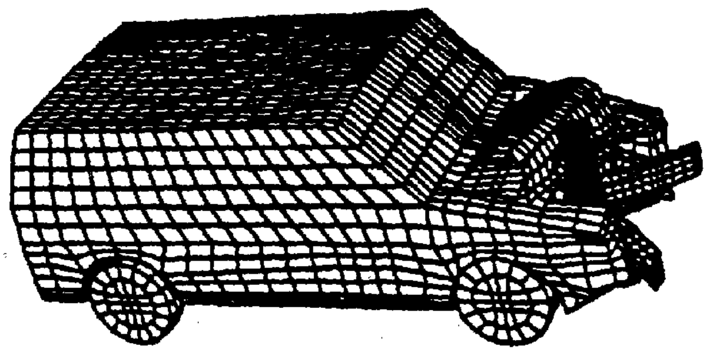

Figure 11. Side view of vehicle for centerline impact: 0 to 120 ms (continued).

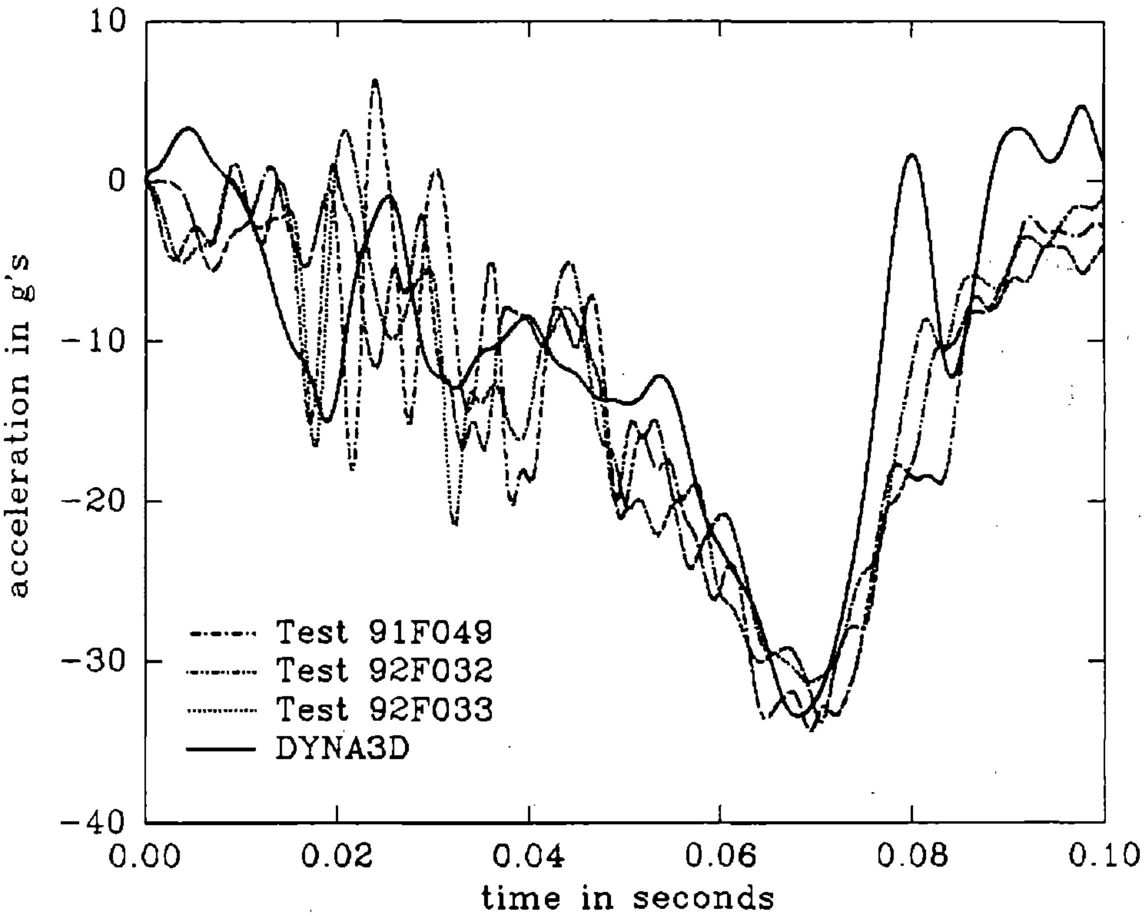

Figure 12. Accelerations at CG of vehicle for centerline impact.

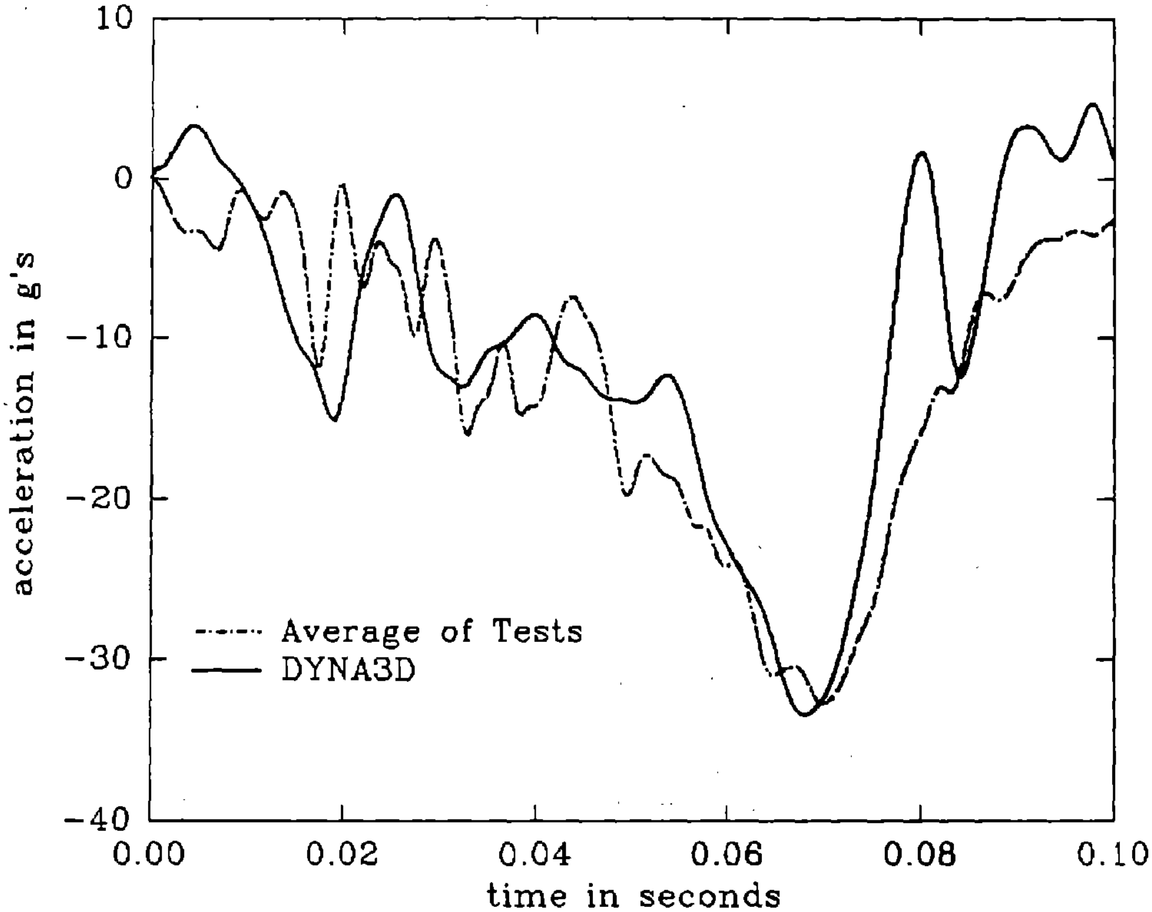

Figure 13. Average accelerations at CG of vehicle for centerline impact.

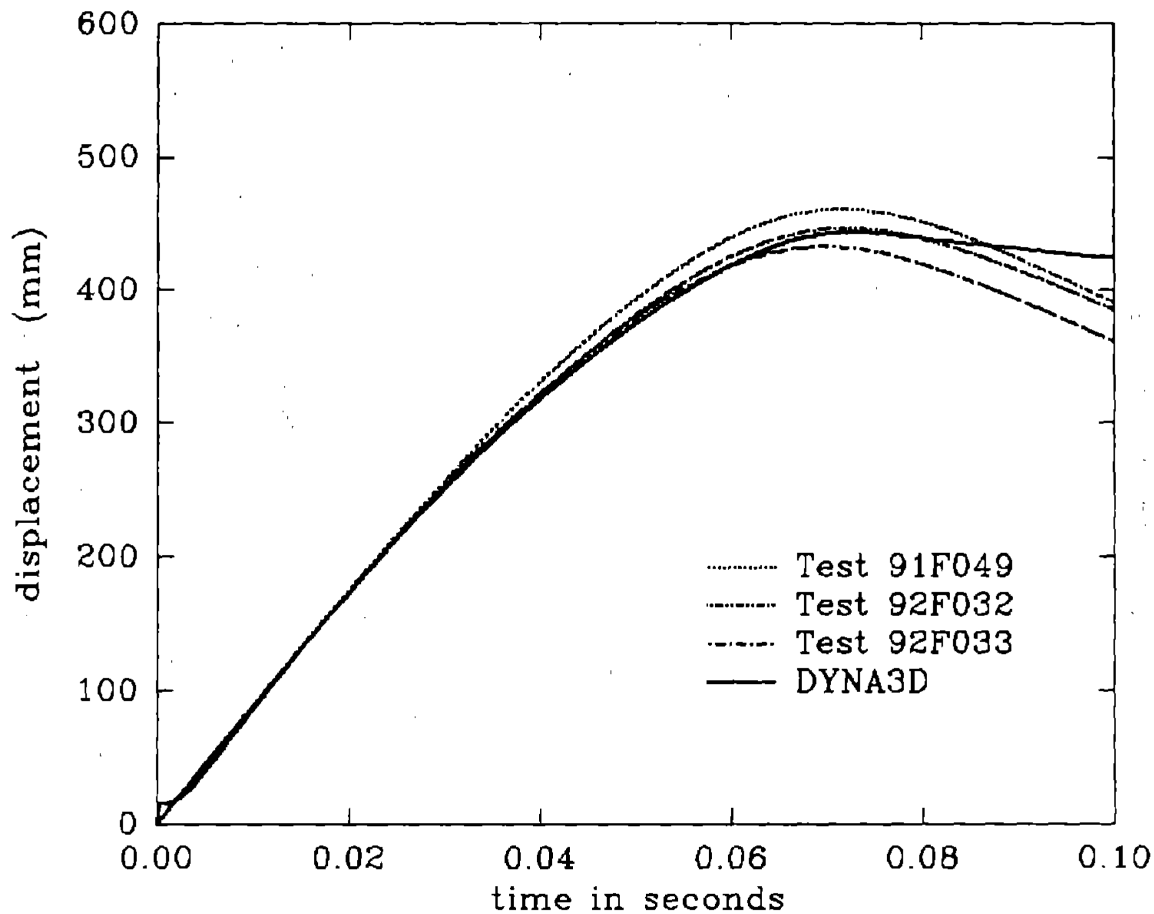

Figure 14. Displacements at CG of vehicle for centerline impact.

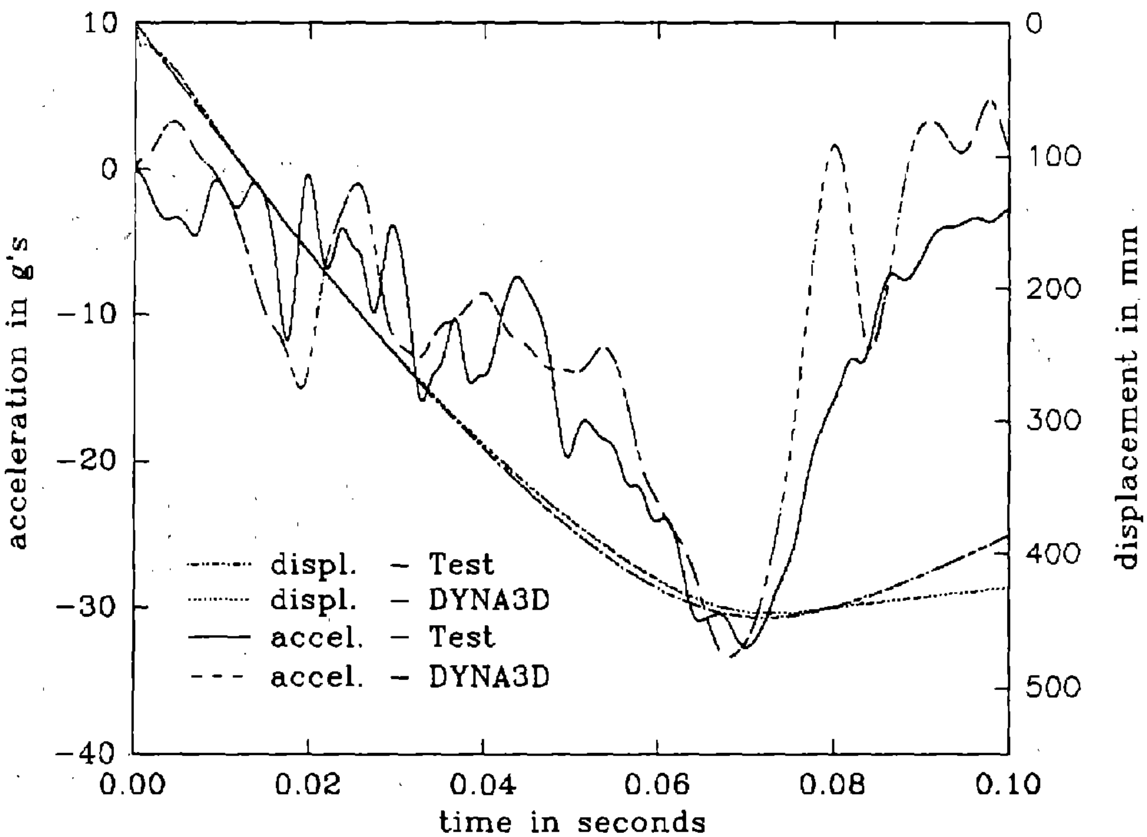

Figure 15. Combined accelerations and displacements at CG of vehicle for centerline impact.

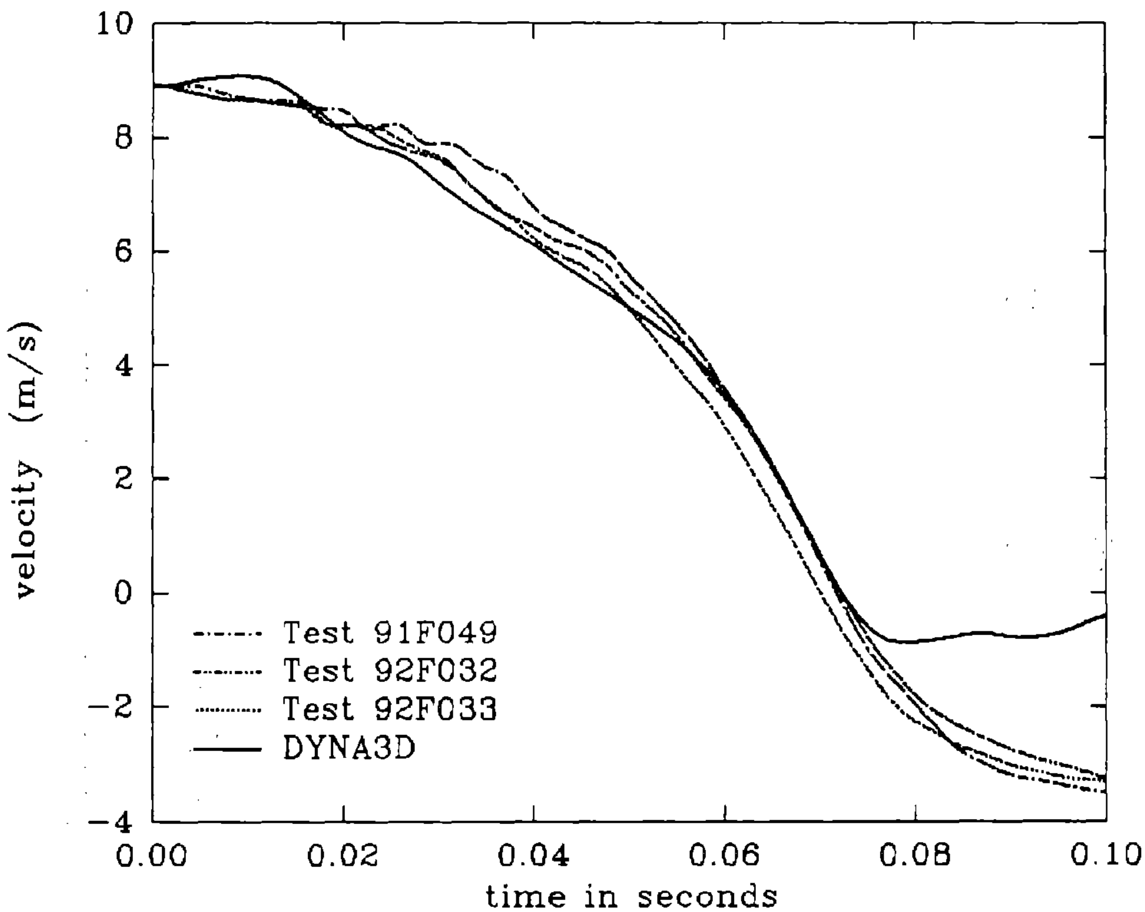

Figure 16. Velocities at CG of vehicle for centerline impact.

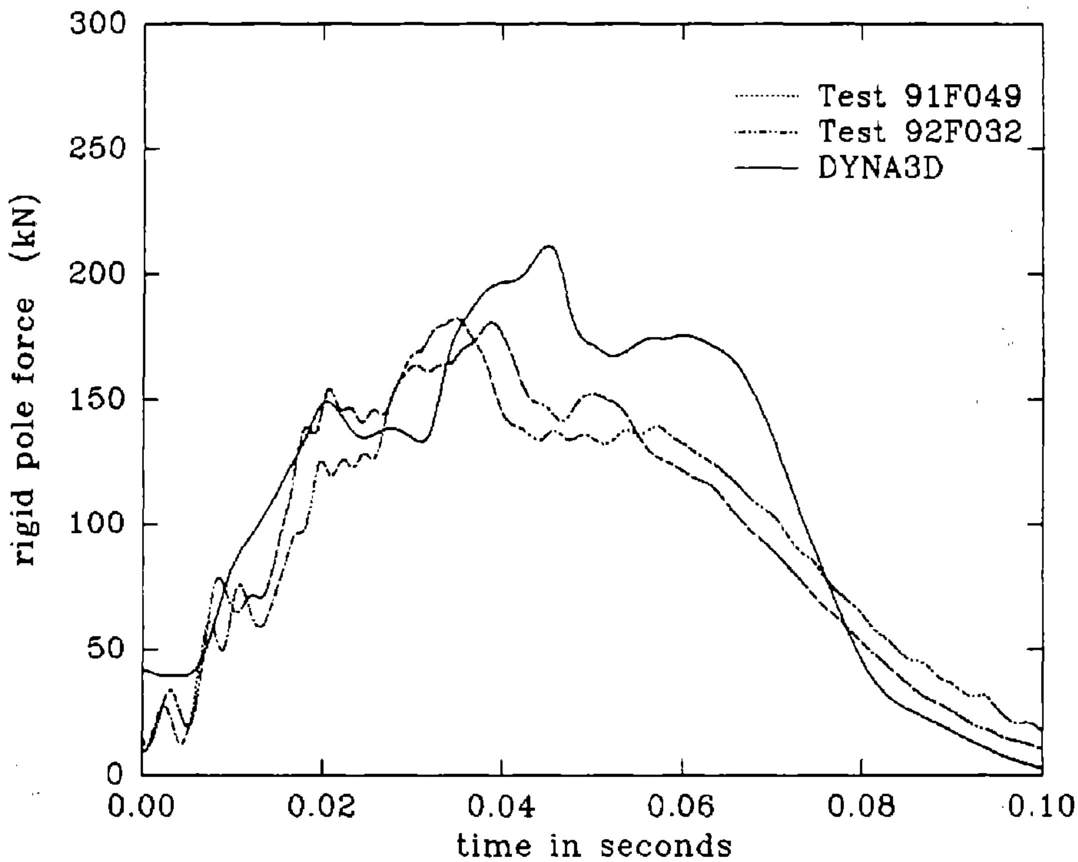

Figure 17. Rigid pole force versus time for centerline impact.

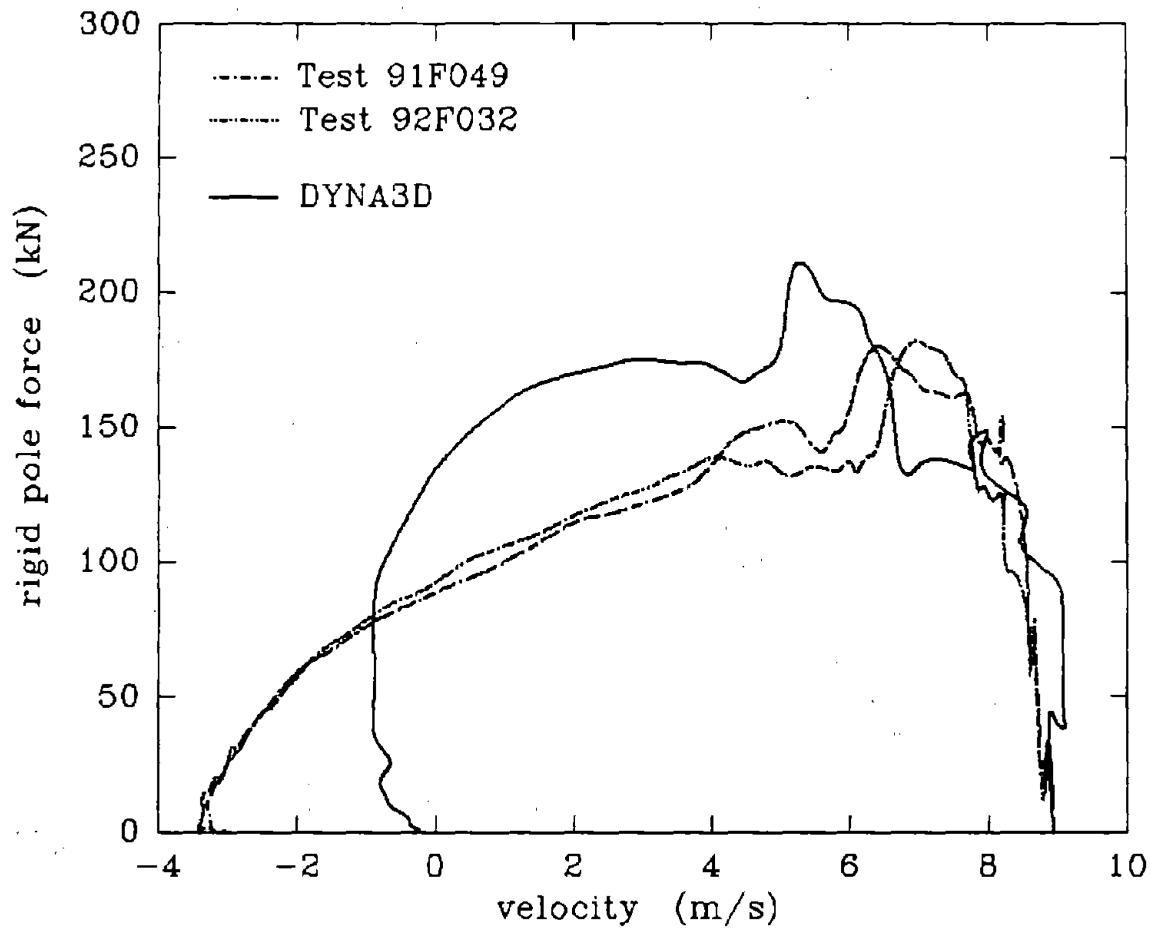

Figure 18. Rigid pole force versus velocity at CG of vehicle for centerline impact.

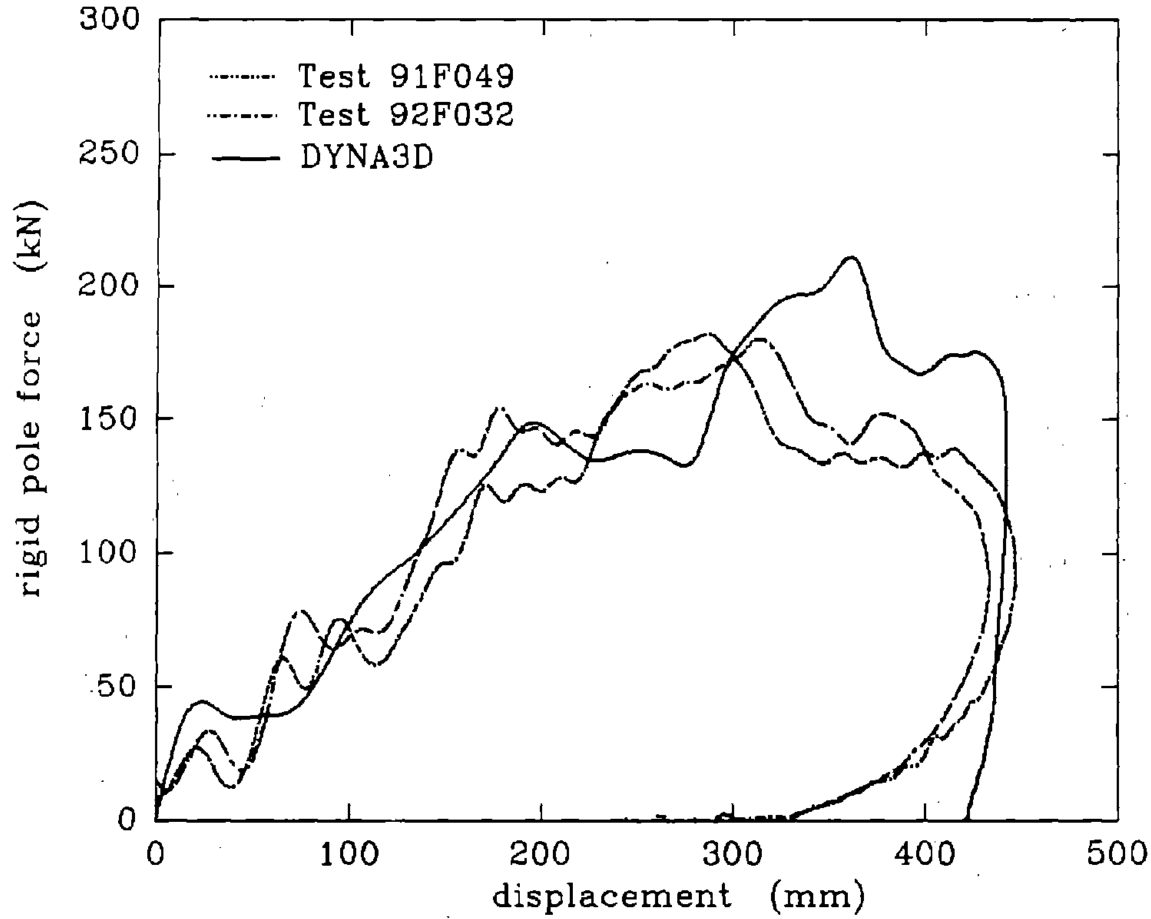

Figure 19. Rigid pole force versus displacement at CG of vehicle for centerline impact.

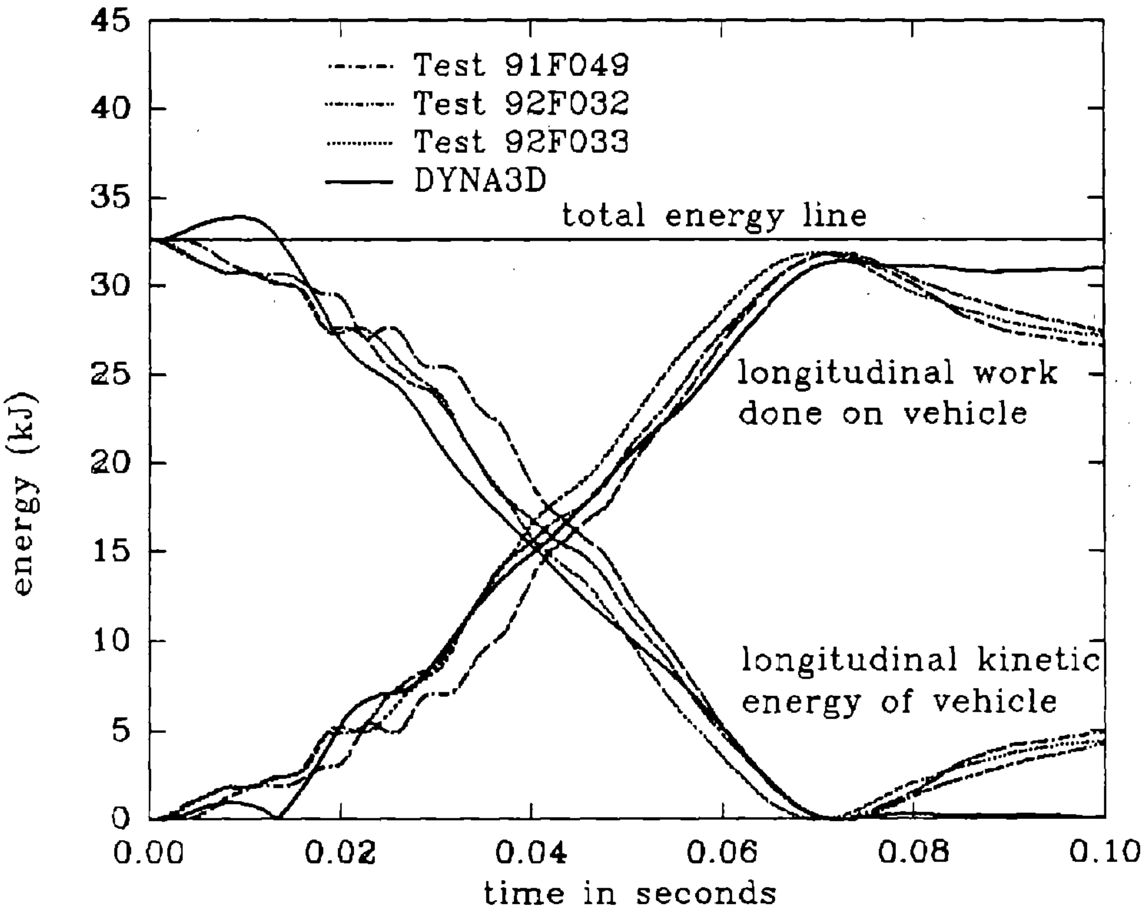

Figure 20. Energy curve versus time at CG of vehicle for centerline impact.

Table 6. Summary of centerline impact results.

	longitudinal change in velocity (m/s)	longitudinal change in kinetic energy (kJ)	longitudinal work done (kJ)	longitudinal impulse transferred (kN·s)
	time = 70 ms			
Simulation	8.9	32.65	32.50	6.33
Test 91F049 Test 92F032 Test 92F033	9.0 8.9 8.9	32.65 32.65 32.65	33.10 32.36 32.36	6.53 6.45 7.0
Percentage difference	0.4 %	0.0 %	0.4 %	5.0 %
	time = 100 ms			
Simulation	9.6	32.65	32.50	8.07
Test 91F049 Test 92F032 Test 92F033	12.5 12.3 12.3	27.40 27.70 27.70	30.0 30.0 29.0	10.17 9.97 9.99
Percentage difference	22.4 %	18.3 %	9.5 %	19.7 %

LEFT-OF-CENTERLINE IMPACT

Figures 21 through 23 show the plots of top view, side view, and bottom view of the deformed state of the vehicle at time intervals between 0.0 ms and 120.0 ms. There was extensive deformation on the left frame horn (impact point) as seen in figure 21, but the damage was restricted to the left half of the vehicle. The vehicle yawed to the left due to the resultant force on the vehicle at the CG, tending to cause the whole vehicle to rotate about the impact point. For this impact scenario, most of the resistance to impact was provided by the left frame horn and fender, as evidenced in figure 21. Most of the energy in the system is dissipated very early in the event. There was very little tilting of the engine block relative to the engine compartment. Penetration of the pole into the engine compartment was restricted to areas around the left frame horn. The engine block never made contact with the firewall because very little damage was done to the engine mounts. Figure 22 shows a view of the bottom of the engine compartment and the deformed state of the cradle during the impact. Very little damage was done to the engine cradle compared to the centerline impact. The event time was also very short. Figure 23 shows a side view of the vehicle with the hood attached, illustrating the deformation and buckling of the left side of the hood.

Even though no full-scale tests were available for comparison study, results of accelerations, displacements, velocities, and rigid pole forces were shown to:

- Demonstrate the reliability of the model in simulating another impact scenario.
- Serve as a guide for designing the full-scale test.
- Provide simulated data for comparison studies should the full-scale test become available.

Acceleration, velocity, and displacement plots were collected at the CG of the vehicle. Rigid pole forces were also collected on the rigid pole material. Figure 24 shows a plot of the acceleration (in g's) versus time. The first peak of about 32 g's occurred very early in the impact and corresponded to the resistance provide by the front face of the frame horn and the bumper when the pole first made contact. The next peak of 35 g's corresponded to contact with the face of the fender — the deformation and buckling of the left frame horn and the fender. Most of the kinetic energy in the vehicle was expended during this stage through the deformation and buckling of these components. Even though the total simulation time was 120.0 ms, a significant portion of the event was completed by 50.0 ms into the event. Also shown in figure 24 were the accelerations in the Y-direction (transverse direction Y). A gradual buildup in acceleration caused by the yawing of the vehicle is apparent, but eventually dies down toward the end of the event. Figures 25 and 26 show plots of the horizontal (X-direction) and transverse (Y-direction) displacements and velocities at the CG of the vehicle. Figure 25 indicates the extent of the yawing. The maximum penetration of the pole into the vehicle was about 165 mm. Also, figure 25 indicates that the vehicle had less than one-tenth of its initial kinetic energy left 40 ms into the event. Figure 27 shows a plot of the rigid pole force. The maximum rigid pole force was about 210 kN and occurred much earlier in the event. The rigid pole force rapidly decayed to zero after the peak value was reached. Figure 28 shows the plot of rigid pole forces versus displacements at the CG.

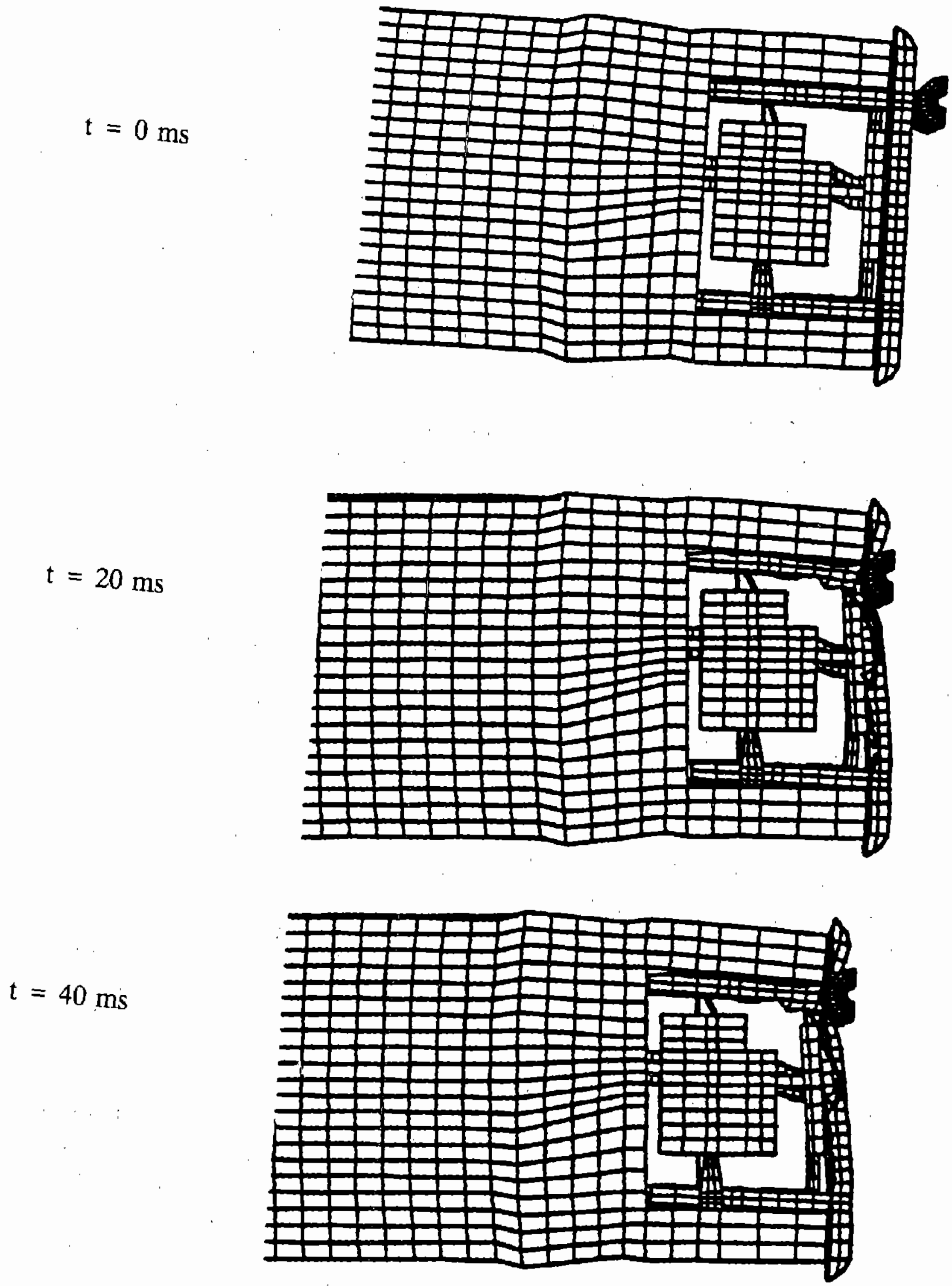

Figure 21. Top view of engine compartment for left-of-centerline impact: 0 to 120 ms.

t = 60 ms

t = 80 ms

t = 120 ms

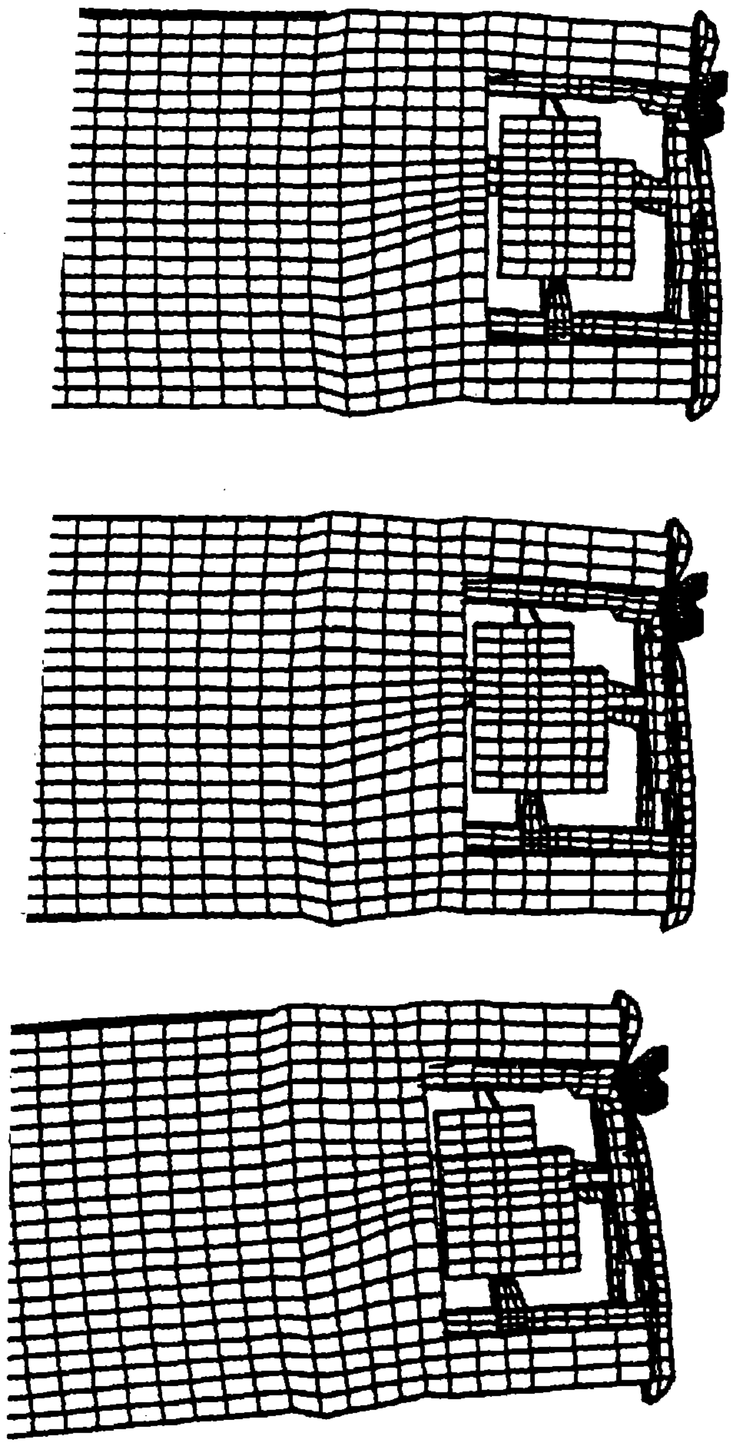

Figure 21. Top view of engine compartment for left-of-centerline impact: 0 to 120 ms (continued).

t = 0 ms

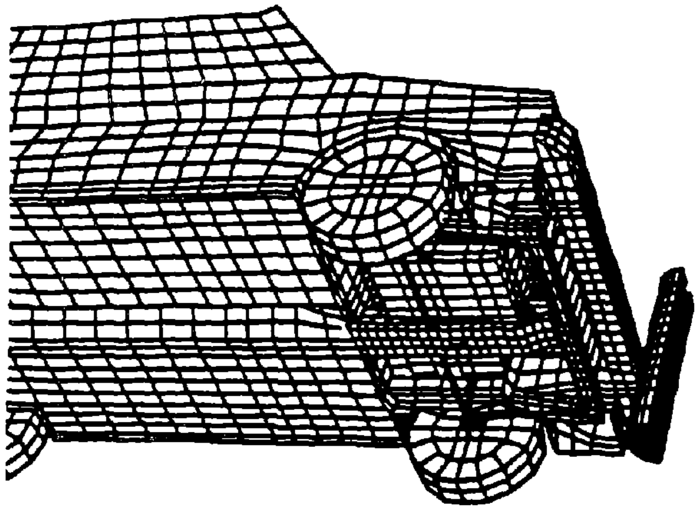

t = 20 ms

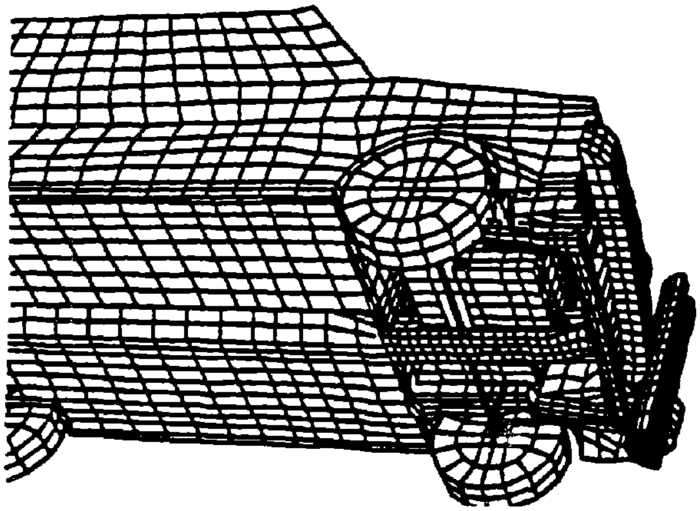

t = 40 ms

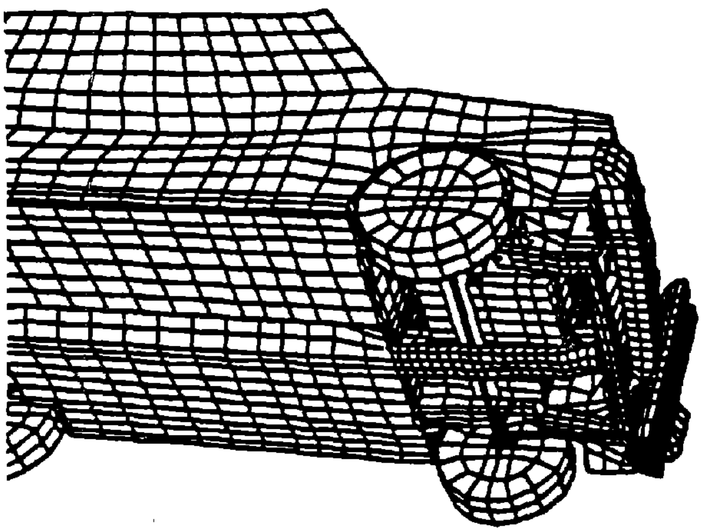

Figure 22. View from below engine compartment for left-of-centerline impact: 0 to 120 ms.

t = 60 ms

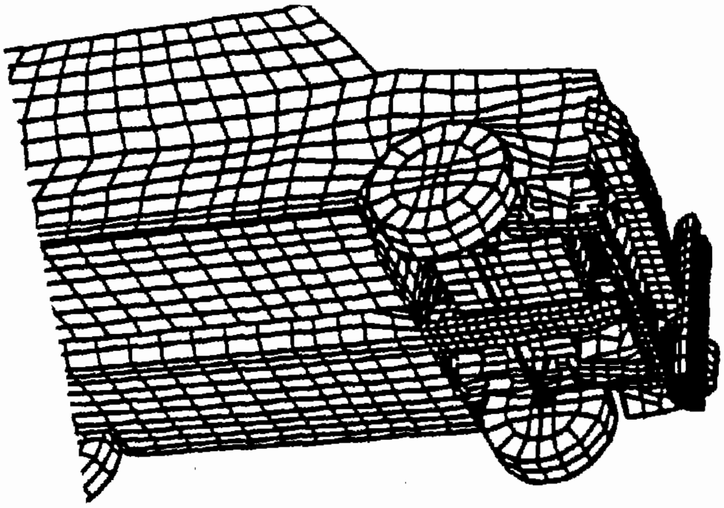

t = 80 ms

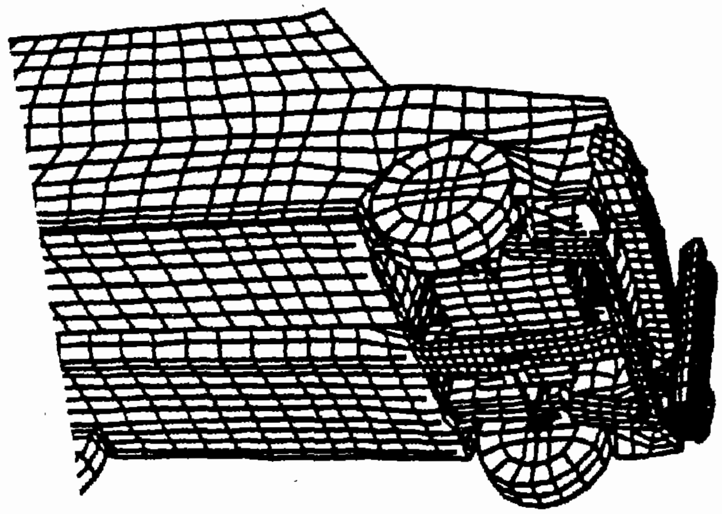

t = 120 ms

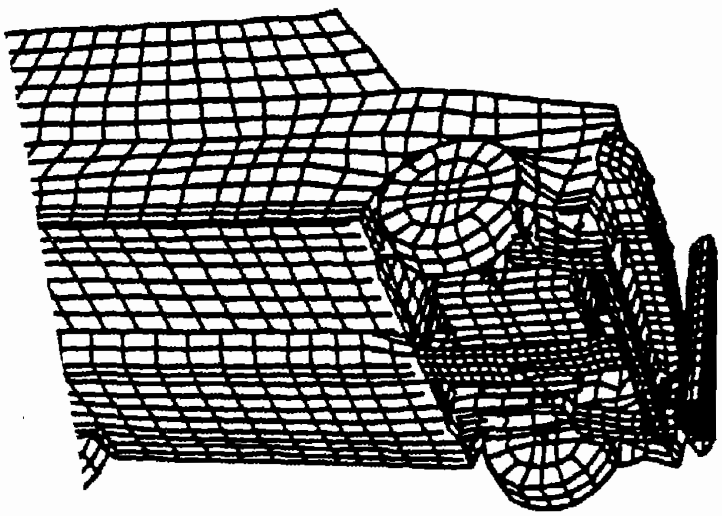

Figure 22. View from below engine compartment for left-of-centerline i
0 to 120 ms (continued).

t = 0 ms

t = 20 ms

t = 40 ms

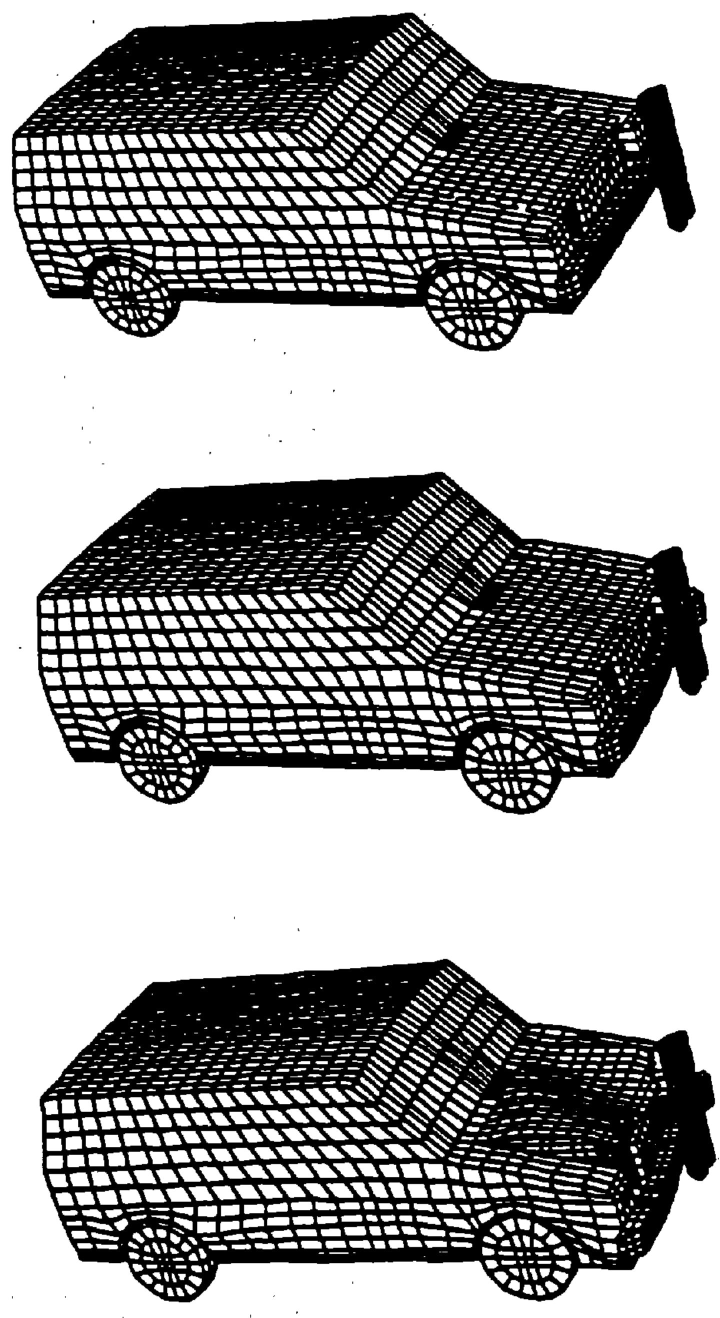

Figure 23. Side view of vehicle for left-of-centerline impact: 0 to 120 ms.

t = 60 ms

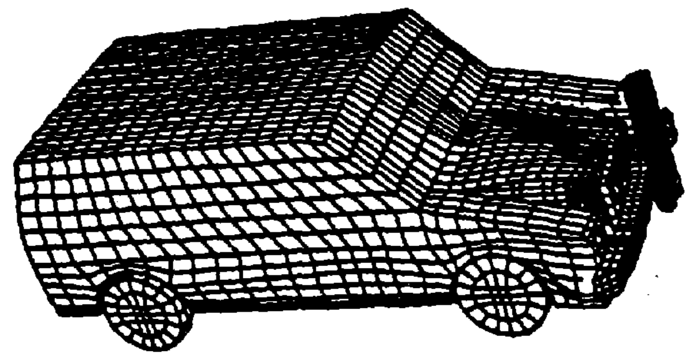

t = 80 ms

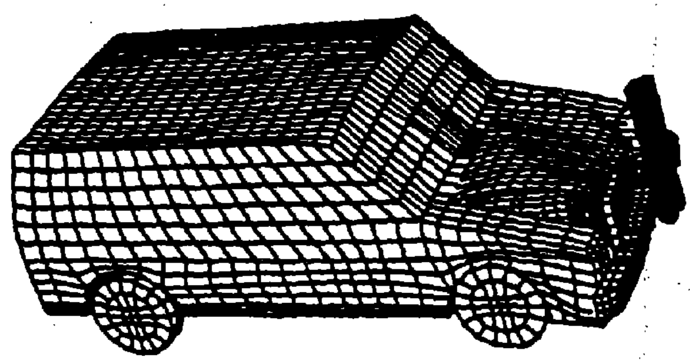

t = 120 ms

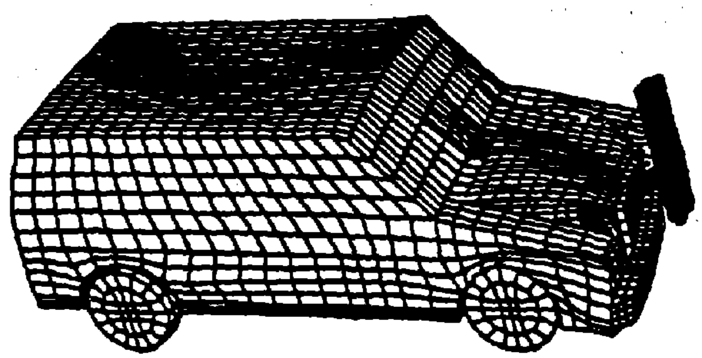

Figure 23. Side view of vehicle for left-of-centerline impact: 0 to 120 ms (continued).

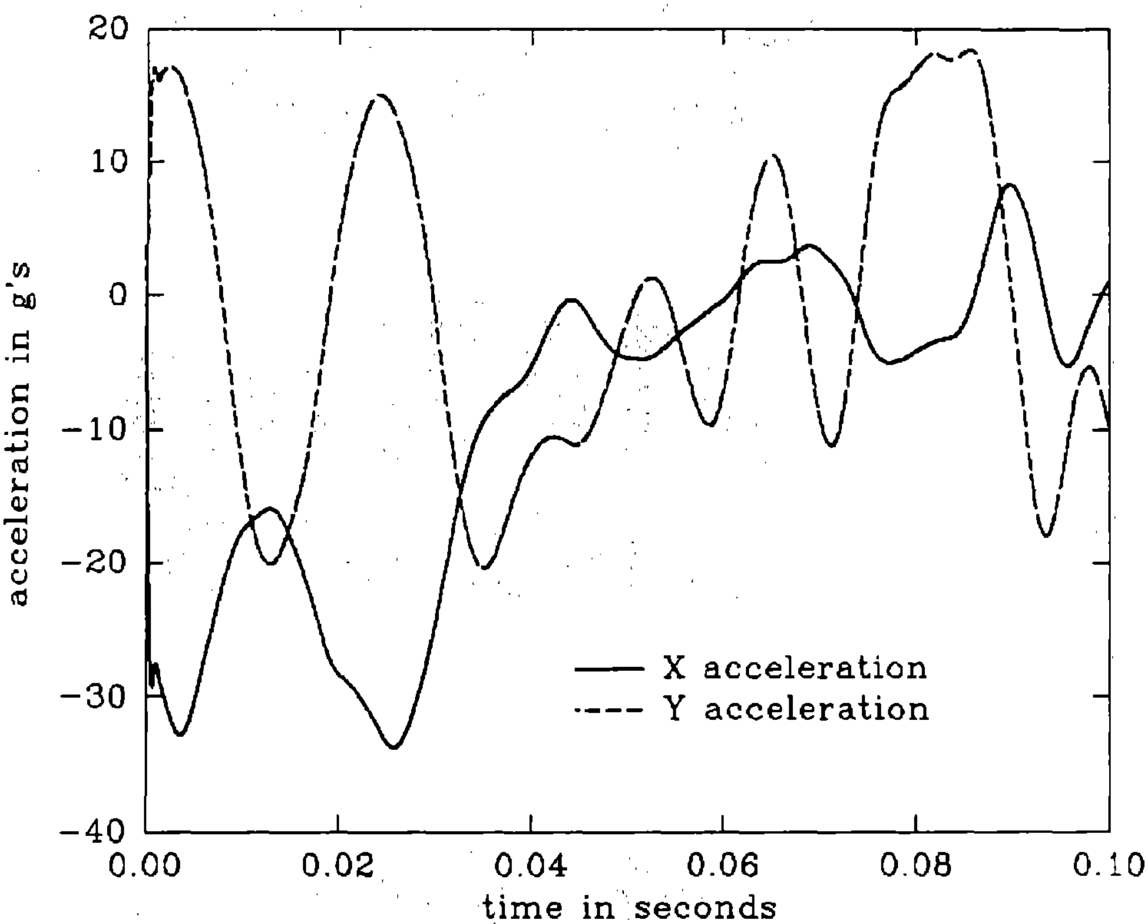

Figure 24. Accelerations at CG of vehicle for left-of-centerline impact.

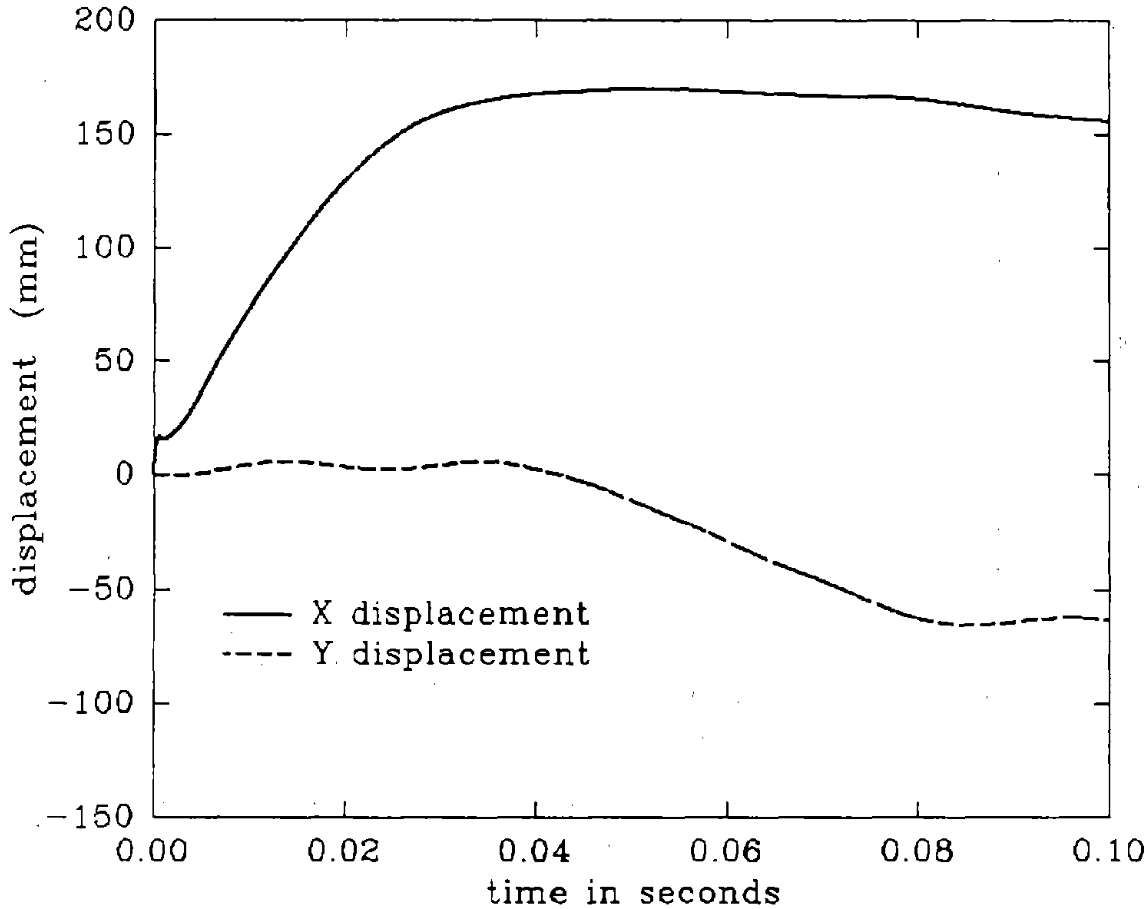

Figure 25. Displacements at CG of vehicle for left-of-centerline impact.

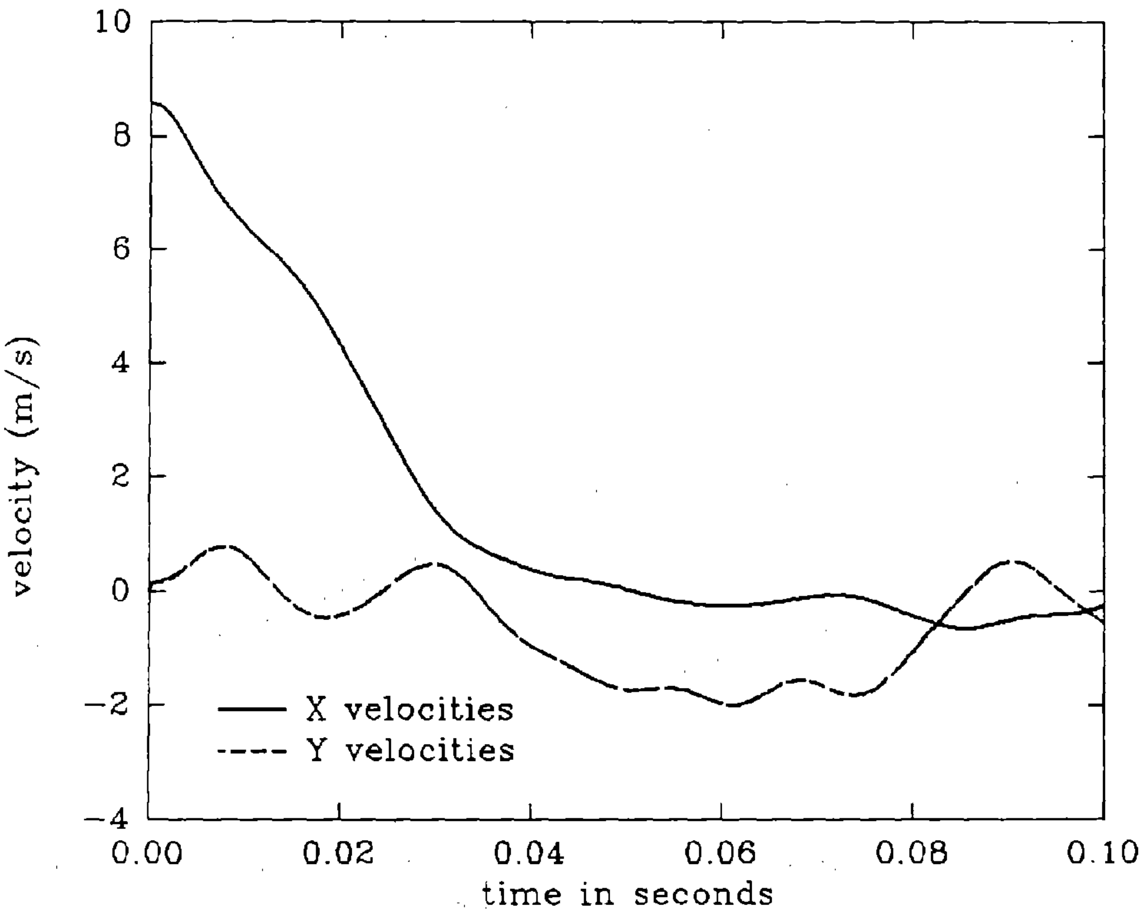

Figure 26. Velocities at CG of vehicle for left-of-centerline impact.

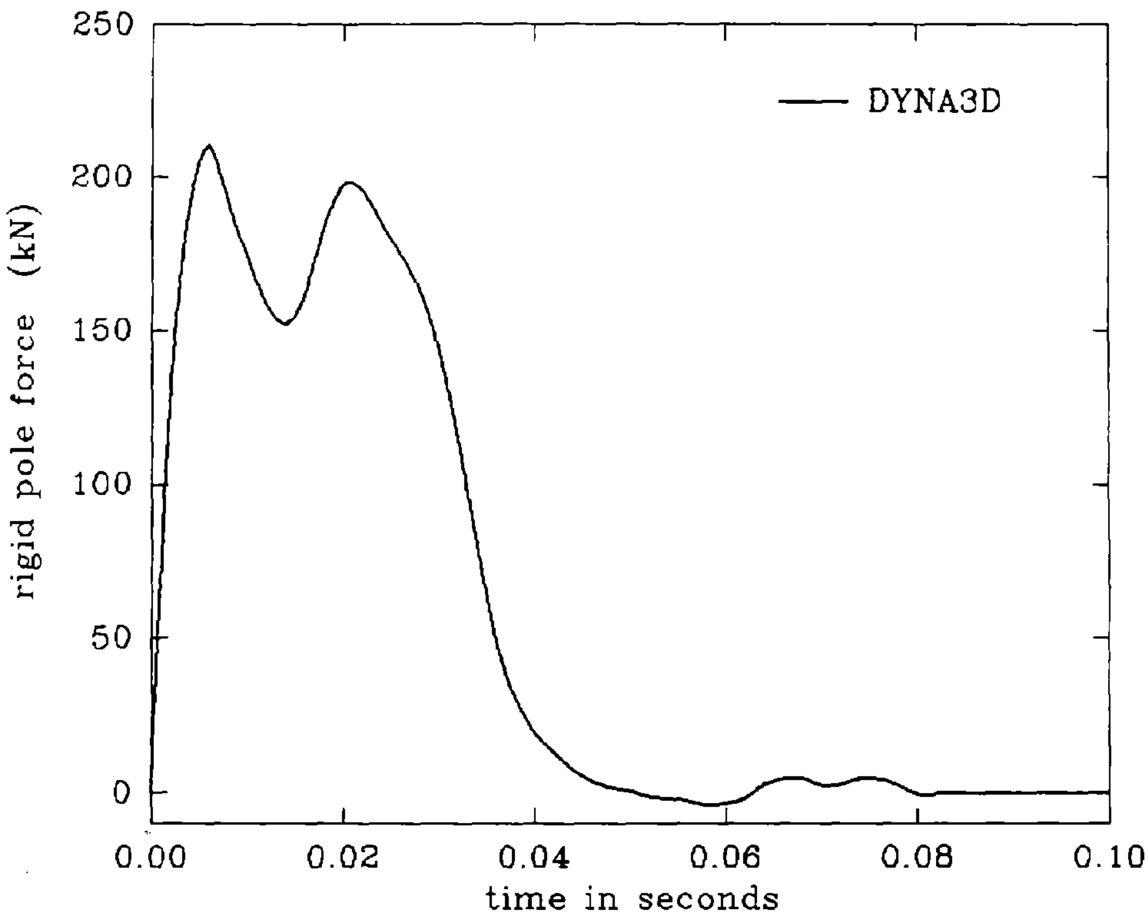

Figure 27. Rigid pole force versus time for left-of-centerline impact.

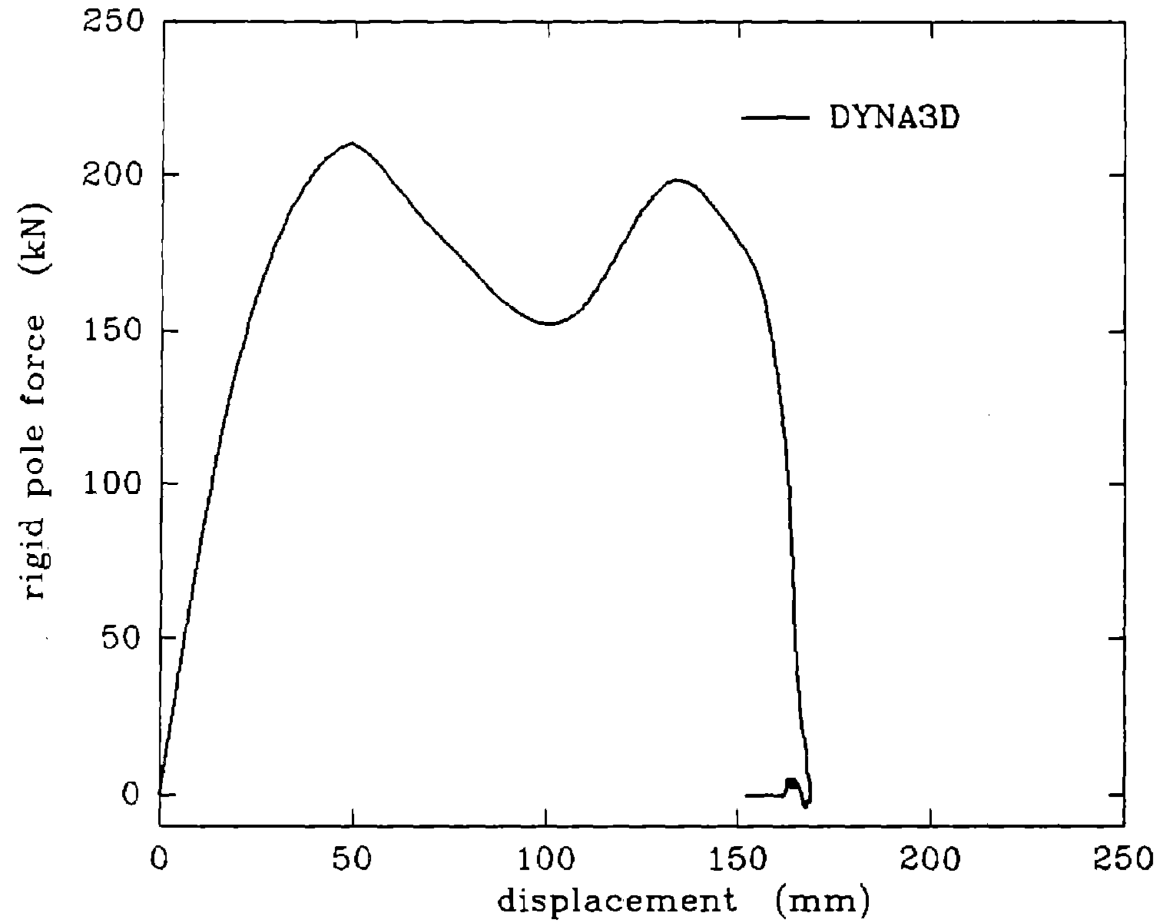

Figure 28. Rigid pole force versus displacement at CG of vehicle for left-of-centerline impact.

RIGHT-OF-CENTERLINE IMPACT

Figures 29 through 31 show the plots of the top view, side view, and bottom view of the deformed states of the vehicle between 0.0 ms and 120.0 ms. Figure 29 shows the damage to the front of the vehicle. Since the impact occurred at the point of least resistance, there was much deeper penetration into the engine compartment during the early stages of impact, when only the bumper, hood, and lower core support resisted the impacting force. Unlike the centerline impact, resistance to the impacting force was provided by the engine mounts only after contact was made with the engine block. The left frame horn and fender also provided more resistance to the motion in this impact than was noticed in the centerline impact (excessive deformation of the frame horn). The back engine mount remained partially intact throughout the impact. As a result, full contact was not made with the firewall by the back of the engine block. The engine block tilted to the right, but there was very little yawing of the vehicle. Pitching of the vehicle also occurred. Figure 30 shows plots of the deformed shape from underneath the engine compartment, illustrating the deformed state of the engine cradle during the event. The deformation was not as extensive as was noticed in the centerline impact. Figure 31 shows a side view of the vehicle with the hood attached. The damage was severe to one side of the vehicle and the local buckling of the right half of the hood is apparent.

t= 0 ms

t = 20 ms

t = 40 ms

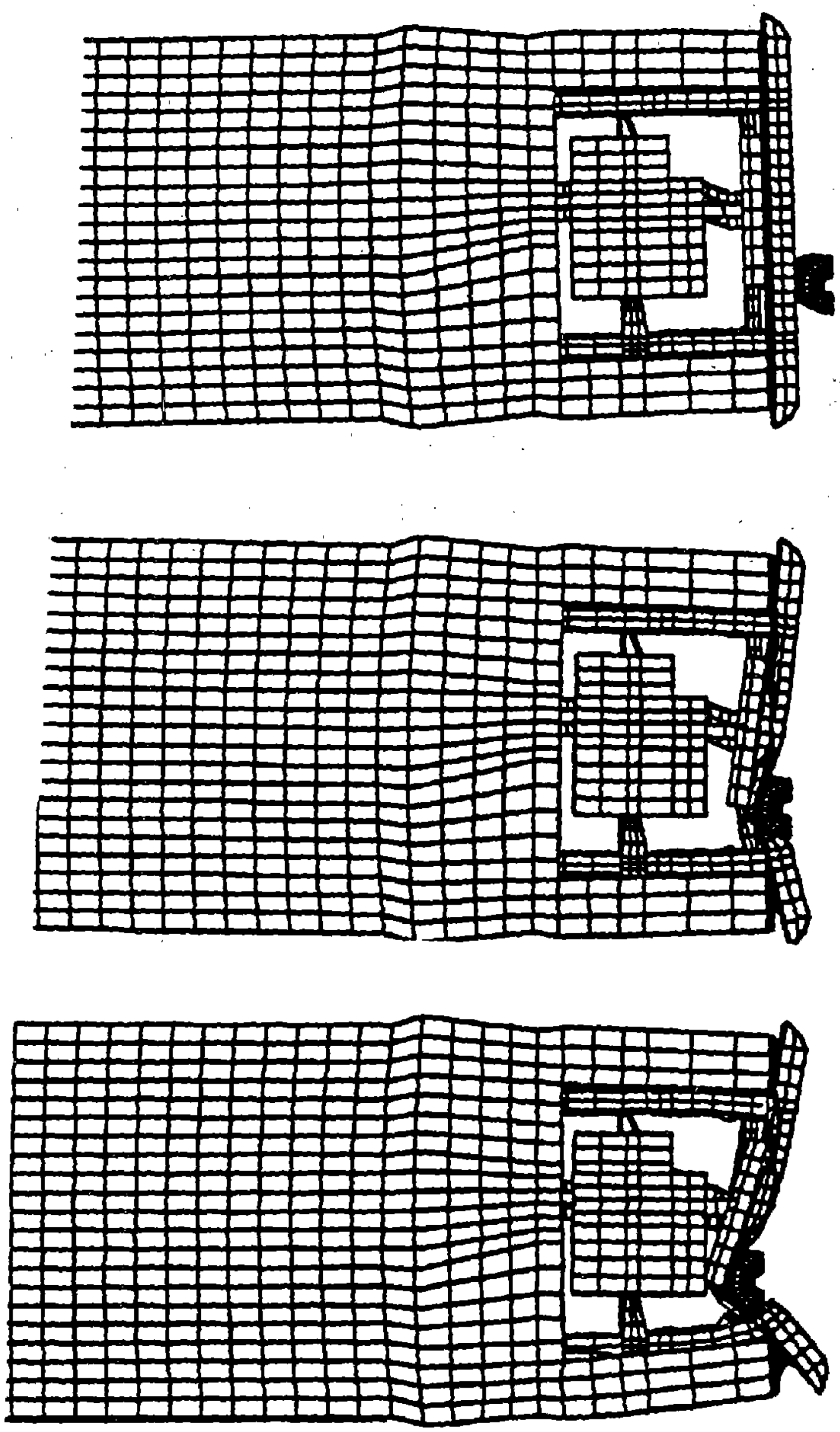

Figure 29. Top view of engine compartment for right-of-centerline impact: 0 to 120 ms.

t = 60 ms

t = 80 ms

t = 120 ms

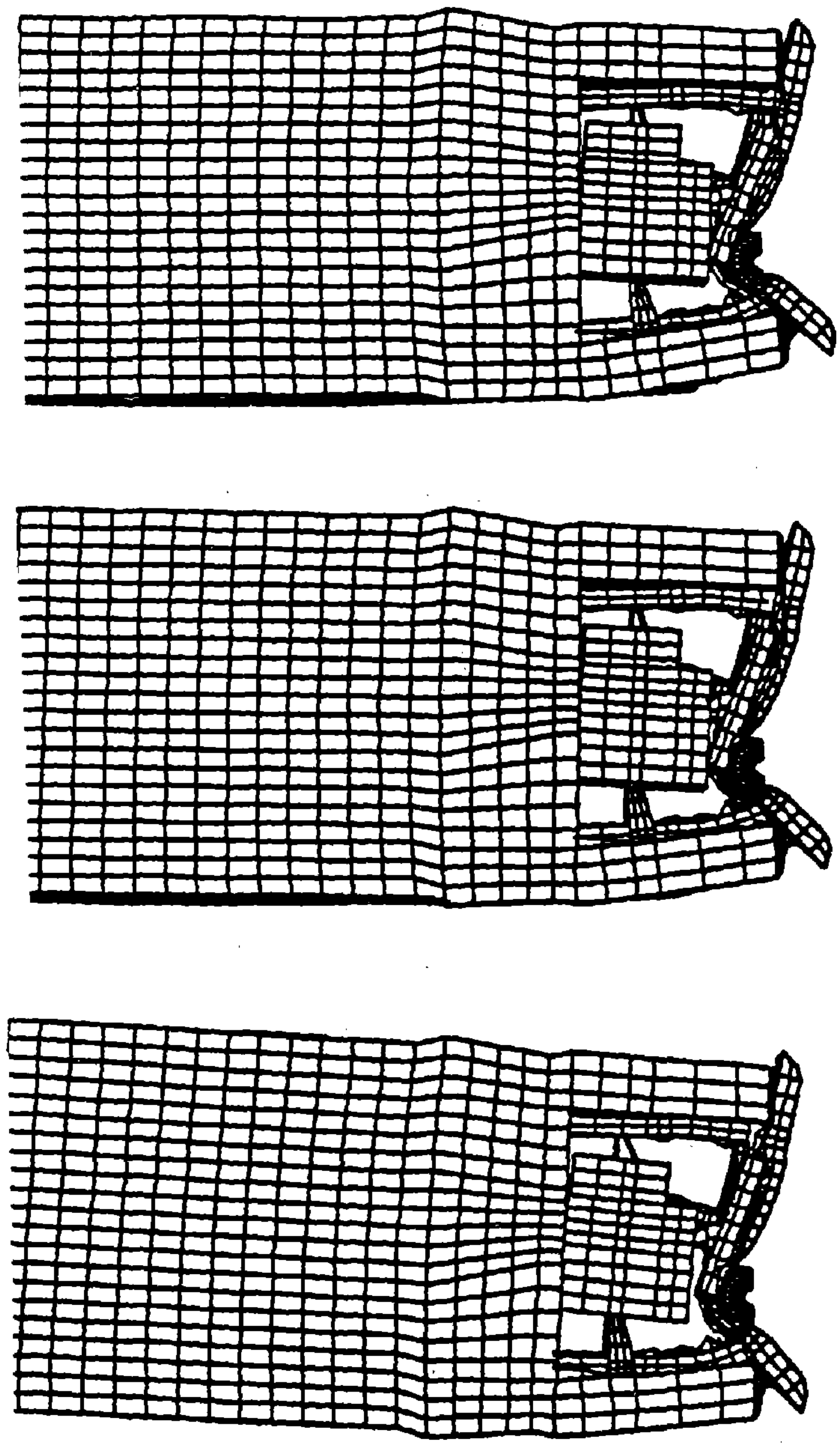

Figure 29. Top view of engine compartment for right-of-centerline impact: 0 to 120 ms (continued).

t = 0 ms

t = 20 ms

t = 40 ms

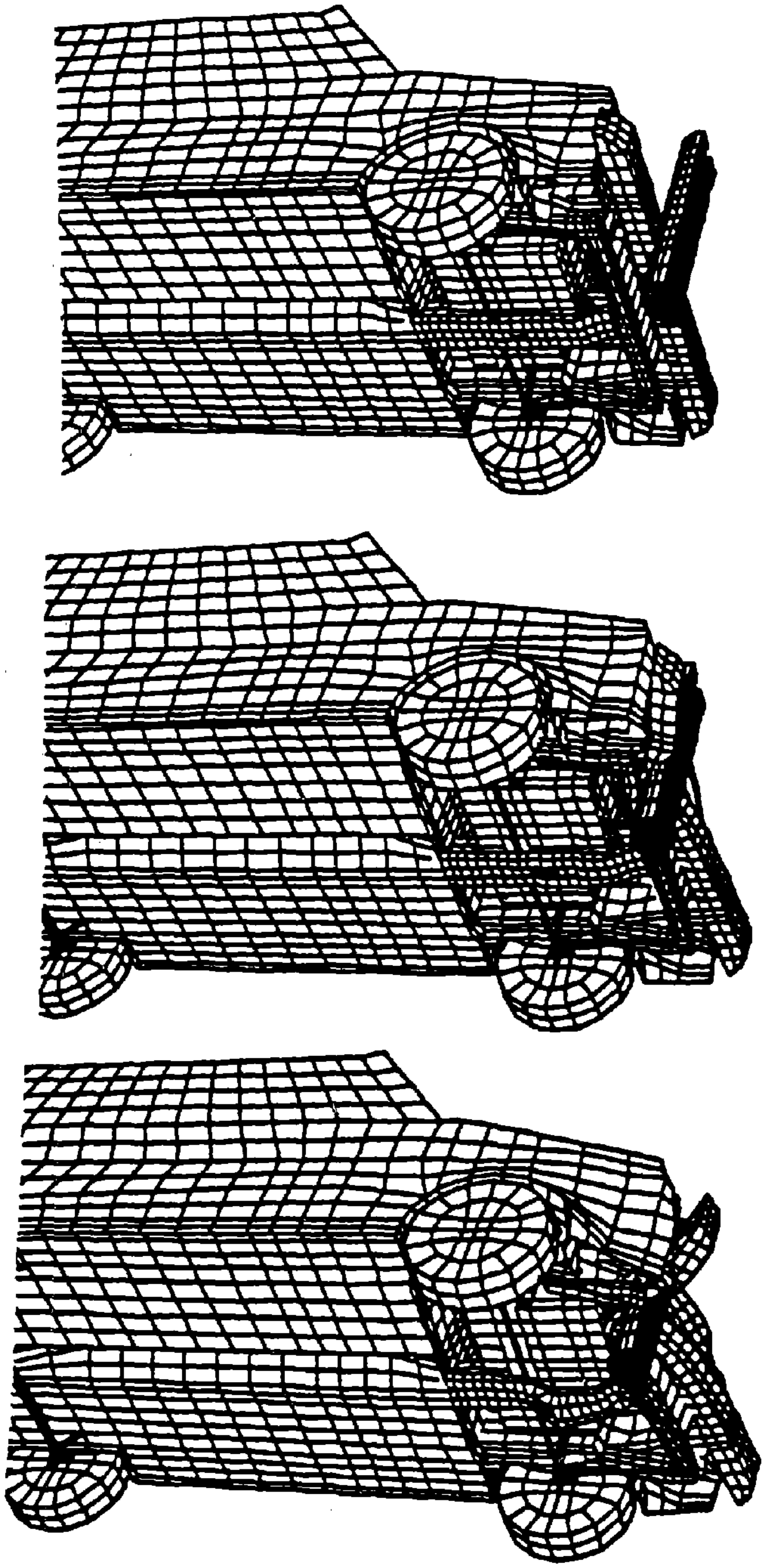

Figure 30. View from below engine compartment for right-of-centerline impact: 0 to 120 ms.

t = 60 ms

t = 80 ms

t = 120 ms

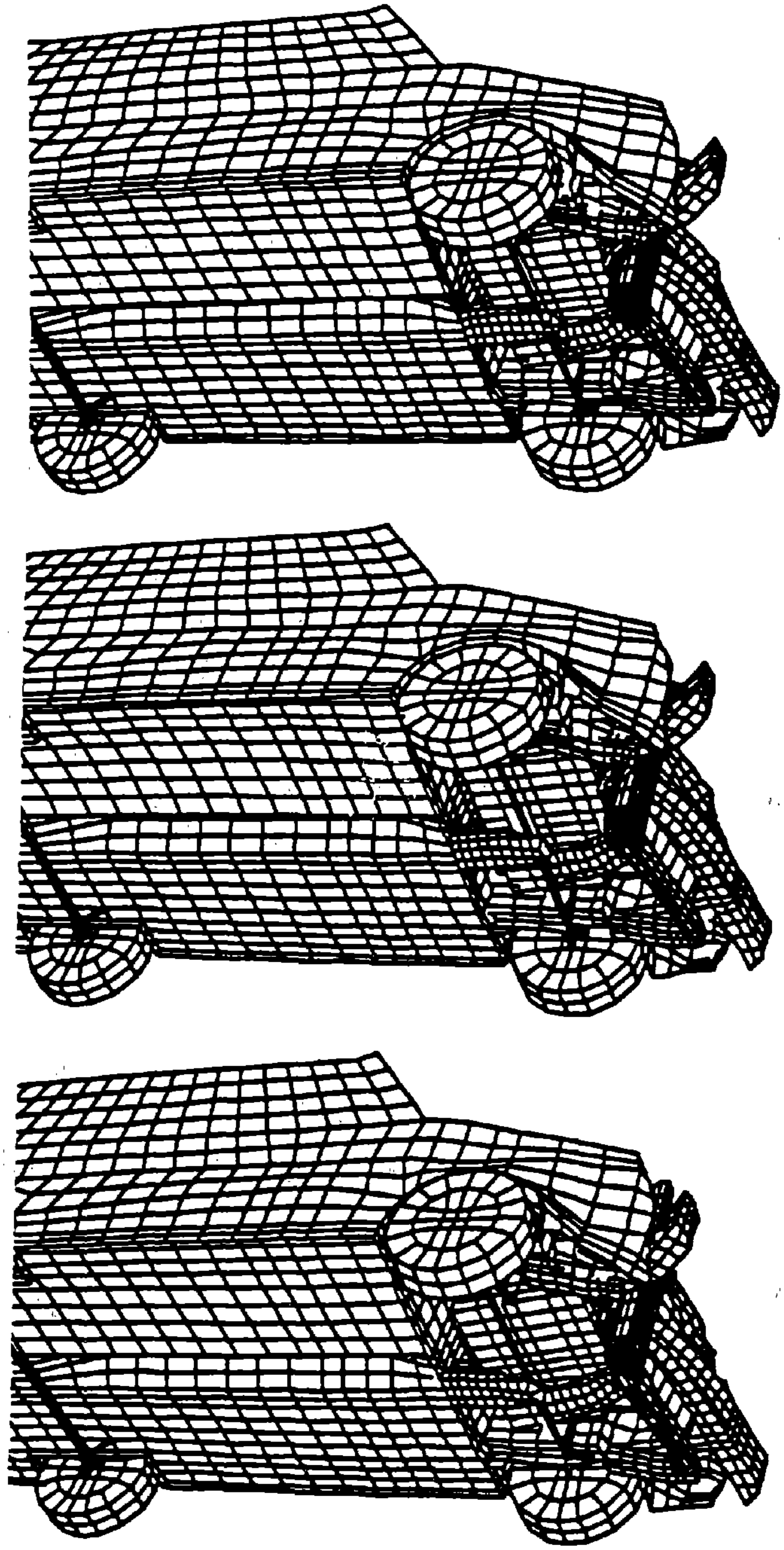

Figure 30. View from below engine compartment for right-of-centerline impact: 0 to 120 ms (continued).

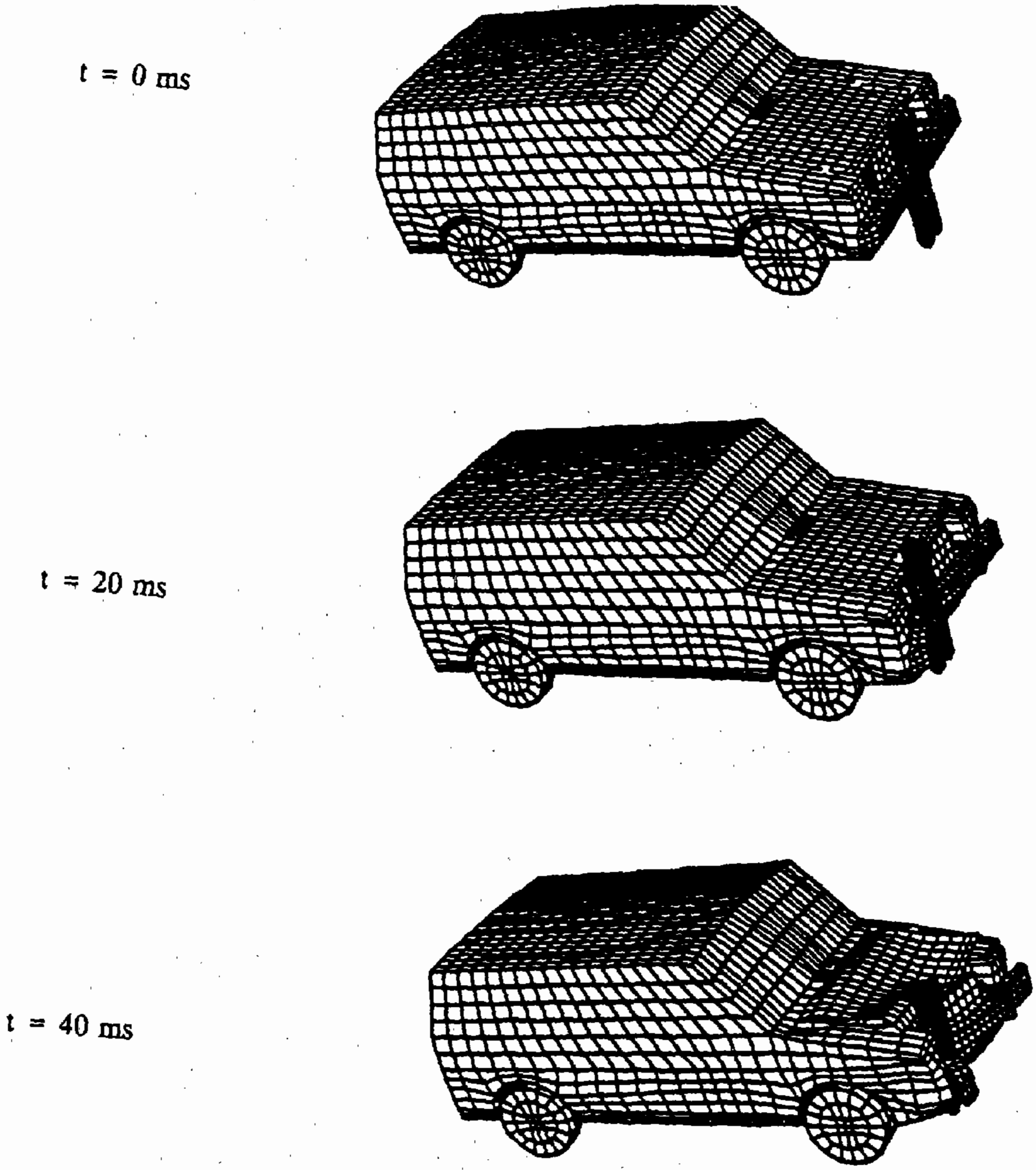

Figure 31. Side view of vehicle for right-of-centerline impact: 0 to 120 ms.

t = 60 ms

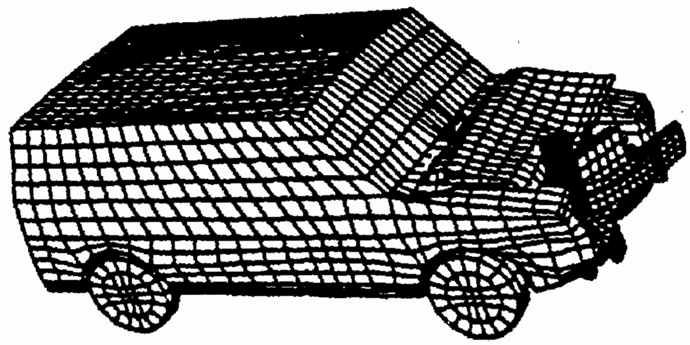

t = 80 ms

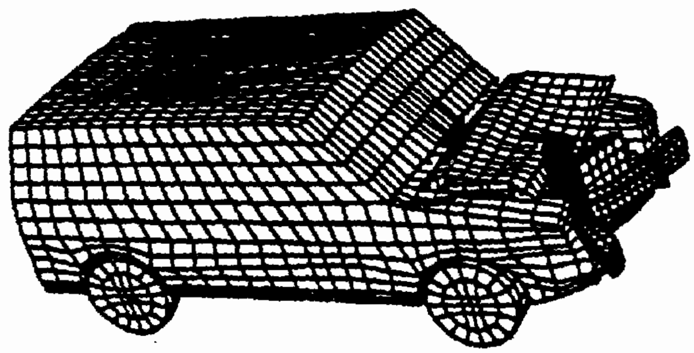

t = 120 ms

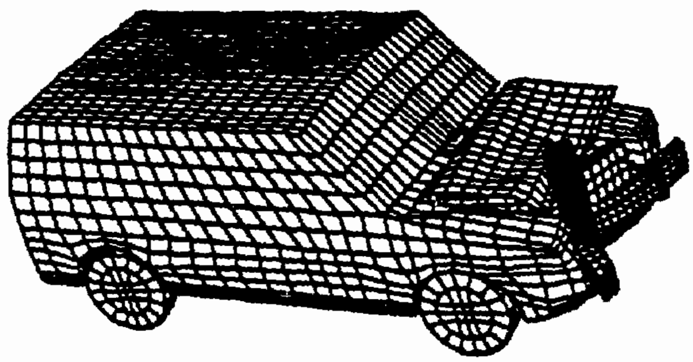

Figure 31. Side view of vehicle for right-of-centerline impact: 0 to 120 ms (continued).

Acceleration, velocity, and displacement plots were collected at the center of gravity of the vehicle. Rigid pole forces were also collected on the rigid pole material. Figure 32 shows a plot of the acceleration (in g's) versus time. Note that the peak acceleration was maintained at a constant value over a much longer period compared to the centerline or left-of-centerline impact. This is due to the sustained resistance to the motion provided by the engine mounts, the frame horn, the fender, and the tilting of the engine block over a long period of time. Also, as was stated earlier, the engine never made contact with the firewall. Figures 33 and 34 show the plots of the displacements and velocities. The peak displacement was 360 mm and occurred at about 60.0 ms, after which the vehicle began to rebound from the pole. Figure 35 shows the rigid pole force versus time. The pole force gradually builds up to a peak of 170 kN and remains relatively constant over a long period of time before decreasing to zero. This indicates that there was no sudden failure of components, but rather a gradual yielding of parts. The peak value was less than that obtained from the centerline impact. Figure 36 shows the plot of rigid pole forces versus displacements at the CG of the vehicle.

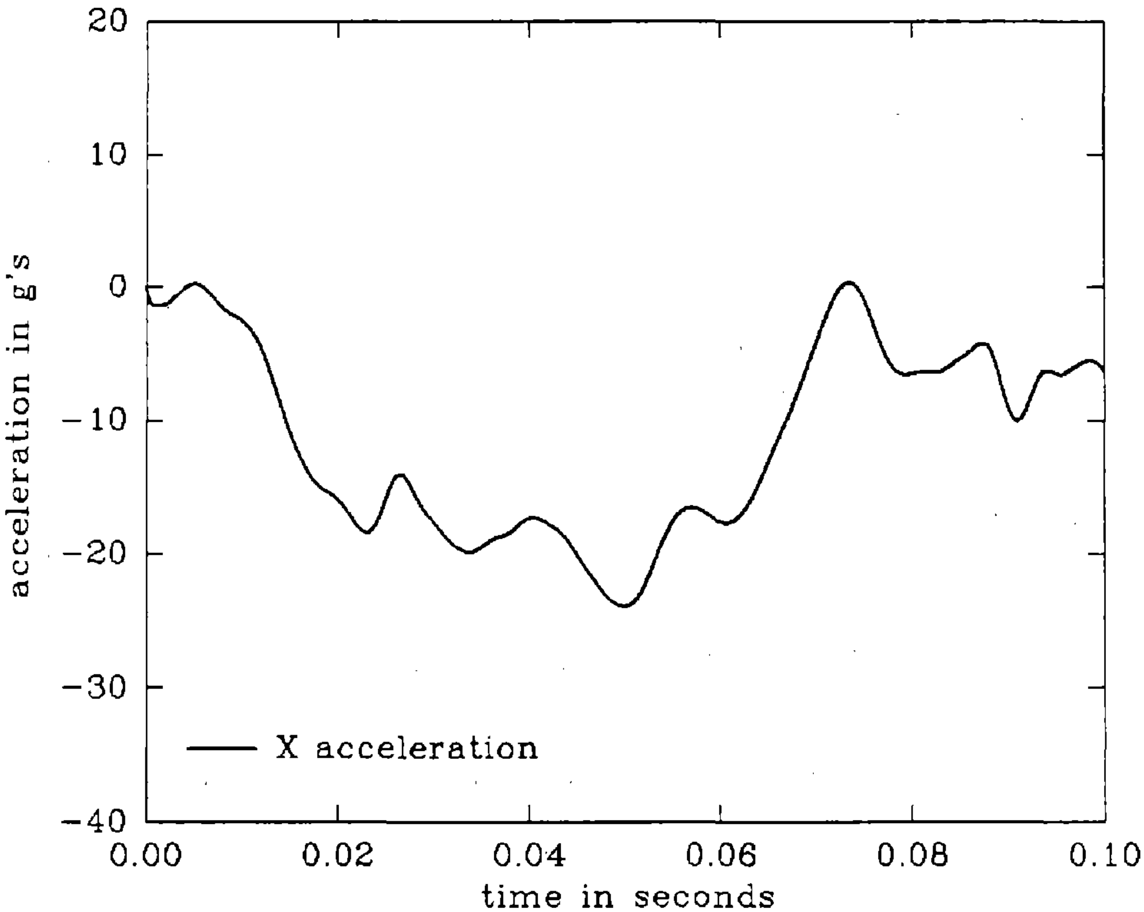

Figure 32. Accelerations at CG of vehicle for right-of-centerline impact.

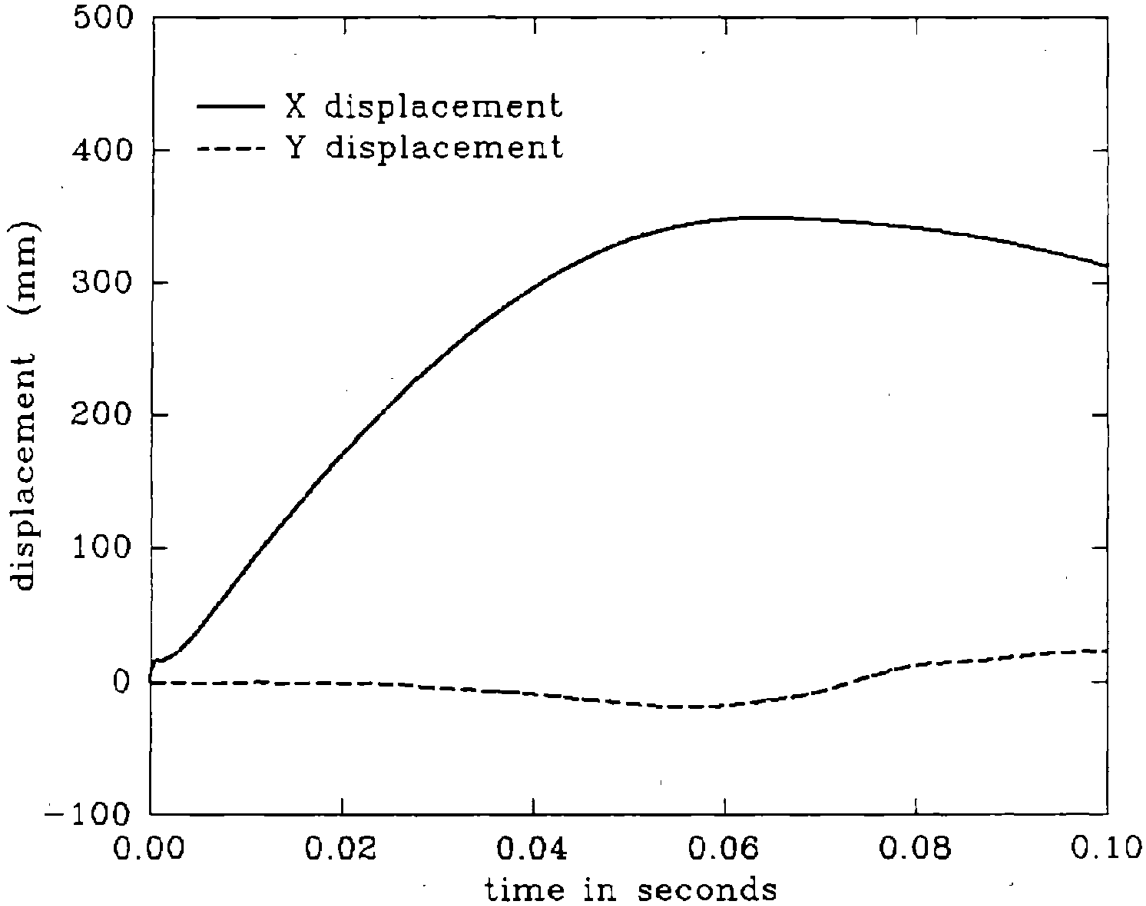

Figure 33. Displacements at CG of vehicle for right-of-centerline impact.

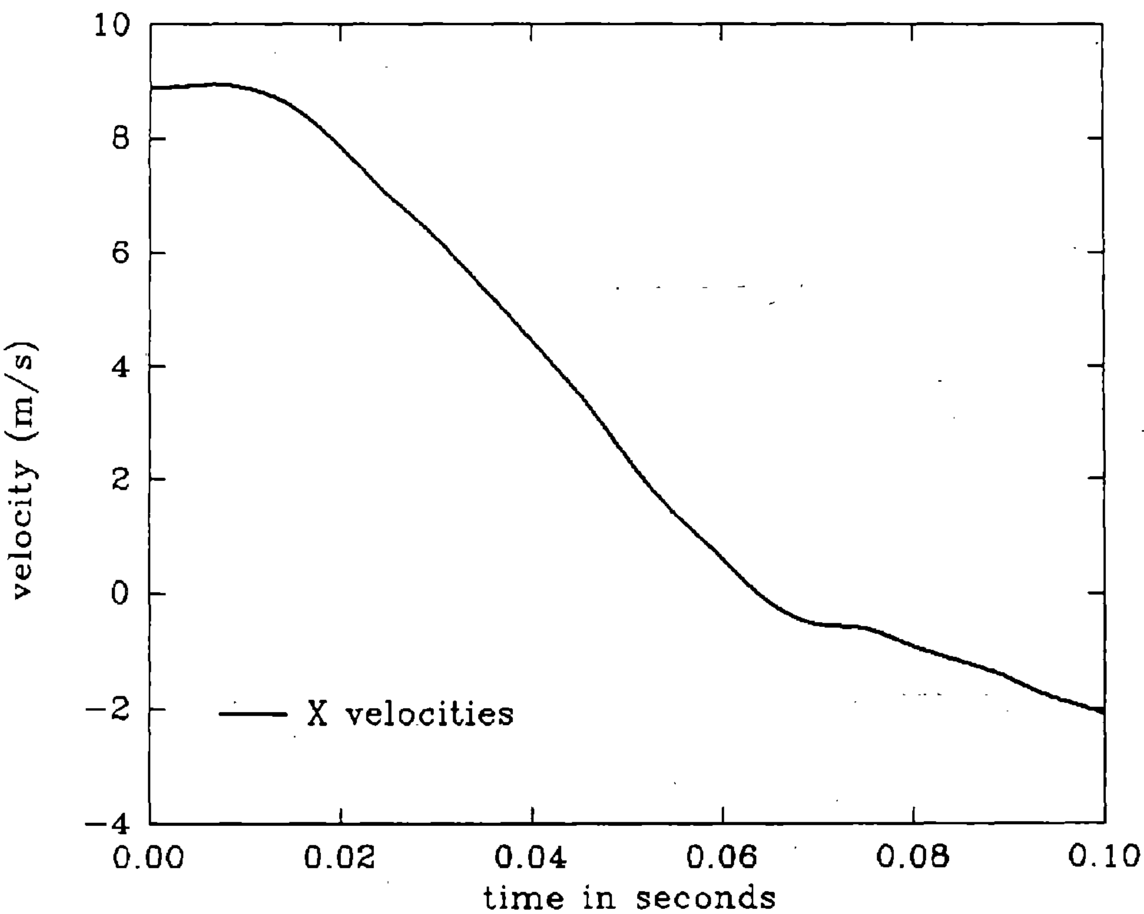

Figure 34. Velocities at CG of vehicle for right-of-centerline impact.

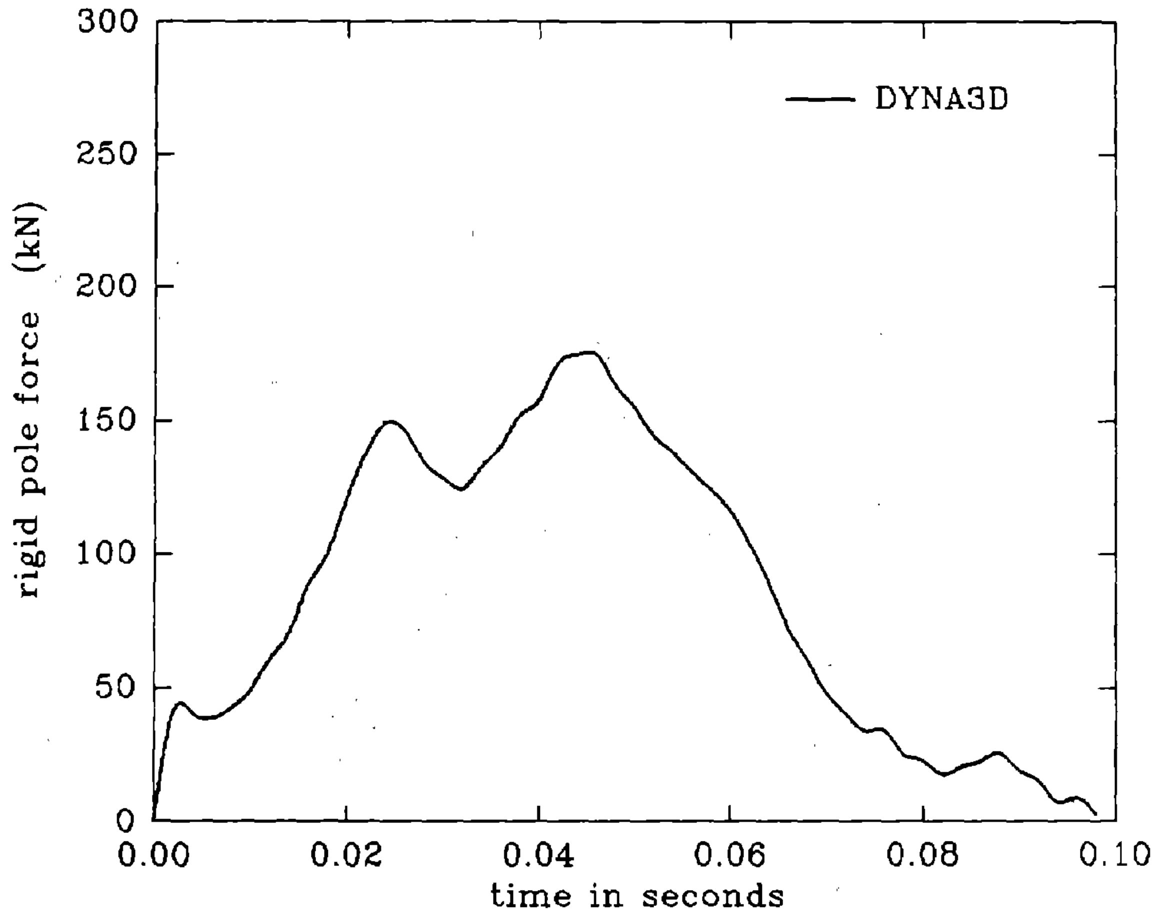

Figure 35. Rigid pole force versus time for right-of-centerline impact.

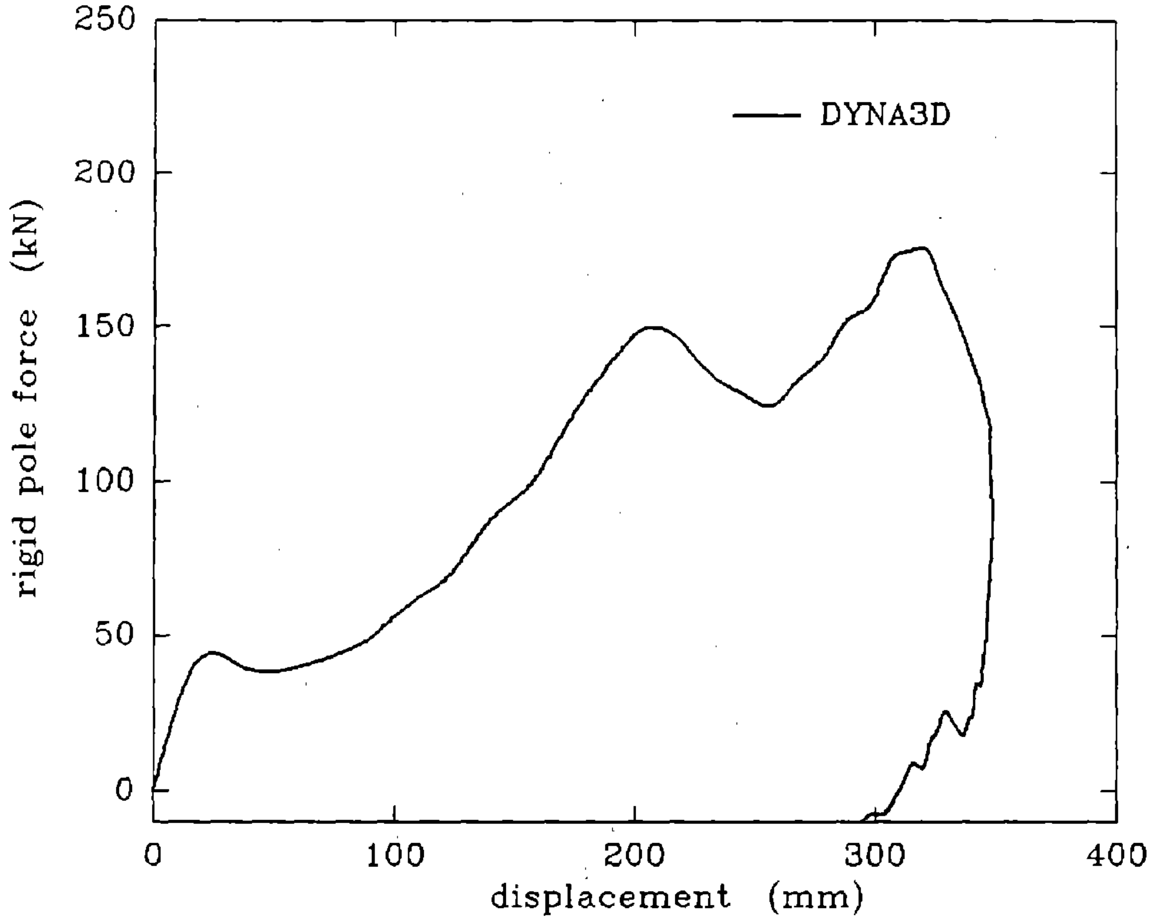

Figure 36. Rigid pole forces versus displacement at CG of vehicle for right-of-centerline impact.

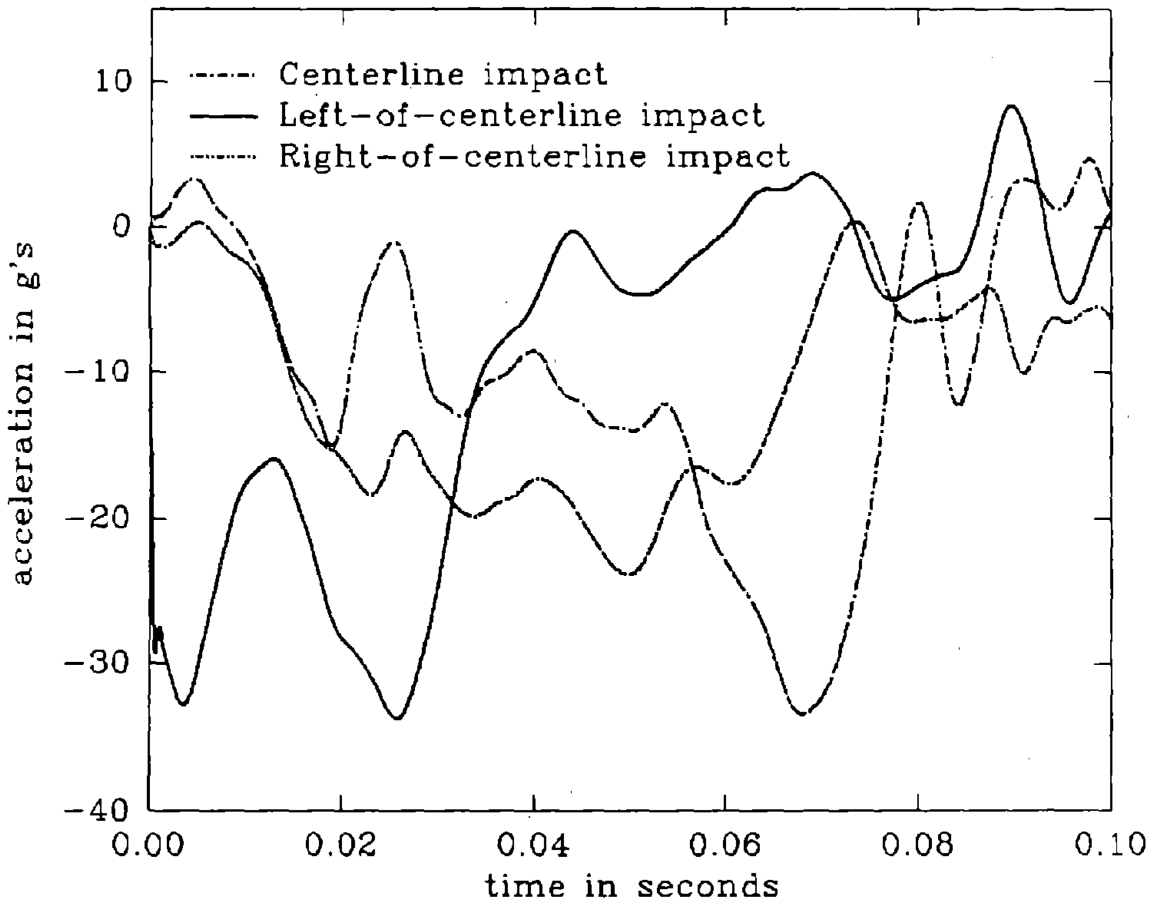

Figure 37. Acceleration at CG of vehicle for all three simulations.

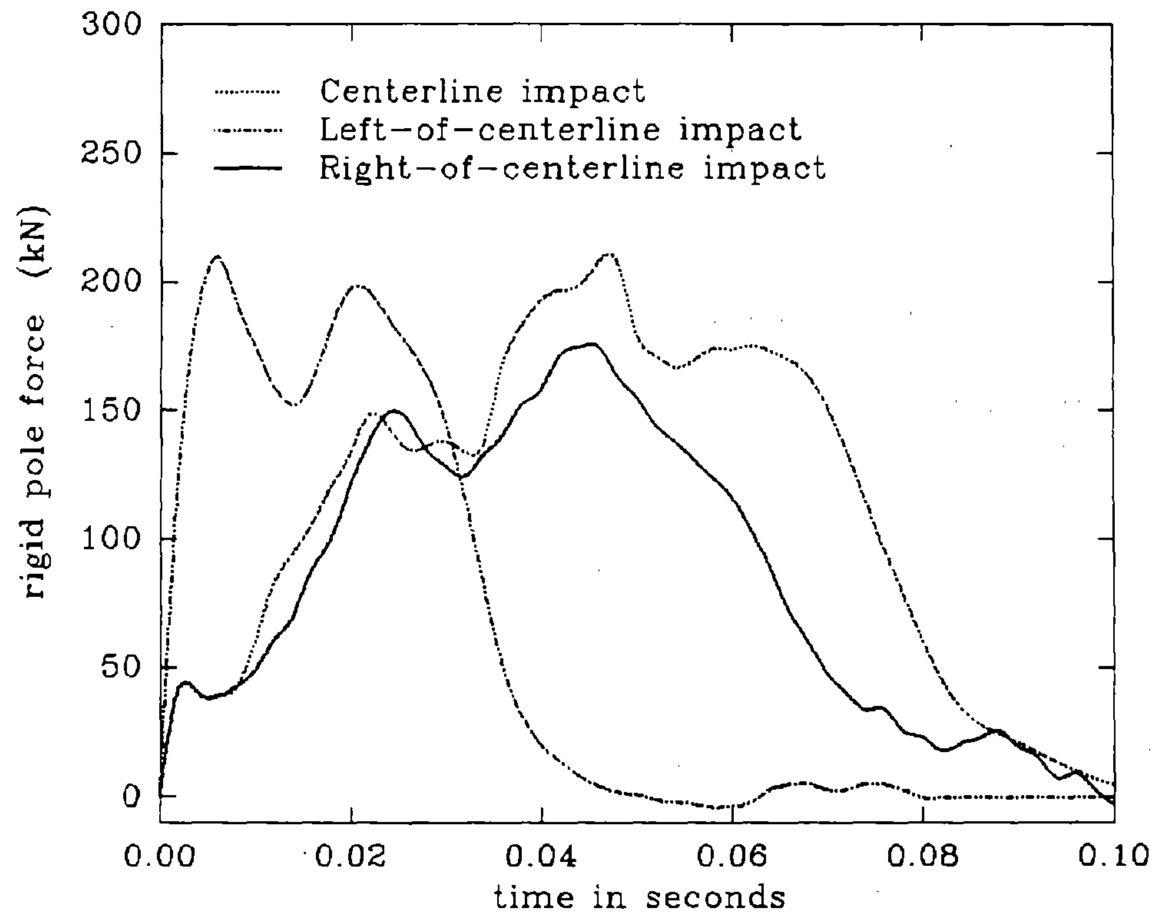

Figure 38. Rigid pole force versus time for all three simulations.

SUMMARY OF RESULTS

Figures 36 and 37 show plots of the acceleration, displacement, and rigid pole force for all three simulated impact cases. The peak accelerations and rigid pole forces were highest in the left-of-centerline (strong side) impact and smallest in the right-of-centerline (weak side) impact. The forces build up and decrease rapidly in both the centerline and left-of-centerline impacts, but tend to maintain a constant value over a much longer period of time in the right-of-centerline impact. The displacements were, however, highest in the centerline impact and smallest in the left-of-centerline impact.

Table 7 is a summary of the simulation and test results. The peak acceleration in all three impact cases, together with the time when these peaks occurred, are shown in the table. Also shown in this table are the maximum displacements at the CG of the vehicle and peak rigid pole forces. Simulation performance of the three impact cases on the Risc 6000/370 are shown in table 8.

Table 7. Summary of results.

	Acceleration	Displacement	Time of peak	Max. pole
Centerline impact				
DYNA3D	35.0	450.0	70.0	210.0
Test 91F049	33.5	455.0	70.0	170.0
Test 92F032	33.0	440.0	70.0	170.0
Test 92F033	31.5	430.0	69.0	---
Left-of-centerline impact	36.0	165.0	26.0	210.0
Right-of-centerline impact	23.0	370.0	50.0	170.0

Table 8. Simulation performance.

<u>Number of elements</u>		Hardware:	Risc 6000/370
Beams	60	Simulated time:	120 ms
Shells	2898		
Solids	633		
<u>Contact surfaces</u>		<u>Type of impact</u>	<u>cpu time</u>
Vehicle-Pole	1	Centerline impact	12.2 h
Vehicle-Vehicle	27	Left-of-centerline impact	12.2 h
		Right-of-centerline impact	10.2 h

CHAPTER 4. CONCLUSIONS

A simple finite element model of a small automobile (820C) impacting a rigid pole has been presented. The purpose of this study was to investigate and validate the reliability of using very simple finite element models in predicting the behavior of vehicles crashing into roadside safety hardware. This simplified model was found to be computationally efficient, reliable, and suitable for the rigid pole impact test. Peak values and shapes of the accelerations, displacements, and force curves agreed well with test data. Peak values were found to corresponded to unique events in the impact that would be clearly identifiable. This model can be used in designing and providing better insight into the behavior and response of vehicles during frontal impacts into roadside hardware.

The location of the engine block, the modeling of the engine mounts, and the way the engine block was supported by the engine mounts were found to play a crucial role in the response of the vehicle. The use of shell elements for the modeling of the engine mounts was found to be most reliable. Beam and truss elements were tried and discarded because they produced unsatisfactory results. Proper modeling of the engine mounts is a topic that deserves much more thought and effort.

The simulated deformation of the hood does not accurately model the actual crash of the test vehicle after impact. This is another area that deserves improvement for cosmetic (not load-producing) purposes only.

One of the setbacks of this model was that no attempts were made at properly matching the mass moments of inertia with that of the actual vehicle. These inertia properties tend to be significant in impact scenarios with large amounts of rolling, pitching, and yawing (e.g., barrier-type impacts), and thus must be corrected for.

During the rebound of the vehicle away from the rigid pole, it is felt that the velocity curves (test data versus simulation) can be better correlated during the rebound phase of the curve if the effect of gravity is included (refer to figure 17). This should be confirmed.

During the initial stages of impact, the velocity curves (test data versus simulation) diverge somewhat (refer to figure 17). This may be related to the fact that the center of gravity changes location during the impact due to deformation of the vehicle. This was not accounted for in the simulation. However, the reason for this deviation is not properly understood.

APPENDIX A

```
c  MODEL OF AN NCHRP REPORT 350 820C VEHICLE
c  By: Emmanuel Cofie, Source: 1992 Ford Festiva, Started: 9-1-93, last touched: 6-22-94
c  **********************
c  car model
c  **********************
c  Total mass of model ~ 0.826 Mg
c  Length of car   =  3761 mm
c  Track width     =  1290 mm
c  Width of car    =  1500 mm
c  Wheel Base      =  2300 mm
c  Total number of materials: 28
c  no. of beam  materials    6
c  no. of shell materials   13
c  no. of solid materials   11
c  Total number of parts:  31
c  Total number of slide  surfaces: 28
c +------------------------------------------------------------
c +  MATERIALS
c +------------------------------------------------------------
c Mat    Part                    Description
c  1     10                      firewall
c  2     10                      front body
c  3     10                      back body material
c  4     10                      windshield
c  5     10                      window
c  6     10                      area around CG
c  7     11                      hood
c  8     12                      engine block
c  9     13,14,15                 rubber tire
c  10    13,14,15                 tire rim
c  11    16                      bumper material
c  12    17                      lower core support
c  13    18                      radiator material
c  14    19                      cradle material
c  15    20,21,22,23,24,25          frame horn
c  16    26                      fun material
c  17    27                      front strip
c  18    1, 3,7                  front axle, back axle, rods to engine
c  19    2                       rod behind lower core
c  20    5                       front shocks
c  21    6                       back shocks
c  22    28,29,30                 engine mount(1)
c  23    4                       attachment to floor pan
c  24    8,9                     bolts, ribs for hood
c  25    31                      box at CG
c  26    32                      rigid pole
c  PARAMETER DEFINITION
c +------------------------------------------------------------
para                   c parameter
c  overall vehicle dimension
body_width  1500          c  maximum width of body
```

Preceding Page Blank

```
in_fndr      535               c  y location of inner fender
front_of_body   0              c  front of body
frnt_overhang  600             c  distance from edge of vehicle to front axle
back_of_body  -3510            c  back of body
body_roof_z  1420              c  roof of car
hood_back_z  914               c  height of hood above ground
f_wall_x -940                 c x distance from front of body to firewall
f_wall_z  742                 c  height of top of firewall
c  tire and wheel position
whgt 267 wrad 267  whgt1 320  c  center of wheel , out and inner radius
tire_diameter   320            c  tire diameter
rim_diameter     165            c  rim diameter
tire_width       150           c  tire width
front_axel_x      -600
rear_axel_x   -2900
trac 1400                     c  track distance
wloc [%body_width/2+%tire_width]  c location of inner edge of tire
wroc [%body_width/2-%tire_width]  c  location of inner edge of tire
efx -270                       c  front of engine block x
ebx -790                       c  back  of engine block x
ecx [(%efx+%ebx)/2]                c  center of engine  x
ely -290                       c  left  location of engine y
ery 350                        c  right location of engine y
flv1 304                       c  floor of car
ucar 254                       c  under of car
etz 720                        c  top of engine
ebz [%flv1+25]                  c
ebz2 [%ebz+100]                  c  bottom of engine
suey1 -25 suey2 125              c
lebp -847  -535                c
bmly2 -457.2 bmry1 457.2          c
rebp 847 bb1x1 102                c
bb1x2 5                        c
bbm1 381 tbm1 520                 c  location of bumper
bbm2 241 tbm2 304 bb2x1 -12        c  location of lower core
rdx1 -32. rdx2 -80 lrdy1 -253.6   c
rrdy2 333.66 lrdy1 -253.6         c  radiator location
xfun -110                      c  fun
cofx2 [%f_wall_x+70] cofx [%rdx2-70]  c  location of engine support
lcgx -1475 lcgz 500 lcgy 0        c  location of accelerometer CG
lcgx1 [%lcgx+50] lcgx2 [%lcgx-50] c nodes around CG
rig1  109  rig2 60             c  radius of rigid pole
lcel1 280  lcel2  840 pcen 213    c  location of load cells egx
ttk1 1.54                      c  thickness of body
ttk2 3.0                       c  thickness of firewall
ttk3 1.54                      c  thickness of bumper (from measurements)
ttk4 1.54                      c  thickness of bumper support
ttk5 2.5                       c  thickness of engine cradle
ttk6 8.0                       c  thickness of box at CG
ttk7 3.0                       c  thickness of floor
ttk8 5.0                       c  thickness of windshield
ttk9 1.54                      c  thickness of inner fender
wse1 200.0e3 wse2 0.33 wse3 207  wse4 200  c
wse5 7.92e-9                   c  material properties for steel
```

```
wge1 80.0e3  wge2 0.33 wge5 2.2e-9  c  material properties for glass
wre1 30.0e3  wre2 0.33 wre3 20. wre4 30. radwse5 1.3e-9 c material properties for radiator
wfe1 20.0e3  wfe3 20.  wfe4 20. funwse5 0.3e-9  c  material properties for fun (thermoplastic)
tmeng  0.17   egwse5 1.518e-9  c  mass of engine block - changed to match test (festiva)
tmbdy1 0.436  bdwse5 1.812e-8  c  mass of part of body - changed to match test (festiva)
tmbdy2 0.014 flwse5 4.8e-8     c  mass of floor around CG
tmbdy3 0.014 bxwse5 1.04e-8    c  mass of box at CG
tmtir1 0.015 tiwse5  2.990e-10 c  mass of tire
tmtir2 0.025 rimwse5 8.78e-10  c  mass of rim
tmrigp  500.  rigwse5  4.05e-5 c   1.5505e-5  mass of rigid pole
bmwse5 7.92e-9  bkwse5 7.92e-9 c
bswse5 7.92e-9  brub1 2.5e-9   c
bst1 7.0e-8                  c
fden1 1.70e-8                 c
egx1 -1436.5 egx2 -1684.7      c
apx1 -140 apx2 [%frnt_overhang+100] apx3 [%f_wall_x+100]  f_wall_z1 900
apx4 [%rear_axel_x+%whgt1+10] apx5 [%rear_axel_x-%whgt1-10]   apz1 520.7 apz2 670 apz3 720
lslide 28    c last slideline number used
lmat 27 ;    c last material number used
c +-------------------------------------------------------------
c  Surface definitions
c  wheel shape
   sd 1 cy %frnt_overhang -%body_width %whgt 0. 1. 0. %whgt1
   sd 2 cy %rear_axel_x -%body_width/2 %whgt 0. 1. 0. %whgt1  c
c the windshield plane
   sd 3 plan %ecar  -%body_width/2 %hood_back_z -21.  0.  7
   sd 4 plan %f_wall_x -%body_width/2 %hood_back_z  21.  0.  18
c  wheel
   sd 5  cy %frnt_overhang -%body_width/2 %whgt 0. 1. 0. %wrad
   sd 6  cy %frnt_overhang -%body_width/2 %whgt 0. 1. 0. %rim_diameter
   sd 7  cy %frnt_overhang [%body_width/2-%tire_width+10] %whgt 0. 1. 0. %wrad
   sd 8  cy %frnt_overhang [%body_width/2-%tire_width+10] %whgt 0. 1. 0. %rim_diameter
   sd 9  cy %rear_axel_x -%body_width/2 %whgt 0. 1. 0. %wrad
   sd 10 cy %rear_axel_x -%body_width/2 %whgt 0. 1. 0. %rim_diameter

c +-------------------------------------------------------------
c +  SLIDELINE DEFINITION
c +-------------------------------------------------------------
sid 1  sv pen kfric 0.25 fric 0.25; c pole[m] to bumper-lower core-front-cradle-radiator[s]
sid 2  sv  pen ; c bumper[m] to radiator-front[s]
sid 3  sv  pen ; c radiator[s] to engine[m]
sid 4  sv  pen ; c engine[s] to firewall[m]
sid 5  sv  pen ; c top radiator-engine[s] to hood_back_z[m]
sid 6  sv pen  ; c engine-radiator[s] to left frame[m]
sid 7  sv pen  ; c engine-radiator[s] to right frame[m]
sid 8  sv pen  ; c engine[s] to left fender[m]
sid 9  sv pen  ; c engine[s] to right fender[m]
sid 10 sv pen  ; c bottom of engine[s] to cradle[m]
sid 11 single pen; c bumper self-contacting
sid 12 single pen; c lower core support self-contacting
sid 13 single pen; c left frame horn self-contacting
sid 14 single pen; c right frame horn self-contacting
sid 15 dnt       ; c left fender[m] to frame[s]
sid 16 dnt       ; c right fender[m] to frame[s]
```

```
sid 17 dnt       ; c mtm accelerometer box[m] to floor[s]
sid 18 sv pen    ; c left fender[m] to wheel[s]
sid 19 sv pen    ; c right fender[m] to wheel[s]
sid 20 single    ; c hood_back_z self-contacting
sid 21 sv pen kfric 0.10 fric 0.15 ; c ground surface[m] to wheel[s]
sid 22 single pen; c cradle self-contacting
sid 23 sv pen    ; c left fender[m] to wheel[s]
sid 24 sv pen    ; c right fender[m] to wheel[s]
sid 25 single pen; c left fender self-contacting
sid 26 single pen; c right fender self-contacting
sid 27 single pen; c engine mount self-contacting
sid 28 single pen; c
c +-------------------------------------------------------------
velocity  8940. 0. 0.
c  --- VEHICLE PARTS -----
c (1) FRONT    AXLE RODS
beam
c   axle nodes
rt %frnt_overhang         [%wloc-10]      %whgt     ; c  node 1
rt %frnt_overhang         [-%in_fndr]     %whgt     ; c  node 2
rt %frnt_overhang         %in_fndr        %whgt     ; c  node 3 intermediate node
rt %frnt_overhang         [%wroc+10]      %whgt     ; c  node 4
rt [%frnt_overhang+200]   0               %whgt     ; c  node 5 reference node
rt [%frnt_overhang+50]    [%wloc-10]      %whgt     ; c  node 6
rt [%frnt_overhang-50]    [%wloc-10]      %whgt     ; c  node 7
rt %frnt_overhang     [%wloc-10]     [%whgt-50]     ; c  node 8
rt %frnt_overhang     [%wloc-10]     [%whgt+50]     ; c  node 9
rt [%frnt_overhang+50]    [%wroc+10]      %whgt     ; c  node 10
rt [%frnt_overhang-50]    [%wroc+10]      %whgt     ; c  node 11
rt %frnt_overhang     [%wroc+10]     [%whgt-50]     ; c  node 12
rt %frnt_overhang     [%wroc+10]     [%whgt+50]     ; c  node 13
rt %ecx     %ely     %ebz          ; c  node 14
rt %ecx     %ery     %ebz          ; c  node 15
c  axle
bm 1  2 1 18 18 5; bm 2  3 1 18 18 5; bm 3  4 1 18 18 5;
bm 6  2 1 18 18 5; bm 7  2 1 18 18 5; bm 8  2 1 18 18 5;
bm 9  2 1 18 18 5; bm 10 3 1 18 18 5; bm 11 3 1 18 18 5;
bm 12 3 1 18 18 5; bm 13 3 1 18 18 5; bm 2 14 1 26 26 5;
bm 15 3 1 26 26 5;
endpart
c (2) Front attachment rod behind lower core
beam
rt %frnt_overhang [-%in_fndr] %whgt   ; c  node 1
rt %rdx2    %bmly2    %bbm2           ; c  node 2
rt %rdx2    %lrdy1    %bbm2           ; c  node 3
rt %rdx2    %suey1    %bbm2           ; c  node 4
rt %rdx2    %rrdy2    %bbm2           ; c  node 5
rt %rdx2    %bmry1    %bbm2           ; c  node 6
rt %frnt_overhang  %in_fndr  %whgt    ; c  node 7
rt %frnt_overhang  0        %bbm2     ; c  node 8 reference node
rt [(%rdx2+%frnt_overhang)/2]  0  %whgt ; c  node 9 reference node
c  axle
bm 1 2 2 19 19 9; bm 2 3 2 19 19 8; bm 3 4 3 19 19 8;
bm 4 5 3 19 19 8; bm 5 6 2 19 19 8; bm 6 7 2 19 19 9;
```

```
endpart
c (3) BACK AXLE
beam
c  rear axle nodes
rt %rear_axel_x     [%wloc-10]     %whgt          ; c  node 1
rt %rear_axel_x     [-%in_fndr]    %whgt          ; c  node 2
rt %rear_axel_x         %bmly2   %whgt            ; c  node 3
rt %rear_axel_x  [%sueyl+50]    %whgt             ; c  node 4
rt %rear_axel_x         %bmryl   %whgt            ; c  node 5
rt %rear_axel_x         %in_fndr   %whgt          ; c  node 6
rt %rear_axel_x  [%wroc+10]    %whgt              ; c  node 7
rt %rear_axel_x       [%sueyl+50]    %flvl        ; c  node 8
rt [%rear_axel_x+200]    0       %whgt            ; c  node 9 reference node
rt [%rear_axel_x+200]    0  [(%whgt+%flvl)/2]     ; c  node 10 reference node
rt [%rear_axel_x+50]     [%wloc-10]    %whgt    ; c  node 11
rt [%rear_axel_x-50]    [%wloc-10]    %whgt    ; c  node 12
rt [%rear_axel_x+50]     [%wroc+10]    %whgt    ; c  node 13
rt [%rear_axel_x-50]    [%wroc+10]    %whgt    ; c  node 14
rt %rear_axel_x     [%wroc+10]    [%whgt-50]    ; c  node 15
rt %rear_axel_x     [%wroc+10]    [%whgt+50]    ; c  node 16
rt %rear_axel_x     [%wloc-10]    [%whgt-50]    ; c  node 17
rt %rear_axel_x     [%wloc-10]    [%whgt+50]    ; c  node 18
c  axle
bm 1  2 1 18 18 9;  bm 2  3 1 18 18 9; bm 3  4 1 18 18 9;
bm 4  5 1 18 18 9;  bm 5  6 1 18 18 9; bm 6  7 1 18 18 9;
bm 4  8 1 18 18 10; bm 11 2 1 18 18 9; bm 12 2 1 18 18 9;
bm 13 6 1 18 18 9;  bm 14 6 1 18 18 9; bm 15 6 1 18 18 9;
bm 16 6 1 18 18 9;  bm 17 2 1 18 18 9; bm 18 2 1 18 18 9;
endpart

c (4)  ATTACHMENT TO FLOOR PAN
beam
c  rear axle nodes
rt  %rear_axel_x   [-%in_fndr]    %whgt            ; c  node 1
rt  [(%rear_axel_x+%apx4)/2]   %bmly2     %flvl   ; c  node 3 intermediate node
rt  %rear_axel_x  %in_fndr    %whgt                ; c  node 2 intermediate node
rt  [(%rear_axel_x+%apx4)/2]   %bmryl %flvl        ; c  node 4 intermediate node
rt  [(%rear_axel_x+%whgt/2)] [(%wloc+%wroc)/2] [%flvl+200]  ; c  node 5 reference node
c  front nodes
rt  %frnt_overhang   [-%in_fndr]     %whgt         ; c  node 6
rt  [%f_wall_x+22] [-%in_fndr]    [%flvl-2]        ; c  node 7 intermediate node
rt  %frnt_overhang   %in_fndr    %whgt             ; c  node 8 intermediate node
rt  [%f_wall_x+22] %in_fndr     [%flvl-2]          ; c  node 9 intermediate node
rt  [(%frnt_overhang+%whgt/2)] [(%wloc+%wroc)/2] [%flvl+200] ; c  node 10 reference node
c  rear attachment
bm 1  2 1 23  23 5; bm 3  4 1 23  23 5;
c  front attachment
c bm 6 7 1 23  23 10;  c bm 8 9 1 23  23 10;
endpart

c  (5)  SHOCKS [spring]
beam
rt %frnt_overhang [-%in_fndr]  %whgt        ; c  node 1
rt %frnt_overhang  %wloc [%whgt+%whgtl]      ; c  node 2
```

```
rt %frnt_overhang %in_fndr  %whgt          ; c  node 3
rt %frnt_overhang  %wroc  [%whgt+%whgt1]    ; c  node 4
rt %frnt_overhang 0 [(%whgt+%apz2)/2]       ; c  node 5 reference node
c  rear axle nodes
rt %rear_axel_x   [-%in_fndr]   %whgt     ; c  node 6
rt %rear_axel_x    %wloc     [%whgt+%whgt1] ; c  node 7 intermediate node
rt %rear_axel_x   %in_fndr   %whgt       ; c  node 8
rt %rear_axel_x    %wroc     [%whgt+%whgt1]; c  node 9 intermediate node
rt %rear_axel_x    0     [(%flv1+%whgt)/2] ; c  node 10 reference node
c front springs
bm 1 2 1 20 20 5; bm 3 4 1 20 20 5;
c  back springs
bm 6 7 1 21 21 10; bm 8 9 1 21 21 10;
endpart

c (6)  front beam
block
-1;1 6 10 16 19; 1 3;
%rdx1
[-%in_fndr+2.5]  %lrdy1 %suey1 %rrdy2 [%in_fndr-2.5]
%apz2 %f_wall_z
pb 1 1 1 1 5 1 x 0
pa 1 1 1 y [-%in_fndr]
pa 1 5 1 y %in_fndr
pa 1 3 2 z [%f_wall_z-4]
thic 1.54
mate 17
orpt  +  %pcen 0 %f_wall_z
sii -1 ; ; ; 1 s
orpt - %pcen 0 %f_wall_z
sii -1 ;2 4 ; ; 2 m
orpt - %pcen 0 %f_wall_z
sii -1 ; ; ; 5  s
orpt off
endpart

c  (7) bolts and brackets
beam
c
rt %rdx1  %lrdy1  %f_wall_z;            c   node 1
rt %rdx1  %lrdy1  [%f_wall_z-4];        c   node 2
rt %rdx1  %rrdy2  %f_wall_z;            c   node 3
rt %rdx1  %rrdy2  [%f_wall_z-4];        c   node 4
rt %rdx1  %suey1  %f_wall_z;            c   node 5
rt %rdx1  %suey1  [%f_wall_z-4];        c   node 6
rt 0  %wloc [(%tbm1+(%bbm1+%tbm2)/2)/2];     c   node 7
rt 5  %wloc  [%bbm1+(%tbm1-%bbm1)/3]  ;     c   node 8
rt 0  %wloc %tbm1   ;                  c   node 9
rt 5  %wloc %tbm1   ;                  c   node 10
rt 0  [(-%body_width/2+%wloc)/2] [(%tbm1+(%bbm1+%tbm2)/2)/2]     ; c node 11
rt 5  [(-%body_width/2+%wloc)/2] [%bbm1+(%tbm1-%bbm1)/3]        ; c node 12
rt 0  [(-%body_width/2+%wloc)/2] %tbm1   ;                  c node 13
rt 5  [(-%body_width/2+%wloc)/2] %tbm1   ;                  c node 14
rt 0  %wroc [(%tbm1+(%bbm1+%tbm2)/2)/2]  ;                  c node 15
```

```
rt 5  %wroc [%bbm1+(%tbm1-%bbm1)/3]   ;                          c node 16
rt 0  %wroc %tbm1   ; c node 17
rt 5  %wroc %tbm1   ; c node 18
rt 0  [(%body_width/2+%wroc)/2] [(%tbm1+(%bbm1+%tbm2)/2)/2]     ; c node 19
rt 5  [(%body_width/2+%wroc)/2] [%bbm1+(%tbm1-%bbm1)/3]        ; c node 20
rt 0  [(%body_width/2+%wroc)/2] %tbm1                    ; c node 21
rt 5  [(%body_width/2+%wroc)/2] %tbm1                    ; c node 22
rt 2.5  [-%body_width/2]   %flv1;                   c node 23
rt 2.5  %body_width/2   %flv1;                      c node 24
rt %rdx1  %lrdy1  [%f_wall_z-4-(%f_wall_z-4-(%ebz2+5))/4];       c node 25
rt 0      %lrdy1  %apz2;                          c node 26
rt %rdx1  %rrdy2  [%f_wall_z-4-(%f_wall_z-4-(%ebz2+5))/4];       c node 27
rt 0  %rrdy2  %apz2;                              c node 28
c
c  tied rods
bm 1  2  1 26  26 23; bm 25 26 1 26  26 23;  bm 3  4  1 26  26 23;
bm 27 28 1 26  26 23; bm 5  6  1 26  26 23;  bm 7  8  1 24  24 23;
bm 9  10 1 24  24 23; bm 11 12 1 24  24 23;  bm 13 14 1 24  24 23;
bm 15 16 1 24  24 24; bm 17 18 1 24  24 24;  bm 19 20 1 24  24 24;
bm 21 22 1 24  24 24;
endpart

c  --- VEHICLE PARTS -----
c (8) BODY
block
 -1 2  -4  5 7 -8 10 12 13 -20 22 -24 25 -26;
 -1 3 -4  5 9 10 11 13 14  15  18  -19  20 -22;
  1 -2 3 -5 7 -9 -13 ;
0 %apx1 %apx2 %frnt_overhang %apx3 %f_wall_x [(%f_wall_x+%lcgx)/2] %lcgx1 %lcgx2
%apx4 %rear_axel_x %apx5 [(%ecar+%apx5)/2] %back_of_body
[-%body_width/2] %wloc [-%in_fndr]  %bmly2 [%suey1-50] %suey1 [%suey1+50] %suey2
[%suey2+50] [%suey2+100] %bmry1  %in_fndr %wroc %body_width/2
%whgt  %flv1 [(%bbm1+%tbm2)/2] %tbm1  %apz2  %hood_back_z  %body_roof_z
c  create front shape of car
  dei  1 6;            ;    -7 ;
  dei  1 6;-1 -3 -12  -14   ; 6    7 ;
  dei  3 5;-3 -12 ;  1 2;
c remove floor for engine placement
  dei  1 5; 4  11  ; 3  5;
  dei  1 6; 3 12   ;  -2 ;
c inside of car
  dei 7 13; 4 11   ; 3  6;
  dei 10 13;-3  -12; 4  7;
  dei 6 14;-3  -12; 6  7;
  dei 6 14; 1  14 ;   -6;
  dei 6 10 0 12 13;-3  -12; 1  6;
  dei -3 -10 -12;3  12;  ;
  dei -3 -10 -12;1 3 0 12 14; 4 7;
  dei 1 3 0 6 10 0 12 13;1 3 0 12 14; -4;
  dei  ; 3 12; -4;
  dei 3 6 0 10 12 ; 1 3 0 12 14; -2;
  dei 1 3 ; 1 3 0 12 14; -2;
c create engine compartment
  dei   -1; 3 12  ;1   6;
```

```
 dei  -1;      ;6  7;
c create shape of hood_back_z
 sfi 1 6;1 14   ; -6; plan  %f_wall_x 0  %hood_back_z  0.189 0. 1.
 dei  1 5; 3 12 ; -6;
c create the wheel wells
 dei     3 6;   -1 3 0 12  -14; 1 4;
 dei    10 12;  -1 3 0 12  -14; 1 4;
 sfi  -3  -6; -1  3 0 12 -14; 1 -4; sd 1
 sfi  -10 -12; -1 3 0 12 -14; 1 -4; sd 2
  mb 7 6 2 10 7 2  z 100
  mb 1 3  6 5  3 6    y 2.5
  mb 1 12 6 5 12 6    y -2.5
c project hatchback
  sfi -14;        ; 6  7;  sd 3
c project windshield
 sfi  -6;1 14   ; 6  7;  sd 4
c create inner and outer shape of body
sfi 6 14;-1 ;1 6;cy %lcgx [-%body_width/2+2500] [(%whgt1+%hood_back_z)/2] 1 0 0 2500
sfi 6 14;-14;1 6;cy %lcgx [%body_width/2-2500] [(%whgt1+%hood_back_z)/2] 1 0 0 2500
sfi 6 14;1 14;-7 ;cy %lcgx 0 [%body_roff_z-8000] 1 0 0 8000
 mb  6 1  7  14 1  7  y   50   c move to y -675
 mb  6 14 7  14 14 7  y  -50   c move to y  675
c  windshield and back body  materials
  thi   -6 -14;2 13; 6 7; %ttk8
  mti   -6 -14;2 13; 6 7; 4
c floor of car
 thi 6 13;  ;   -2; %ttk7
c firewall
 thi   -6;   ; 1 6; %ttk2
 mti   -6;   ; 1 6; 1
cpl 6 1  7  14 14  7  i
cpl 6 1  7  14 14  7  j
cpl 6 1  6  14 1 6
cpl 6 14  6  14 14 6
c  front of car
mt 1 1 1 5 14 7  2  c
mti 8 9;4 11 ; -2; 6      c  isolate floor for accelerometer
c  side window - glass
mti 6 13; -1  -14 ; 6 7; 5       c
thic %ttk1
mate 3

c  contact surfaces
orpt + 213.  0.   440      c [ rigid pole barrier to face of car ]
sii -1;1 3 0 12  14; 1 6  ; 1  s
orpt +  50  0. [(%bbm1+%tbm1)/2]     c bumper to fender
sii -1;1 3 0 12  14 ;1 4  ; 2  s
orpt + [(%f_wall_x+%ebx)/2] 0. [(%etz+%flv1)/2] c firewall to engine
sii  -6;     3 12;    2 6; 4  m
orpt + %ecx %ely [(%etz+%flv1)/2] c right fender to engine
sii  1 5;-3      ;     2 5; 8  m
orpt +  %ecx %ery [(%etz+%flv1)/2] c right fender to engine
sii  1 5;-12     ;     2 5; 9  m
orpt + %ecx  0.  [(%etz+%flv1)/2] c left fender to frame  tied node
```

```
sii  1 5;-3     ;    1 4;  15 m
orpt + %ecx 0. [(%etz+%flv1)/2] c right fender to frame  tied node
sii  1 5;-12  ;    1 4;  16 m
orpt + %lcgx 0 %lcgz  c l fender to wheel
sii  8 9; 6 7 ;-2;  17 m
orpt - %frnt_overhang 0 [(%whgt+%flv1)/2] c left fender to wheel
sii  1 5;-3     ;    1 5;  18 m
orpt - %frnt_overhang 0 [(%whgt+%flv1)/2] c right fender to wheel
sii  1 5;-12       ; 1 5;  19 m
orpt + %frnt_overhang [(-%body_width/2+%wloc)/2]  %whgt c left fender to wheel
sii  3 6; 1 3  ; -4;  23 m
orpt + %frnt_overhang [(-%body_width/2+%wloc)/2]  %whgt c left fender to wheel
sii  -3 -6; 1 3  ; 2 4;  23 m
orpt + %frnt_overhang [(%body_width/2+%wroc)/2]  %whgt c right fender to wheel
sii  3 6; 12 14 ; -4;  24 m
orpt + %frnt_overhang [(%body_width/2+%wroc)/2]  %whgt c right fender to wheel
sii  -3 -6; 12 14 ; 2 4;  24 m
orpt + %frnt_overhang [(-%body_width/2+%wloc)/2]  [(%whgt+%hood_back_z)/2] c left fender self-
contacting
sii  3 6;  -1 -3 ; ;  25 s
orpt + %frnt_overhang [(-%body_width/2+%wloc)/2]  [(%whgt+%hood_back_z)/2] c left fender self-
contacting
sii  3 6;   1 3 ; -4;  25 s
orpt + %frnt_overhang [(%body_width/2+%wroc)/2]  [(%whgt+%hood_back_z)/2] c right fender self-
contacting
sii  3 6; -12 -14 ;  ;  26 s
orpt + %frnt_overhang [(%body_width/2+%wroc)/2]  [(%whgt+%hood_back_z)/2] c right fender self-
contacting
sii  3 6; 12 14 ; -4;  26 s
orpt off
endpart

c Hood_back_z  PART (9)
block
1 3 11 13 ;1 2  8  15 16; -1 ;
0 -100 [%f_wall_x+100] %f_wall_x  [-%in_fndr] %bmly2  %sueyl %bmryl in_fndr  %hood_back_z
sfi  ;     ; -1; plan  %f_wall_x 0  %hood_back_z  0.189 0. 1.
dei 3 4 ; ;-1 ;
mb 2 3 1 3 3 1 z 10
thic 1.65     c
mate 7
c  contact surfaces
orpt + %ecx 0. %hcar  c  post
sii   ;  ; -1;  1 s
orpt +  %ecx  0. [(%etz+%ebz)/2]  c  top of engine to fender
sii   ;  ; -1;  5 m
orpt +  %ecx  0. [(%etz+%ebz)/2]  c  self-contacting
sii   ;  ; -1; 20 s
orpt off
endpart

c (10) ENGINE
block
1 3 4 5 7 ;1 5 6 7 8 9 12;1 3 4 8;
```

```
%ebx [%ecx-50] %ecx [(%ecx+%efx)/2] %efx
%ely %sueyl  [%sueyl+50] [%sueyl+100] %suey2 [%suey2+50] %ery c
%ebz  %ebz2  %tbm1  %etz
dei    ; 6 7 ; 3 4;
dei 4 5; 6 7 ; 1 3;
mti 1 4; 6 7 ; 1 3; 27
mate 8
c  contact surfaces
orpt  +  %pcen   0. [(%etz+%ebz)/2]   c to pole
sii   -5;   ;   ; 1 s
orpt  +  %pcen   0. [(%etz+%ebz)/2]   c to pole
sii   -4;6 7 ;  ; 1 s
orpt  +  %apx1   0. [(%etz+%ebz)/2]   c to radiator
sii   -5;   ;   ; 3 m
orpt  +  %apx1   0. [(%etz+%ebz)/2]   c to radiator
sii   -4;6 7 ;  ; 3 m
orpt  +  %f_wall_x  0. [(%etz+%ebz)/2]   c to firewall
sii   -1;   ;   ; 4 s
orpt  +  %ecx   0. %hood_back_z    c to hood_back_z
sii     ;   ;   -4; 5 s
orpt - %ecx  0 [(%etz+%ebz)/2] c left frame horn
sii     ;   -1;   ; 6 s
orpt - %ecx  0 [(%etz+%ebz)/2] c right frame horn
sii     ;   -7;   ; 7 s
orpt - %ecx  0 [(%etz+%ebz)/2] c left fender
sii     ; -1;     ; 8 s
orpt - %ecx  0 [(%etz+%ebz)/2] c right fender
sii     ;-7 ;     ; 9 s
orpt  +  %ecx [(%sueyl+%suey2)/2]  0  c  engine to cradle
sii     ;    ;  -1; 10 s
orpt off
endpart

c (11) FRONT WHEELS
block
1  2 3 4 5 6 7; 1 3; 1 2 3 4 5 6 7;
[(%frnt_overhang-127)] [(%frnt_overhang-127)] [(%frnt_overhang-50)] %frnt_overhang
[(%frnt_overhang+50)] [(%frnt_overhang+127)] [(%frnt_overhang+127)]
[-%body_width/2]  [-%body_width/2+%tire_width-10]
127  127 [%whgt-50]  %whgt  [%whgt+50] 381 381
dei 1 2 0 6 7;  ; 1 2 0 6 7;
sfi -1 -7;  ;      ;sd 5
sfi       ;  ;-1 -7 ;sd 5
sfi -2 -6;  ; 2 6  ;sd 6
sfi  2 6 ;  ;-2 -6 ;sd 6
c swi   ;  ; -1;  1
mti 2 6;1 2 ;2 6; 10
mate 9
c  contact surfaces
orpt  +   %frnt_overhang %ely  [(%whgt+%flv1)/2]    c inner wall of fender
sii   ;-2;  ; 18 s
orpt -  %lcgx  0  %hood_back_z
sii   ; ;-1  ; 21 s
orpt - %frnt_overhang   [(-%body_width/2+%wloc)/2]  %whgt c right fender to wheel
```

```
sii   ;  ; -7 ;  23 s
orpt - %frnt_overhang   [(-%body_width/2+%wloc)/2]  %whgt c right fender to wheel
sii  -1 -7; ;  ;  23 s
orpt off
c lct 1 rxz;
c lrep 0 1;
endpart

c (12) FRONT WHEELS
block
1  2 3 4 5 6 7; 1 3; 1 2 3 4 5 6 7;
[(%frnt_overhang-127)] [(%frnt_overhang-127)] [(%frnt_overhang-50)] %frnt_overhang
[(%frnt_overhang+50)] [(%frnt_overhang+127)] [(%frnt_overhang+127)]
[%body_width/2-%tire_width+10]  %body_width/2
127  127 [%whgt-50]  %whgt  [%whgt+50] 381 381
dei 1 2 0 6 7;  ; 1 2 0 6 7;
sfi -1 -7;  ;      ;sd 7
sfi      ;  ;-1 -7 ;sd 7
sfi -2 -6;  ; 2 6  ;sd 8
sfi  2 6 ;  ;-2 -6 ;sd 8
c swi    ;  ; -1;  1
mti 2 6;1 2 ;2 6; 10
mate 9
c  contact surfaces
orpt +  %frnt_overhang %ery [(%whgt+%flvl)/2]    c inner wall of fender
sii   ;-1;  ; 19  s
orpt -  %lcgx  0  %hood_back_z
sii   ; ;-1  ; 21 s
orpt - %frnt_overhang [(%body_width/2+%wroc)/2]  %whgt c right fender to wheel
sii   ;  ; -7 ;  24 s
orpt - %frnt_overhang [(%body_width/2+%wroc)/2]  %whgt c right fender to wheel
sii  -1 -7;  ; ;  24 s
orpt off
endpart

c (13) REAR WHEELS
block
1  2 3 4 5 6 7; 1 3; 1 2 3 4 5 6 7;
[(%rear_axel_x-127)] [(%rear_axel_x-127)] [(%rear_axel_x-50)] %rear_axel_x [(%rear_axel_x+50)]
[(%rear_axel_x+127)] [(%rear_axel_x+127)]
[-%body_width/2]  [-%body_width/2+%tire_width-10]
127  127 [%whgt-50]  %whgt  [%whgt+50] 381 381
dei 1 2 0 6 7;  ; 1 2 0 6 7;
sfi -1 -7;  ;      ;sd 9
sfi      ;  ;-1 -7 ;sd 9
sfi -2 -6;  ; 2 6  ;sd 10
sfi  2 6 ;  ;-2 -6 ;sd 10
c swi   ; ; -1;  1
orpt -  %lcgx  0  %hood_back_z
sii   ; ;-1  ; 21 s
c orpt -  %rear_axel_x 0 %whgt     c to inner wall
c sii    ; ;-7  ; 21  s
c mti 2 6;1 2 ;2 6; 10
mate 9
```

```
lct 1 rxz;
lrep 0 1;
endpart

c (14) BUMPER
block
-1  -3; -1 2 4 5 7 23 25 26 28 -29 ; -1 -4;
5.  102. %lebp [-%body_width/2] %wloc [-%in_fndr] %bmly2 %bmry1 %in_fndr %wroc [%body_width/2]
%rebp
%bbm1  %tbm1
mb 2 1 1 2 1 2 xy -30 45   c  curved shape at end
mb 2 10 1 2 10 2 xy -30 -45 c
thic %ttk3
mate 11
c  contact surfaces
orpt +  213. 0. [(%bbm1+%tbm1)/2]
sii   -2;2 9   ;       ; 1  s   c  to post
orpt -   50. 0. [(%bbm1+%tbm1)/2]
sii      ;2 9   ;-1 -2  ; 1  s    c  to post
orpt - 110. 0. [(%bbm1+%tbm1)/2]
sii -1; 2 9  ;     ; 2  m        c   to radiator
orpt - 50. 0. [(%bbm1+%tbm1)/2]
sii 1 2  ; 2 9  ;-1 -2; 2  m         c    to radiator
orpt  + 50. 0. [(%bbm1+%tbm1)/2]
sii   ;         ;-1 -2; 11 s        c self-contacting
c added front and back self-contact
orpt  + 50. 0. [(%bbm1+%tbm1)/2]
sii  -1 -2;    ;      ; 11 s        c self-contacting
orpt off
endpart

c (15) LOWER CORE SUPPORT
block
-1 -3; -1 3 6 9 10 11 12 16 18 -20; -1  -3;
%rdx2  %rdx1 [-%in_fndr] %bmly2 %lrdy1 %suey1 [%suey1+50] [%suey2-50] %suey2 %rrdy2
%bmry1 %in_fndr  %bbm2  %tbm2
thic %ttk3
mate 12
c  contact surfaces
orpt +     %pcen  0. %whgt
sii      -2;    ;      ; 1 s        c    to post
orpt - [(%rdx2+%rdx1)/2]  0. [(%bbm2+%tbm2)/2]
sii         ;  ;-1  -2; 1 s         c     to post
orpt + [(%rdx2+%rdx1)/2]  0. [(%bbm2+%tbm2)/2]
sii         ;2 9 ;-1  -2;12 s    c   self-contacting
orpt  + [(%rdx2+%rdx1)/2]  0. [(%bbm2+%tbm2)/2]
sii  -1 -2 ;2 9 ; ;12 s    c  self-contacting
orpt off
endpart

c (16) RADIATOR
block
1 2; 1 4 6 9; 1 2  6;
%rdx2 %rdx1  %lrdy1 %suey1 %suey2 %rrdy2  %flv1 [%ebz2+5] [%f_wall_z-4]
```

```
orpt + 213  0.  [(%bbm1+%tbm1)/2] c post
sii -2; ;      ; 1 s
orpt +  213  0.  [(%bbm1+%tbm1)/2] c bumper
sii -2; ;      ; 2 s
orpt +  %apx1 0.  [(%etz+%flv1)/2]  c engine
sii -1;   ;1 2 ; 3 s
orpt +   [(%rdx2+%rdx1)/2]  0.   %hood_back_z
sii   ;  ; -3  ; 5 s
orpt -  %ecx [(%lrdy1+%rrdy2)/2] [(%etz+%flv1)/2]  c left frame horn
sii  ;-1 ;     ; 6 s
orpt -  %ecx [(%lrdy1+%rrdy2)/2] [(%etz+%flv1)/2]  c right frame horn
sii  ;-4 ;     ; 7 s
orpt off
endpart

c (17) evaporator core
block
1 2; 1 4 6 9; 1 5;
%xfun %rdx2  %lrdy1 %suey1 %suey2  %rrdy2 [%ebz2+5]  [%f_wall_z-4]
mb 1 1 1 1 4 1 x 20
mate 16
c  contact surfaces
orpt  +  %efx 0 [(%etz+%flv1)/2]    c engine
sii   -1;  ;  ; 3 s
orpt  +  [(%rdx2+%xfun)/2] 0 %hood_back_z   c to hood_back_z
sii    ;  ; -2 ; 5 s
orpt off
endpart

c (18) ENGINE CRADLE
block
1 3 5 8 10 11 12 14 17 20 22 23; -1 2 3 -4; -1 2 ;
%f_wall_x %cofx2 %ebx [(%ebx+%ecx)/2] [%ecx-50] %ecx [%ecx+50]
[(%efx+%ecx)/2] %efx %cofx %rdx2 [(%rdx2+%rdx1)/2]  %suey1 [%suey1+50] [%suey2-50] %suey2
%whgt %flv1
mb 1  1 1 9 4 2 y 50
pb 10 1 1 12 1 1 z [(%bbm2+%tbm2)/2]
pb 10 4 1 12 4 1 z [(%bbm2+%tbm2)/2]
dei 5 7 ; 2 3; -1;
thic %ttk5
mate 14
c  contact surfaces
orpt  +  %ecx [%suey1+30] 0.
sii 1 12; ; -1;  1 s
orpt  +  %ecx [(%suey1+%suey2)/2]  %ebz  c  engine to cradle
sii ; ; -1; 10 m
orpt  +  %ecx [(%suey1+%suey2)/2]  %ebz2  c engine to cradle
sii ;-1 -4 ;   ; 10 m
orpt  +  %ecx [(%suey1+%suey2)/2]  [(%whgt+%flv1)/2]  c   cradle
sii ;      ; -1; 22  s
orpt  +  %ecx [(%suey1+%suey2)/2]  [(%whgt+%flv1)/2]  c   cradle
sii ;-1 -4 ;   ; 22  s
orpt off
endpart
```

```
c (19) HORN TO BUMPER (L)  c left frame horn
block
1 3 5 8;-1 -3;-1 -3 ;
102. 5. -150. -400.  [-%in_fndr] %bmly2  %bbm1  %tbm1
pb 4 1 1 4 2 1 z [(%bbm1+%tbm2)/2]
thic %ttk4
mate 15
c  contact surfaces
c orpt  +  %pcen [(-%in_fndr+%bmly2)/2] [(%bbm1+%tbm1)/2] c to pole
c sii -1  ; ;  ;  1 s
orpt  +  %ecx %ely [(%bbm1+%tbm1)/2]  c left side of engine
sii    ;-2;  ; 6 m
orpt - %ecx 0.  [(%bbm1+%tbm1)/2]   c tied to left fender
sii    ;-1;  ; 15 s
orpt  +  %ecx [(-%in_fndr+%bmly2)/2]  [(%bbm1+%tbm1)/2]   c self-contacting
sii    ;-1 -2;  ; 13 s
orpt off
endpart

c (20) HORN TO BUMPER (R)  right frame horn
block
1 3 5 8;-1 -3;-1 -3 ;
102 5. -150. -400.  %in_fndr %bmry1  %bbm1  %tbm1
pb 4 1 1  4 2 1 z [(%bbm1+%tbm2)/2]
thic %ttk4
mate 15
c  contact surfaces
c orpt  +  %pcen [(%bmry1+%in_fndr)/2] [(%bbm1+%tbm1)/2] c to pole
c sii -1  ; ;  ;  1 s
orpt  +  %ecx %ery [(%bbm1+%tbm1)/2]  c left side of engine
sii    ;-2;  ; 7  m
orpt - %ecx 0.  [(%bbm1+%tbm1)/2]   c tied to right fender
sii    ;-1;  ; 16 s
orpt  +  %ecx [(%bmry1+%in_fndr)/2]  [(%bbm1+%tbm1)/2]   c self-contacting
sii    ;-1 -2;  ; 14 s
orpt off
endpart

c  (21) HORN TO LOWER CORE SUPPORT (L)
block
1 2 4 8;-1 -3 ;-1 -3 ;
%rdx1  %rdx2  -150. -400. [- %in_fndr] %bmly2 %bbm2 %tbm2
pb 4 1 2  4 2 2  z [(%bbm1+%tbm2)/2]
mb 4 1 1  4 2 1  z [(%bbm1-%tbm2)/2]
thic %ttk4
mate 15
c  contact surfaces
c orpt  +  %pcen [(-%in_fndr+%bmly2)/2] [(%bbm2+%tbm2)/2] c to pole
c sii -1  ; ;  ;  1 s
orpt  +  %ecx %ely [(%bbm2+%tbm2)/2] c left side of engine
sii     ;-2;  ;  6 m
orpt - %ecx 0.  [(%bbm2+%tbm2)/2] c tied to left fender
sii     ;-1;  ; 15 s
orpt  +  %ecx [(-%in_fndr+%bmly2)/2]  [(%bbm1+%tbm1)/2]  c self-contacting
```

```
sii    ;-1 -2;  ; 13 s
orpt off
endpart

c  (22) HORN TO LOWER CORE SUPPORT (R)
block
1 2 4 8;-1 -3 ;-1 -3 ;
%rdx1 %rdx2  -150. -400.  %in_fndr %bmry1 %bbm2 %tbm2
pb 4 1 2  4 2 2  z [(%bbm1+%tbm2)/2]
mb 4 1 1  4 2 1  z [(%bbm1-%tbm2)/2]
thic %ttk4
mate 15
c  contact surfaces
c orpt  +  %pcen [(%bmry1+%in_fndr)/2] [(%bbm2+%tbm2)/2] c to pole
c sii -1  ; ;  ;  1 s
orpt  +  %ecx %ery [(%bbm2+%tbm2)/2] c left side of engine
sii     ;-2;  ; 7 m
orpt - %ecx 0.  [(%bbm2+%tbm2)/2] c left fender
sii     ;-1;  ;16 s
orpt  +  %ecx [(%in_fndr+%bmry1)/2]  [(%bbm1+%tbm1)/2]    c self-contacting
sii    ;-1 -2;  ; 14 s
orpt off
endpart

c (23) HORN TO FIREWALL (L)
block
1 4 5 6 7; -1 -3; -1 3 -4;
%f_wall_x %frnt_overhang %apx2 -450 -400  [-%in_fndr] %bmly2
%tbm1 [%tbm1-2*(%tbm1-(%bbm1+%tbm2)/2)/3] [(%bbm1+%tbm2)/2]
mb 5 1 3 5 2 3 z [-((%bbm1+%tbm2)/2-%bbm2-(%bbm1-%tbm2)/2)]
pb 5 1 2 5 2 2 z [(%bbm1+%tbm2)/2]
thic %ttk4
mate 15
c  contact surfaces
orpt  +  %ecx %ely [(%tbm2+%bbm1)/2]  c left side to engine
sii  ;-2;   ; 6 m
orpt - %ecx 0.  [(%tbm2+%bbm1)/2]  c left fender
sii  ;-1;   ; 15 s
orpt  +  %ecx [(%+%bmly2)/2]  [(%bbm1+%tbm1)/2]    c self-contacting
sii    ;-1 -2;  ; 13 s
orpt off
endpart

c (24) HORN TO FIREWALL (R)
block
1 4 5 6 7; -1 -3; -1 3 -4;
%f_wall_x %frnt_overhang %apx2 -450 -400  %in_fndr %bmry1
%tbm1 [%tbm1-2*(%tbm1-(%bbm1+%tbm2)/2)/3] [(%bbm1+%tbm2)/2]
mb 5 1 3 5 2 3 z [-((%bbm1+%tbm2)/2-%bbm2-(%bbm1-%tbm2)/2)]
pb 5 1 2 5 2 2 z [(%bbm1+%tbm2)/2]
thic %ttk4
mate 15
c  contact surfaces
orpt  +  %ecx %ery [(%tbm2+%bbm1)/2]  c left side to engine
```

```
sii ;-2; ; 7 m
orpt - %ecx 0. [(%tbm2+%bbm1)/2] c left fender
sii ;-1; ; 16 s
orpt + %ecx [(%in_fndr+%bmry1)/2] [(%bbm1+%tbm1)/2] c self-contacting
sii ;-1 -2; ; 14 s
orpt off
endpart

c (25) LEFT SIDE ENGINE MOUNT
block
-1 -4; -1 -4; -1 -4 ;
%apx2 %frnt_overhang [-%in_fndr] %ely %tbm1 %apz2
pa 1 2 1 xyz %ecx %ely %tbm1
pa 2 2 1 xyz [%ecx-50] %ely %tbm1
pb 1 2 2 2 2 2 y %bmly2
thic 2.0 c
mate 22
endpart

c (26) FRONT ENGINE MOUNT
block
-1 -3 ; -1 -2; -1 3 -4;
%rdx2 %cofx [%suey1+50] [%suey2-50] %whgt [%ebz2-125/3] %ebz2
mb 1 1 3 1 2 3 x -5
mb 2 1 2 2 2 2 x [2*(%efx-%cofx)/3]
pb 2 1 3 2 2 3 x %efx
thic 2.0
mate 22
orpt + %pcen [(%suey1+%suey2)/2] [(%apz2+%f_wall_z)/2] c to radiator
sii -1; ; ; 3 m
orpt + [(%cofx+%efx)/2] [(%suey1+%suey2)/2] [(%apz2+%f_wall_z)/2] c to radiator
sii ; ; -3; 3 m
orpt - %pcen [(%suey1+%suey2)/2] [(%apz2+%f_wall_z)/2] c to radiator
sii -2; ;1 2 ; 3 s
orpt + [(%rdx2+%xfun)/2] [(%suey1+%suey2)/2] [(%flv1+%ebz2)/2] c self-contacting
sii -1 -2 ; ; ; 27 s
orpt + [(%rdx2+%xfun)/2] [(%suey1+%suey2)/2] [(%flv1+%ebz2)/2] c self-contacting
sii ; ; -1 -3 ; 27 s
endpart

c (27) BACK ENGINE MOUNT
block
-1 -3 ; -1 -2; -1 3 -4;
%f_wall_x %cofx2 [%suey1+100] %suey2 %whgt [%ebz2-125/3] %ebz2
mb 1 1 3 1 2 3 x 5
mb 2 1 2 2 2 2 x [2*(%ebx-%cofx2)/3]
pb 2 1 3 2 2 3 x %ebx
orpt + %f_wall_x [(%suey1+%suey2)/2] [(%apz2+%f_wall_z)/2] c to firewall
sii -1; ; ; 4 s
orpt + [(%cofx2+%ebx)/2] [(%suey1+%suey2)/2] [(%apz2+%f_wall_z)/2] c to firewall
sii ; ; -3; 4 s
orpt - %f_wall_x [(%suey1+%suey2)/2] [(%apz2+%f_wall_z)/2] c to firewall
sii -2; ;1 2; 4 m
orpt + [(%cofx2+%f_wall_x)/2] [(%suey1+%suey2)/2] [(%flv1+%ebz2)/2] c self-contacting
```

```
sii  -1 -2  ;   ; ; 28 s
orpt + [(%cofx2+%f_wall_x)/2] [(%suey1+%suey2)/2] [(%flv1+%ebz2)/2] c self-contanting
sii  ; ; -1 -3  ; 28 s
thic 2.0
mate 22
endpart

c (28)  box AT CG
block
1 3; 1 3 ;1 2;
%lcgx1 %lcgx2  %suey1 [%suey1+50]  [%flv1+100] %lcgz
mate 25
orpt - %lcgx 0 %lcgz
sii ; ;-1 ; 17 s
orpt off
npb 1 1 2 2 2 2
npb 1 1 1 2 2 1
endpart

c MATERIALS ------
c firewall
tmm 3 %tmbdy1  tmm 6 %tmbdy2 tmm 8 [0.6*%tmeng] tmm 9  %tmtir1 tmm 10 %tmtir2
tmm 13 0.009 tmm 16 0.004 tmm 25 %tmbdy3 tmm 27 [0.4*%tmeng] tmm [%lmat+1] %tmrigp
c  material 1 - firewall
dynamats 1 3  shell e %wse1 pr 0.33 sigy %wse3 etan %wse4 beta 0. rho %wse5 tsti 3 ;
c material 2 -  front body
dynamats 2 3  shell e %wse1 pr  %wse2 sigy %wse3 etan %wse4 beta 0. rho %wse5 tsti 3 ;
c material 3 - back body material
dynamats 3 1  shell e %wse1 pr   %wse2 rho %bdwse5 tsti 3 ;
c  material 4 - windshield
dynamats 4 1  shell e %wge1 pr   %wge2 rho %wge5 tsti  3 ;
c material 5 - windshield
dynamats 5 1  shell e %wge1 pr %wge2 rho %wge5 tsti 3 ;
c  material 6 - floor around CG
dynamats 6 1  shell e %wse1 pr %wse2 rho %flwse5 tsti 3 ;
c  material 7 hood_back_z material
dynamats 7 3  shell e %wse1 pr %wse2 sigy %wse3 etan %wse4 beta 0. rho %wse5 tsti 3 ;
c material 8 - rigid engine mass
dynamats 8 1 e %wse1 pr %wse2 rho %egwse5 ;
c material 9 - wheel tire material
dynamats 9 1 e 2.46e3 pr 0.35 rho %tiwse5 ; c 2461
c material 10 - rim
dynamats 10  1 e  %wse1 pr  %wse2 rho %rimwse5 ;
c material 11 - bumper material
dynamats 11 3 shell e %wse1 pr %wse2 sigy %wse3 etan %wse4 beta 0. rho  %wse5 tsti 3 ;
c material 12 -  lower core support
dynamats 12 3  shell e %wse1 pr %wse2 sigy %wse3 etan %wse4 beta 0. rho  %wse5 tsti 3 ;
c material 13 - radiator material
dynamats 13 3 e %wre1 pr %wre2 sigy %wre3 etan %wre4 beta 0. rho %radwse5 tsti 3 ;
c material 14 - support under engine material
dynamats 14 3  shell e  %wse1 pr %wse2 sigy %wse3 etan %wse4 beta 0. rho  %wse5  tsti 3 ;
c  material 15 - support for bumper and lower core material
dynamats 15 3  shell e %wse1 pr %wse2 sigy %wse3 etan %wse4 beta 0. rho  %wse5   tsti 3 ;
c material 16 - evaporator core
```

```
dynamats 16 3 e %wfe1 pr 0.33 sigy %wfe3 etan %wfe4 beta 0. rho %funwse5 tsti 3 ;
c material 17 - front strip
dynamats 17 3 shell e %wse1 pr %wse2 sigy %wse3 etan %wse4 beta 0. rho %wse5 tsti 3;
c material 18 - front axle
dynamats 18 3 beam e %wse1 pr %wse2 rho %bmwse5 sigy %wse3 etan %wse4 beta 0. bmcross 1
elfom hl sthi 25 tthi 2 quad 3 sloc 0 tloc 0 ;
c material 19 - rods behind lower core
dynamats 19 1 beam e %wse1 pr %wse2 c sigy %wse3
rho %bmwse5 bmcross 1 elfom hl sthi 15 tthi 0 quad 3 sloc 0 tloc 0 ;
c material 20 - front shocks-springs modeled as axial elements
dynamats 20 3 beam e %wse1 pr %wse2 rho %bswse5 sigy %wse3 etan %wse4
beta 0. bmcross 1 elfom hl sthi 75 tthi 2 quad 3 sloc 0 tloc 0 ;
c material 21 - rear shocks
dynamats 21 1 beam e %wse1 pr %wse2 rho %bswse5 bmcross 1 elfom hl sthi 75
tthi 2 sloc 0 tloc 0 quad 3;
c material 22 - engine mounts
dynamats 22 3 shell e %wse1 pr %wse2 rho %bmwse5 tsti 3 sigy %wse3 etan %wse4 beta 0 ;
c material 23 - back axle
dynamats 23 3 beam e %wse1 pr %wse2 sigy %wse3 etan %wse4 beta 0.
rho %bmwse5 bmcross 0 elfom hl sthi 30 tthi 10 quad 3 sloc 0 tloc 0;
c material 24 - bolts
dynamats 24 3 beam e %wse1 pr %wse2 sigy [0.8*%wse3] etan [%wse4/2] beta 0. rho %bst1
bmcross 1 elfom truss carea 30 sloc 0 tloc 0 ;
c material 25 - solid at CG
dynamats 25 1 e %wse1 pr %wse2 rho %bxwse5 tsti 3 ;
c material 26 - tied rods
dynamats 26 3 beam e %wse1 pr %wse2 sigy %wse3 etan %wse4 beta 0. rho %bst1
bmcross 1 elfom truss carea 200 sloc 0 tloc 0 ;
material 27 - rigid engine mass
dynamats 27 1 e %wse1 pr %wse2 rho %egwse5 ;
dynamats [%lmat+1] 1 e %wse1 pr %wse2 rho %rigwse5 tsti 3 ; c rigid pole
dynamats [%lmat+2] 20 e %wse1 pr %wse2 rho %rigwse5 tsti 3 ; c ground
```

REFERENCES

1. G. H. Powell. *BARRIER VII: A Computer Program for Evaluation of Automobile Barrier Systems, Report No. FHWA-RD-73-51,* Federal Highway Administration, McLean, VA, April 1973.

2. R. W. Bruce, E. E. Hah, and N. R. Ankh. *Guardrail/Vehicle Dynamic Interaction, Report No. FHWA-RD-77-29,* NTIS No. P 286119/AS.

3. R. G. Whirley and J. O. Hallquist. *DYNA3D: A Nonlinear, Explicit, Three-Dimensional Finite Element Code for Solid and Structural Mechanics - User Manual,* University of California, Lawrence Livermore National Laboratory, *Report UCRL-MA-107254,* May 1991.

4. M. M. Kamal and J. A. Wolf. *Modern Automotive Structural Analysis.* Van Nostrand Reinhold Company, NY, 1982.

5. J . W. Wekezer, M. S. Oskard, R. W. Logan, and E. Zywicz. "Vehicle Impact Simulation" *J. of Transportation Engineering,* Vol. 119, No. 4, pp. 598-617.

6. H. E. Ross (Jr.), D. L. Sickling, and J. D. Michie. *Recommended Procedures for the Safety Performance Evaluation of Highway Features, NCHRP Report 350,* Transportation Research Board, 1993.

7. C. Brown. *Crush Characteristics of Four Mini-Sized Vehicles, Test Numbers 91F049, 92F032, and 92F033, Report No. FHWA-RD-93-075,* Federal Highway Administration, McLean, VA, May 1993.

8. D. W. Stillman and J. O. Hallquist. *INGRID: A Three-Dimensional Mesh Generator for Modeling Nonlinear Systems,* University of California, Lawrence Livermore National Laboratory, *Report UCID-20506,* July 1985.

9. R. Rainesburger. *TRUEGRID MANUAL, Version 0.99* XYZ Scientific Applications, September 1993.

10. F. P. Beer and E. R. Johnston (Jr.). *Mechanics of Materials,* McGraw-Hill Book Company, New York, 1981.

11. AISI. *Automotive Steel Design Manual,* American Iron and Steel Institute, Washington, DC, February 1993.

12. B. E. Brown and J. O. Hallquist. *TAURUS: An Interactive Post-Processor for the Analysis Codes NIKE3D, DYNA3D & TOPAZ3D,* University of California, Lawrence Livermore National Laboratory, *Report UCID-19392,* May 1991.